Title
The Role of Cortical Beta Transients in Parkinson Disease

Author
O'Keeffe, Andrew Brian

Publication Date
2021

Peer reviewed|Thesis/dissertation

UNIVERSTIY OF CALIFORNIA

Los Angeles

The Role of Cortical Beta Transients in Parkinson Disease

A dissertation submitted in partial fulfillment of the requirements for the degree

Doctor of Philosophy in Neuroscience

by

Andrew Brian O'Keeffe

2021

ABSTRACT OF THE DISSERTATION

The Role of Cortical Beta Transients in Parkinson Disease

by

Andrew Brian O'Keeffe

Doctor of Philosophy in Neuroscience

University of California, Los Angeles, 2021

Professor Nader Pouratian, Co-Chiar,

Professor Nanthia Suthana, Co-Chair

Parkinson disease is a common neurodegenerative disorder characterized by deficits of balance, resting tremor and voluntary movement. The study of this dopamine-depleted state has come to focus upon the role of beta oscillations (12-35 Hz) as a means of explaining the movement deficits that dominate the constellation of symptoms. It remains unclear what the precise role of beta oscillations is in the healthy state and why they feature so prominently in the pathophysiology of Parkinson disease. Deep brain stimulation in movement disorders affords a valuable opportunity to invasively record from cortical and subcortical structures in patients undergoing the procedure. This dissertation embarks upon an in-depth analysis of beta oscillations in the motor cortices of Parkinsonian patients undergoing deep brain stimulation and contrasts the findings in this cohort with those observed in the dopamine-intact state of essential tremor patients.

The findings detailed here show that transient increases in beta power (beta bursts)

constitute periods of high interregional cortical synchrony and that these episodes are associated with stereotyped changes in waveform morphology. Beta bursts are furthermore characterized by high beta-phase to broadband gamma amplitude coupling. Beta bursting is preceded by increases in cortico-cortical synchrony which is proposed here to act as a driver for beta burst episodes in the motor cortex. Parkinson patients display disordered temporal patterns of beta bursting compared with essential tremor patients. Correlation between the duration of beta bursts and Unified Parkinson's Disease Rating Scale (UPDRS) scores of bradykinesia and rigidity suggests that electrophysiological dysfunction in the timing of beta bursts has direct relevance to clinical manifestations of the dopamine-depleted state. Waveform analysis shows that, when compared with Parkinson disease patients, essential tremor patients exhibit greater degrees of waveform change during bursting compared with non-burst epochs. The extent of waveform morphology change also correlates inversely with severity of bradykinesia and rigidity as measured by UPDRS scores.

Analysis of movement onset in patients shows that beta oscillations are transiently suppressed at the time of movement initiation in both Parkinson disease and essential tremor cohorts. Only essential tremor patients demonstrated a significant reduction in cortico-cortical synchrony prior to movement onset. The probability of beta bursts immediately following movement onset was reduced for both cohorts however this beta burst suppression occurred earlier for the essential tremor cohort and could be identified a full second prior to movement initiation. Waveform morphology during beta bursting was significantly altered during movement compared to rest and initial changes in waveform morphology occurred as early as three seconds prior to movement onset. Beta-phase to broadband gamma amplitude during

bursting was reduced during movement but there was no difference between the cohorts in absolute levels of burst-associated phase-amplitude coupling.

The findings presented are consistent with a model of hypersynchrony across cortico-basal ganglia loops driving disordered beta bursting in motor cortices, resulting in impairments of voluntary movement. Evidence is presented to show that burst timing pathology occurs as a direct result of synchrony abnormalities and acts to impair movement via phase-amplitude coupling and waveform morphology changes noted to occur therein. Higher burst synchrony and extended burst durations may be acting as a physiological tamponade on development and updating of movement plans. This interpretation offers a unified explanatory framework for a body of literature that has uncovered seemingly contradictory findings regarding beta oscillations and lays the groundwork for targeted therapies directed towards restoring the dopamine-intact electrophysiological features of voluntary movement.

The dissertation of Andrew Brian O'Keeffe is approved.

Marco Iacoboni

Michael Levine

Martin Monti

Nader Pouratian, Committee Co-Chair

Nanthia Suthana, Committee Co-Chair

University of California, Los Angeles

2021

Table of Contents

List of Figures

List of Tables

List of Equations

List of Abbreviations

a.u. = Arbitrary Units

CV = coefficient of variation

DBS = deep brain stimulation

dwPLI = debiased weighted phase lag index

EEG = electroencephalography

ECoG = electrocorticography;

GPi = globus pallidus internal capsule

IPG = implantable pulse generator

LFP = local field potential

M1 = primary motor cortex

MSN = medium spiny neurons

PAC = phase-amplitude coupling

PD = Parkinson disease

PSI = phase synchrony index

SNc = substantia nigra pars compacta

STN = subthalamic nucleus

SMA = supplementary motor area

tACS = transcranial alternating current stimulation

UPDRS = Unified Parkinson's Disease Rating Scale

µV = microvolts

Acknowledgements

Dedication

To Humphrey,
with all my heart.

Appreciation

Family

Shobna O'Keeffe, BSc
Geraldine Walford, MD
Declan O'Keeffe, MD

Doctoral Committee

Nader Pouratian, MD, PhD
Marco Iacoboni, MD, PhD
Nanthia Suthana, PhD
Martin Monti, PhD
Michael Levine, PhD

Pouratian Laboratory

William Speier, PhD
Mahsa Malekmohammadi, PhD
Evangelia Tsolaki, PhD
Nicholas Au Yong, MD PhD
Hiro Sparks, MD

UCLA

Jennifer Lee
Suzie Vader

Funding Sources

This dissertation was made possible by the generous support of the Fulbright International Science and Technology Scholarship Program, overseen by the U.S. Department of State.

The Pouratian laboratory was supported by the National Institute of Biomedical Imaging and Bioengineering (Grant K23-EB-014326), by the National Institute of Neurological Disorders and Stroke (Grant R01-NS-097782), and by philanthropic support from the Casa Colina Center for Rehabilitation.

Previously Published and Copyrighted Material

Figure 1. Is reproduced with permission from the author and has been previously published as; Beta burst dynamics in Parkinson's disease OFF and ON dopaminergic medication, Gerd Tinkhauser, Alek Pogosyan, Huiling Tan, Damian M Herz, Andrea A Kühn, Peter Brown, *Brain*, Volume 140, Issue 11, November 2017, Pages 2968–2981, https://doi.org/10.1093/brain/awx252

Chapters 1 and 2 contain material previously published by the author as;
Synchrony Drives Motor Cortex Beta Bursting, Waveform Dynamics, and Phase-Amplitude Coupling in Parkinson's Disease, Andrew B. O'Keeffe, Mahsa Malekmohammadi, Hiro Sparks and Nader Pouratian, Journal of Neuroscience, Volume 40, Issue 30, July 2020, Pages 5833-5846; DOI: https://doi.org/10.1523/JNEUROSCI.1996-19.2020

Biographical Sketch

Education

Bachelor's Degree in Mathematics and Statistics, Open University (Ongoing)

Master of Arts, Keble College, University of Oxford (2011)

History of Mathematics, with commended performance, Open University (August 2010)

Bachelor of Medicine, Bachelor of Surgery, University of Oxford (2009)

Bachelor's Degree in Physiology, Psychology and Philosophy, University of Oxford (2004)

Peer Reviewed Publications

O'Keeffe AB, Malekmohammedi M, Sparks H, Pouratian N**,** Synchrony Drives Motor Cortex Beta Bursting, Waveform Dynamics, and Phase-Amplitude Coupling in Parkinson's Disease. J Neurosci. Jul 2020 22;40(30)

Malekmohammadi M, Shahriari Y, AuYong, **O'Keeffe A**, Bordelon Y, Hu X, Pouratian N**.** Pallidal stimulation in Parkinson disease differentially modulates local and network beta activity. J Neural Eng. Oct 2018. 15(5)

Machado AR, Zaidan HC, Paixão AP, Cavalheiro GL, Oliveira FH, Júnior JA, Naves K, Pereira AA, Pereira JM, Pouratian N, Zhuo X, **O'Keeffe A,** Sharim J, Bordelon Y, Yang L, Vieira MF, Andrade AO. Biomed Eng Online. Dec 2016. 15(1).

O'Keeffe AB, Lawrence T, Bojanic S. Oxford Craniotomy Infection Database: A Cost Analysis of Craniotomy Infection. British Journal of Neurosurgery. April 2012; 26(2): 265-269

O'Keeffe AB. Oxford Craniotomy Infections Database: a cost analysis of craniotomy infection. Abstract published in the British Journal of Neurosurgery 2011;25:pp576

O'Keeffe AB, Terris J Post-traumatic swelling. BMJ 2012;345:e6363

O'Keeffe AB, Terris J, Hormbrey P. A sinister cause of back pain 2012;344:e3015 BMJ.

O'Keeffe AB, Lawrence T P, Agombar D, Bojanic S**.** Post Craniotomy Infection. Abstract published in the British Journal of Neurosurgery 2011;25.2:165-166

Chapter 1. Background and Introduction

1.1 Parkinson Disease

In his seminal tract "An Essay on the Shaking Palsy", published in 1817, James Parkinson, described six case studies characterized by the gradual onset of "a slight sense of weakness, with a proneness to trembling in some particular part; sometimes in the head, but most commonly in one of the hands and arms".[1] In his succinct writings Parkinson describes many of the cardinal features of the eponymously named pathological progression, outlining slowness of movement, stiffness, tremor and festinating gait as hallmarks of the degenerative disease. Parkinson disease (PD) affects approximately seven million people worldwide and is the second most common neurodegenerative disorder after Alzheimer disease.[2] The economic impact of PD in the United States alone has been estimated at $51.9 billion and the impact on quality of life for most patients is remarkably debilitating.[3] Much progress has been made in understanding the pathophysiology of PD since Parkinson's first description; however, we remain in large part unaware of the etiology, and pathophysiological consequences of dopaminergic degeneration of the substantia nigra pars compacta (SNc), a characteristic feature of the disease considered to be critical in producing PD symptomatology[4].

The diagnosis of "Parkinsonism" is primarily a clinical one based upon the presence of bradykinesia (slowness of movement) together with at least one of tremor, rigidity and postural

instability[5]. A key indicator for a diagnosis of PD is responsiveness of symptoms to levodopa therapy.[6] Since initial studies showing dopamine depletion in the caudate and putamen of human cadavers,[7] followed by pioneering experiments to test the efficacy of levodopa in PD,[8] dopamine has been considered as central to the pathophysiological process' producing the symptoms of the disorder. Several diseases feature the central motor symptoms of "parkinsonism" sometimes combined with other prominent symptoms as is the case in progressive supranuclear palsy and dementia with Lewy bodies. Idiopathic PD stands in contrast to these 'Parkinson plus' syndromes and is so named because of a lack of any clear familial history, genetic etiology or causative environmental agent.[9]

The classical (sometimes called the 'rate') model of PD pathophysiology conceives of the basal ganglia as playing host to two competing cortico-basal ganglia loops, the direct and indirect pathways[10], which govern movement or movement inhibition respectively. Loss of dopaminergic tone to the striatum is thought to bias the cortical output of the basal ganglia to adopt an akinetic pattern as a result of hyperactivation of the indirect pathway. The indirect pathway is purported to exist in counterpoise to the direct pathway which instead exerts a prokinetic influence on the motor cortex.[10] Distinct populations of medium spiny neurons (MSN) in the striatum possess D1 and D2 receptors, and the rate model considers the activation or suppression of cortical activity as arising from an asymmetric dopaminergic activation of these receptors. Thus Parkinsonism is deemed to result from a relative hyperactivation of the indirect pathway preventing movement initiation and generating the cardinal motor symptoms of PD.

Deep brain stimulation (DBS) of the basal ganglia is a surgical approach to ameliorating the symptoms of PD. The technique is complimentary to pharmacological PD treatments and involves implanting stimulating electrodes in the deep nuclei of the brain, most often the

subthalamic nucleus (STN) or the internal capsule of the globus pallidus (GPi), and connecting these leads to an implantable pulse generator (IPG) sited subcutaneously in the pectoral region of the thoracic wall. Application of current at various frequencies across the contacts of the implanted electrodes can improve the movement symptoms of PD, particularly tremor and bradykinesia, reducing dependence upon medications, reducing side effects and improving quality of life.[11] One major tangential benefit of DBS is that it allows recording of local field potentials (LFPs) from the tissues surrounding the electrode contacts. It also permits recording of LFPs during the application of stimulating current across two of the contacts, or from one of the contacts with return at an extra-cranially placed ground. Combined with clinically obtained measurements of PD symptomatology from conscious patients intraoperatively this model provides an important window on the electrophysiological changes that accompany PD symptoms. For example, the amplitude and peak frequencies of beta oscillations (12-35Hz) in the STN have been correlated with severity of PD symptoms[12, 13] and high frequency stimulation has been shown to effect both a suppression of the beta band amplitude and symptomatic relief.[14] Other lines of evidence are compatible with the general claims of the rate model. For example, GPi or STN ablation reduces PD symptoms purportedly by decreasing the activation of the indirect pathway, and restoring a relative hyperactivation of the direct pathway[15,16]. However, while apomorphine, a non-selective dopamine agonist does decrease activity in the GPi, it does not appear to modulate the firing rate of STN neurons suggesting that other factors besides the mere levels of activation in the two pathways are at play.[17]

It remains unclear how exactly DBS may be acting within a rate model to effect symptomatic relief but it has been suggested that stimulating current acts as a 'physiological ablation' to bias activation towards the prokinetic direct pathway. Although this model of basal ganglia function

has not gone unchallenged[18] there is good evidence from animal studies to suggest that at least in broad terms the model outlines key aspects of basal ganglia function.[19] It remains unclear how neural oscillations fit into the traditional two-pathway model of basal ganglia function.

Some of the challenges facing the rate model can be resolved with the idea that the absolute levels of activation in the competing pathways are not the most pertinent feature for PD symptomatology. Rather, we might suppose that what is producing the akinetic/rigid motor symptoms of PD is the temporal pattern of activation within the basal ganglia. Recent research has focused on hypersynchronization of the neural oscillations of the basal ganglia as a phenomenon which may constitute an important component of the pathophysiology underlying the condition.[20] For example, increased cortico-cortical synchrony in the beta band has been found to correlate with PD symptoms and is reduced by levodopa therapy.[21] Similarly, stimulation of the STN at 20Hz to synchronize oscillations results in clinical bradykinesia in PD patients.[22] Such findings have led some researchers to postulate that PD is a disorder of excessive neuronal synchrony across cortico-basal ganglia circuits. DBS affords an excellent opportunity to study the large-scale population level activity of neurons in the nuclei of the basal ganglia. More recently, the simultaneous insertion of electrodes into the deep brain structures and placement of cortical electrode strips, means that large amounts of rich electrophysiological data can be simultaneously acquired from across the cortico-basal ganglia network[23]. This dissertation uses such techniques to test the hypothesis that a major functional disturbance in Parkinson disease is a hypersynchrony throughout cortical motor systems by focusing in particular on the premotor and motor cortices. We propose that this synchrony disturbance, while it may not overtly modulate gross measures of cortical functioning such as oscillatory power, causes disturbances in temporal patterning of neural oscillations, resulting in network level dysfunction. It has been

shown that the frequency of transient increases in beta power (beta bursts) during continuous movements is a superior predictor for bradykinesia than absolute beta power alone[24] however it remains unclear precisely what it is that gives beta bursting an important role in PD movement symptomatology. We draw on previously published research[25] and propose that beta bursts are increased in duration and frequency by cortico-cortical hypersynchronization in the beta band. We suggest that the synchronous nature of bursts and their waveform morphology remains invariant throughout rest and movement but that their frequency of occurrence and duration is modulated in order to permit movement to occur.

Several studies have implied an important role in PD for exaggerated phase-amplitude coupling between the phase of beta oscillations and the amplitude of gamma oscillations (phase-amplitude coupling, or PAC) in the motor cortex.[26] Therapeuitc DBS has also been observed to modulate this exaggerated PAC suggesting that this phenomenon plays a crucial role in the symptomatic expression of PD.[27] Of note however, is that in these studies PAC is not exaggerated in all subjects with symptomatic PD, potentially providing a rebuttal to the hypothesis that PAC occupies a causative role in PD symptomatology. To reconcile these findings we suggest that coupling of low frequency oscillation phase to high frequency amplitude is particularly elevated during beta bursts rather than continuously throughout the time-series, accounting for inconsistencies in the literature surrounding this phenomenon and providing an explanatory mechanism for the role we propose for burst episodes. The bursting nature of the beta band may also serve to explain other outstanding inconsistencies within the literature such as the fact that motor cortical beta oscillations are variously reported as elevated[28] or no different from healthy controls.[29] This dissertation employs several novel analytic approaches to show the relevance of time varying signal features to network level

electrophysiological activity and clinical features of PD. We attempt to break new ground regarding the pathophysiological basis of PD by drawing together several separate strands of research into a unified model of PD dysfunction with hypersynchrony of cortico-basal-ganglia hypersynchrony at its core.

1.2 Human Cortical Electrophysiology

The study of intracranial neural oscillations can be traced back to the work of Richard Caton (1842-1926), a physician and subsequently Lord Mayor of Liverpool, who in 1875 reported his findings[30] regarding electrical currents in the brains of animals. In his short piece featured in the British Medical Journal, Caton describes the fluctuations of a galvanometer in response to the positioning of electrodes at two points of monkey cortex or while referencing one electrode to the surface of the skull. Interestingly, the seeds of the present field of electrophysiology were nascent in his description as he refers to the modulation of those electrical fields in response to specific behavioral tasks. Similar, nearly contemporaneous experiments performed by Adolf Beck in Krakow in 1890, related sensory stimuli to fluctuations of cortical electrical fields and have led some authors to accredit joint responsibility to Caton and Beck in founding the field of electroencephalography (EEG). The work of these two pioneering electrophysiologists received little attention among their peers and it would not be until Hans Berger recorded the first human EEG in 1924 that the field of human cortical electrophysiology began to take the shape we currently recognize today[31].

Hans Berger not only coined the term 'electroencephalogram' but also went on to publish a total of 23 papers on the subject and systematically investigated changes in the EEG in response to attentional changes, the effects of anesthesia and cerebral injury. Berger's impact on the field is still felt today in the terminology used to describe bands of oscillatory frequency, having identified and first described alpha and beta frequencies in his early studies.[32] The next major pioneering efforts in the field would be undertaken by the American polymath, Alfred Loomis (1887-1975) in the form of refinements made to amplifier technology and the application of the EEG to the study and characterization of sleep stages.[33]

Subsequent development of cortical electrophysiological recording came as a result of the neurosurgeon Wilder Penfield's attempts to delineate and surgically resect areas of epileptogenic cortical tissue at the Montreal Neurological Institute[34] in the 1930s. Working closely with a renowned electrophysiologist Herbert H. Jaspers, Penfield and his team developed, refined and documented the Montreal treatment for epilepsy[35] together with the functional cortical maps that the procedure yielded.[36] By weaving together the complimentary fields of neurology, electrophysiology and the surgical treatment of epilepsy, Penfield and Jasper inculcated a new understanding of the human brain, one that still resonates through and informs our current approaches to the electrophysiology of the human cortex. Their focus upon the electrophysiology of the cortex was a key component of this scientific revolution and led to a bias in the literature, perhaps unfairly, that the cortex occupies a privileged position as the seat of sophisticated high-level neural operations. With the advent of detailed anatomical imaging, diffusion weighted tractography[37] and deep brain stimulation permitting direct recording from subcortical structures, attention has begun to shift to circuit-based theories of cerebral function with neural oscillations occupying a prominent role within these frameworks.

1.3 Neural Oscillations

One of the corollaries of the approaches outlined in the foregoing section was the development of a description of the cortical current fluctuations in terms of neural oscillations. Placing electrodes subdurally on the pial surface of the brain (electrocorticography or ECoG) records synchronous activity of large populations of neurons lying beneath or in close proximity to the recording electrode. It is difficult to define the network size that is typically recorded from an ECoG electrode as different frequencies of neural oscillations propagate over different distances with lower frequencies tending to propagate over greater distances.[38] Electrode size also affects the signals optimally acquired by an array and it has been demonstrated experimentally that large electrodes of the type similar to those used in our experiments, are well suited to acquisition of LFPs with a high signal to noise ratio, although the trade-off in terms of recording performance is the effect of spatial averaging resulting from a large electrode surface area.[39] Relatively large electrode sizes are also well suited to the investigation of cortical functioning as this is primarily concerned with elucidating the features of inter-regional neural communication on a macro scale (centimeters) and aims to capture a diverse temporal and frequency range from multiple sources (axon, dendrites and soma of neurons). Neural oscillations are highly dependent on the cellular and network properties of inhibitory interneurons in the cortex[40] and have been implicated in processes as diverse as consciousness,[41] perception,[42] motor control,[43] and memory,[44] to name but a few. They are thought to be highly dependent on network structure and connectivity[45] and have increasingly been seen as playing a prominent role in many disease states collectively referred to in some of the literature as 'oscillopathies'.[46] Accordingly, pathological features of neural oscillations, and hypersynchrony

in particular, has been held to account for disorders of cognition such as schizophrenia,[47] autism and ageing.[48] Of particular interest is a recent trend to apply deep brain stimulation to psychiatric disorders on the supposition that modulation of activity in deep networks could effect a normalization of neural communication on a network level.[49] The rationale here has been similar for deep brain stimulation in movement disorders where it has been established that therapeutic deep brain stimulation can cause changes in the cross-frequency coupling of cortical beta oscillations as well as absolute beta power.[50] In the basal ganglia the precise relative phases of neural oscillations has been shown to shape effective connectivity between nuclei[51] and multiple studies have implicated increased power of beta oscillations as central to the pathology of PD.[52,53,54]

Measurement of neural oscillations by techniques such as ECoG requires that there be some synchrony in the membrane currents of the underlying tissue. Entirely uncoordinated activity would manifest as white noise due to the fact that oppositely aligned dipoles would cancel each other out.[55] Instead the typical power spectrum of a cortical region displays a 1/f (where f = frequency in Hertz) logarithmic decrease spanning roughly five orders of magnitude.[38] Until recently Fourier analysis was the favored methodology for decomposing an oscillatory signal into the relative powers of its frequency components. However, developments in the field such as wavelet decomposition[56] and multitaper analysis[57] offer effective means by which to quantify a power spectrum and have the advantage that they are less constrained by assumptions of signal stationarity, the idea that the stochastic properties of the signal are invariant across time. In recent years attention has focused on the relevance of the raw, undecomposed oscillation waveform shape, with suggestions in the literature that certain aspects of the waveform shape have implications for underlying cortical network functioning.[58]

One major purported role for neural oscillations is the binding together of distinct neural populations or networks into computationally cooperative units.[59] Still other potential roles include contributions to the representation of information or facilitation of the storage and retrieval of information in neural networks.[60] It may be the case that neural oscillations subserve many or all of these functions or that they occupy different functional roles in different neural contexts with specific frequency bands performing dedicated communicative tasks in different regions. Proponents of ideas such as 'communication through coherence' suggest that anatomically distinct regions of the brain exchange information in a time-selective way using synchrony in specific frequency bands.[61] Later sections will discuss in more depth the potential roles for synchrony in neural networks, and the relevance this has to pathophysiological states.

The field of neural electrophysiology has recently seen a renaissance of techniques geared to the analysis of the fine structure of oscillations. Initial investigations of oscillations recorded at the scalp and cortical surface drew attention to prominent stereotyped features of the recording trace. It is, for example, because of the similarity of waveform shape to the Greek letter 'μ' that the mu waveform is named as such. Early investigators lighted upon these easily recognizable features of the waveform as important objects for study,[62] and indeed, in certain fields such as hippocampal electrophysiology they have for many years been consistently regarded as informative by investigators.[63] Because of the computational power of modern computers and the ease with which techniques such as Fourier analysis can be implemented, fields based on technologies such as scalp EEG that generate large datasets have veered towards approaches that neglect the moment-to-moment variability of neural oscillations. This is beginning to change however, with new appreciation for the relevance of non-sinusoidal features of neural oscillations in disease states such as PD,[58] and a renewed interest in the analytic

approaches that permit their study.[64] As an emerging field in the study of PD the non-sinusoidal features of neural oscillations require further characterization to determine their importance with regards cortical function, neural communication and the pathological disease states observed in neurological disorders. Forthcoming sections of this dissertation will investigate directly the relationship between non-sinusoidal oscillations, the beta band and parkinsonian disease states.

1.4 The Beta Band

Abnormalities of the beta band have come to occupy a prominent role in the electrophysiological study of PD. In particular, beta oscillations have been found to be elevated in the STN,[54] GPi,[65] and are reduced in both nuclei by DBS.[66,65] Stimulation of both the STN and GPi is associated with changes in remote, connected locations, as seen in the reduction of beta oscillations in motor cortical regions,[67,68] although this finding has not been consistent.[23] This suggests that the reduction of beta power may be a mechanism by which DBS effects symptomatic improvements. Interestingly there have been conflicting reports regarding the levels of resting beta in PD with some authors finding elevated[28] and others finding normal levels[29, 23] of beta oscillations in M1. Similar results have been observed for beta oscillations in the subcortical structures, some studies finding that beta oscillations are elevated in only around a half of PD subjects,[69] whereas others report much more consistent elevations of beta power.[23] Beta-encoded PAC, whereby the amplitude of high frequency oscillations is tightly linked to low frequency oscillation phase, has also been heavily implicated in the pathophysiology of PD. PAC is enhanced in the cortex,[26] reduced by DBS of the STN and GPi,[27,50] and in the GPi correlates

inversely with severity of PD symptoms.[70] Yet beta to gamma PAC is not markedly elevated in the cortex of all individuals suffering from PD.[26] It can be seen therefore that there is conflicting evidence regarding the significance of elevations in beta power, and associated beta features such as PAC, in the cortico-basal ganglia network of PD patients.

Some aspects of movement-related beta suppression also raise questions about whether it is beta power per se that is important in regulating movement. GPi DBS does not reduce cortical beta power[23], a phenomenon which we might expect to observe if cortical beta oscillations were movement inhibitory. Movement-related cortical beta suppression in healthy individuals appears to be invariant with regards to movement parameters such as speed,[71] force[72] or whether a movement is ballistic or sustained.[73] Although beta suppression during movement is more pronounced on the side contralateral to movement execution it is observed bilaterally in the sensorimotor cortices.[73] Furthermore, post-movement beta rebound is more spatially extensive than the movement-related suppression that precedes it.[74] These features of the beta signal constitute one strand of inquiry that has prompted a closer analysis of the properties of the beta band in order to gain a deeper understanding of the functional role of these oscillations in movement.

If it is not beta power in and of itself that is relevant for movement inhibition, or at least appears to lack the spatial and parameter specificity to perform such a function, it may be that synchrony of beta oscillations throughout the cortico-basal ganglia network is the crucial movement-inhibiting feature of the beta band in the healthy and diseased state. A large body of research has accumulated to suggest that synchrony within the beta band can act as an important component of PD pathophysiology.[75,76,77,78] The beta band has been shown to display increased levels of synchrony in the PD state at the cortico-cortical[79] and the subcortical[80] levels as well as

between cortex and subcortical structures.[78,23] Moreover, beta band coherence between the STN and GPi is attenuated by movement.[81] Stimulation of the GPi in PD has been shown to reduce cortico-GPi beta coherence which is pathologically elevated in the PD state.[65] Experimental studies combined with computational modeling of synchrony in the STN of PD patients supports the view that the beta band embodies periods of high relatively high phase synchrony interrupted by short, transient episodes of lower phase synchrony.[76] A persistent, highly synchronized beta band could reflect an inability to shift between periods of high and low synchrony, potentially "locking closed" a crucial information channel between cortical areas.[80,52] This focus upon short, transient episodes of synchronization has led to analyses of beta power directed towards elucidating the fine temporal structure of beta oscillations and relating these features to information processing in PD pathology.[20]

All spectral analysis approaches aim to concisely represent the average contributions of given frequencies over a unit of time, often several seconds or several minutes[82]. Whilst this method of waveform decomposition and temporal averaging allows for useful summary measures and comparisons of oscillatory activity, it neglects the fine temporal structure of waveform activity that is increasingly being seen as a crucial feature of neural processing.[58]. The PD literature contains both reports of increased,[28] and unaltered[29] cortical beta power, a finding that is hard to reconcile with the hypothesis that beta oscillations occupy a central role in the orchestration of voluntary movment.[83]

Tinkhauser et al have studied beta bursting in the STN and observed the effect that levodopa had on the curtailment of these high amplitude transients. Their findings demonstrate that the duration of beta bursting in the STN is correlated with severity of PD symptoms and that beta burst duration is reduced with therapeutic levodopa treatment. Furthermore, the baseline PD

state was characterized by increased overlap of beta bursts between the STN bilaterally. Such overlapping bursts were also found to be episodes of high phase locking between the bilateral STN oscillations suggesting a tantalizing link between synchrony and beta burst dynamics.[84] A summary of these findings have been reproduced here with permission from the author (see Figure 1, A-E). Subsequent studies looked at short trains of stimulation targeted at STN beta bursts and found that this closed-loop stimulation protocol was equally or more therapeutically effective than continuous stimulation trains[25].

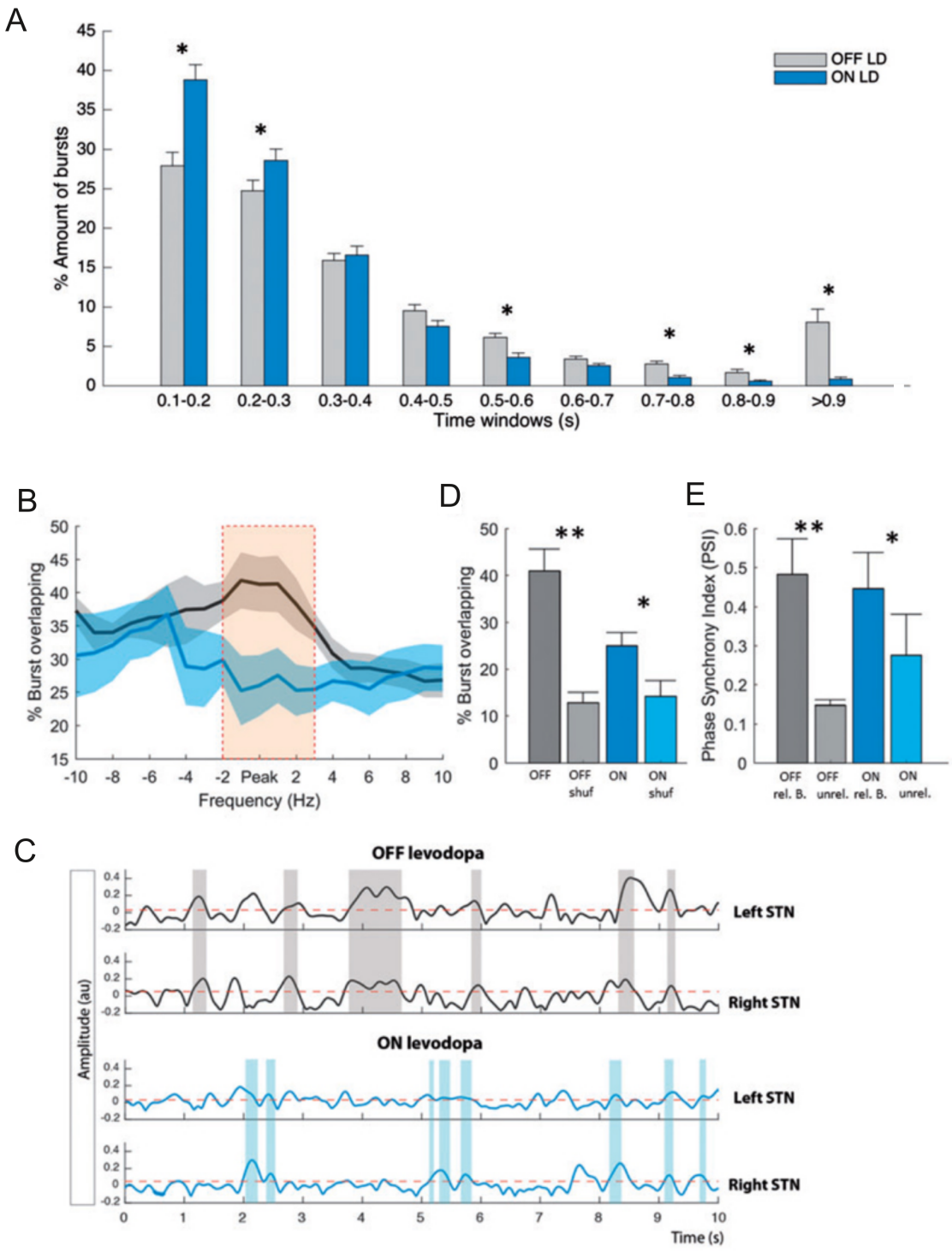

Figure 1. An illustration of beta burst properties adapted from Tinkhauser et al, (2017). Adapted from Tinkhauser et al, (2017) with permission. A) Distribution of burst durations averaged across 16 sides as a percentage of total number of bursts on each side, during

OFF levodopa and ON levodopa, where bursts are defined as periods of beta activity that exceed the 75th percentile amplitude threshold with a minimum duration of 0.1 s. During ON levodopa the percentage amount of shorter bursts (0.1–0.2 s, 0.2–0.3 s) is higher and the percentage amount of long bursts (0.5–0.6 s, 0.7–0.8 s, 0.8–0.9 s, >0.9 s) is lower in comparison to the OFF levodopa state. Values are represented as mean + SEM; *P_{corr} < 0.05. LD = levodopa. B) The percentage of the total number of bursts that overlap in time between hemispheres for the peak frequency of beta (averaged across the two sides) and surrounding frequencies. Data were realigned to the frequency of the beta peak in each STN and then averaged. During OFF levodopa the percentage burst overlapping is significantly higher compared to ON levodopa and also frequency-specific around the beta peak (cluster-based permutation test significance shown by orange bar). C) Illustrates 10 s of simultaneous time evolving wavelet amplitude for the beta peak frequency for the left and right hemisphere and both OFF (grey) and ON (blue) levodopa. This illustrates the stronger burst overlapping (shaded areas) during OFF levodopa compared to ON levodopa (Subject 7). D) Contrasts the difference in percentage overlapping between the conditions for the beta peak frequency, with the overlapping by chance (shuf = shuffled data). Both the conditions show a stronger overlapping compared to that expected by chance, with no difference in the overlapping by chance between the conditions. E) The PSI between hemispheres for related-overlapping and shuffled unrelated-overlapping burst (B = bursts) periods OFF and ON levodopa. The PSI for related bursts is much higher compared to unrelated bursts for both the conditions. Beta bursts were determined using the 75th percentile amplitude threshold. Values are represented as mean + SEM; *P < 0.05.

In a similar vein, Cagnan et al have investigated the relationship between phase locking and beta amplitude between the STN and GPi. By taking advantage of patients implanted with DBS leads in both nuclei the researchers were able to identify beta amplitude enhancing phase relationships between the beta oscillations in the STN and the GPi. The duration of time that the two nuclei spent in such phase relationships correlated with the increases in beta amplitude observed. Finally, the study revealed that levodopa therapy reduced the duration and frequency of beta amplifying phase alignments which the authors suggest is associated with more improved processing capabilities and resultant symptomatic improvements.[80] Studies of beta bursting in the GPi have identified that increased beta power in this nucleus (compared to dystonia controls) is associated with reduced beta burst amplitudes and unchanged burst durations.[23] The same study found that GPi stimulation was associated with decreased beta-band coherence between the motor cortex and the GPi.

Our hypothesis proposes that a close analysis of the cortical beta band with particular attention to the temporal fluctuations of beta oscillatory power will enable resolution of some of these apparently conflicting findings outlined in the preceding paragraphs. This dissertation proposes to test the hypothesis that the fine temporal structure of the beta band, and in particular the phenomenon of beta transients, can explain the discrepancies in overall beta power and will proceed to test the hypothesis that transients in beta power can be closely related to severity of PD symptoms. Central to this hypothesis is the notion that beta transients are critical epochs in the inhibition of movement arising from increases in circuit synchrony and exhibiting concentrated episodes of phase-amplitude coupling (PAC), a phenomenon discussed in more depth in subsequent sections.

Malekmohammadi et al found that stimulation of the GPi reduced excessive cortical beta PAC in the cortex in a similar manner to that effected by stimulation of the STN.[50] They also noted a differential modulation of high (20-35 Hz) and low beta (13-20 Hz) bands during movement and stimulation. Movement reduced low beta power in the motor and premotor cortex but did not have any effect on high beta power in these cortices. Reduced high beta PAC during GPi stimulation was not associated with a reduction of cortical power in either the high or low beta bands. Linear mixed effects modeling showed the two components of the beta band to be modulated independently. This finding parallels studies of the STN which have shown that DBS in this nucleus selectively suppresses oscillations in the low beta range and that degree of suppression in this band correlates with symptomatic improvement.[85] There are also notable differences in the cortical PAC profiles of ET and PD with the latter showing greater levels of high beta-to-gamma PAC and the former preferentially coupling alpha and low beta oscillations to high gamma.[86] These findings have buttressed the hypothesis that high and low beta bands are distinct in their functional roles. One interpretation of this sub-band segregation is that they comprise distinct synchrony channels for the processing and communication of movement plans across cortico-subcortical loops.[52] We draw upon these lines of research to justify our approach to dissecting the beta band into low and high components here hypothesized to occupy distinct functional roles.

The finding that synchrony is intimately linked to changes in the amplitude of beta oscillations, and that both are increased in the dopamine-depleted basal ganglia, has lent support to the idea of communication through coherence.[61] This hypothesis states that a key role for neuronal oscillations in processing of information is to render spatially remote populations of neurons hyperexcitable within specific time windows, allowing the receiving population to favor

inputs from sending populations to which they are phasically entrained. Other authors have sought to couch this notion within a more general schema of cortico-basal ganglia processing by suggesting that the network occupies a narrow state space between synchronized and unsynchronized activity. The ability to shift rapidly between these states could constitute an important factor in regulating the processing capacity of the system. The hypersynchronized state of PD would, under this interpretation, represent a narrowing of computational bandwidth at the network level, resulting in a pattern of oscillation that favors maintenance of the status quo[20]. These two theories of the functional role of beta oscillations are mutually complimentary and it could be the case that each highlights a distinct but crucial role for the beta band in the cortico-basal ganglia network. Our proposal states that the phase of beta band synchrony plays a more subtle role in motor cortical movement regulation and that rather than acting as a channel for the relay of information, cortico-cortical synchrony is instead driving beta transients to occur and it is the occurrence of these phenomena that exerts an informational tamponade on the enactment of cortically generated movement plans.

1.5 Deep Brain Stimulation

Deep brain stimulation (DBS) involves the careful placement of stimulating electrodes in the subcortical structures of the brain with the intention to treat the symptoms of a neurological disorder. The technique has its origins in the Montreal Procedure developed by Wilder Penfield[87] in the 1930s and described above. The Montreal Procedure advocated the use of epilepsy semiotics and intraoperative electrophysiology to elucidate areas of abnormal neural tissue for

resection. The advent of stereotactic approaches to localizing deep brain structures[88] rendered it feasible to ablate well circumscribed regions beyond the direct visual field of the surgeon. Application of Penfield's ideas to tissues beyond the cortex brought neurostimulation of neurological tissue for therapeutic purposes to a vastly increased range of neurological disorders[89]. Before the introduction of levodopa in 1968, PD was a common and intractable neurological disease that quickly became an important object of study for physicians practicing neurostimulation and ablative stereotactic therapies[90]. During exploratory neurostimulation to find targets for ablation, some surgeons noted that high-frequency stimulation could alleviate symptoms and there was a natural progression to attempt chronic neurostimulation of such locations[91]. There followed a brief period of experimental work on DBS and attempts to adapt it to numerous intractable neuropathies[92].

In the 1970's the advent of levodopa therapy for PD, together with a political climate that bundled DBS together with psychosurgery such as frontal lobotomy, meant that DBS was practiced by fewer and fewer surgeons. In tandem with the decline of stereotactic neurosurgery over the 1970s this decade also saw the rise to prominence of the cardiac pacemaker, developed and refined by the medical devices manufacturer Medtronic. Later development of the chronically implantable neurostimulator effectively piggybacked on the technology used in the cardiac pacemaker[89]. Pioneering uses of the chronically implantable neurostimulator were carried out on a small subset of patients suffering from pharmacologically intractable chronic pain and used modified Medtronic radiofrequency systems[93]. Promising results encouraged the uptake of the procedure across several locations in the United States and Medtronic developed the first commercially available neurostimulator in 1968.

Having become increasingly rare in late 1960s and early 1970s, functional neurosurgery made a resurgence in the early eighties. This resulted from two main drivers, first, from the finding that medical therapies offered only a time-limited relief of symptoms before the side effect profile became almost as challenging to manage as the untreated disease state, and second, from the development of rating scales used to quantify PD severity. The UPDRS scale allowed physicians to meaningfully compare the efficacy of their target locations and therapeutic stimulation protocols as well as having the advantage of allowing the Food and Drug Administration to license and regulate the technology with reference to a standardized evidence base[89]. The UPDRS comprises a five-part assessment with each symptom rated on a scale from 0-4. A broad spectrum of disease features are sampled such as gait, bradykinesia, rigidity, mentation, speech, facial expression and tremor[94]. In 1997 DBS was approved for treatment of PD in the United States and was subsequently approved for dystonia. Close collaboration between industry and clinicians has been attempting to expand the indications for DBS and it has been applied with some success to conditions as diverse as depression[95], epilepsy[96] and obsessive compulsive disorder[97]. Despite increasing interest in the technique of DBS the means by which it exerts therapeutic benefit is still poorly understood. As the most common indication for DBS, this has rendered PD an important model for researching the mode of action of DBS, and by proxy, the functioning of the cortico-basal ganglia circuits.

1.6 The Primary Motor Cortex in PD

The motor cortex is considered to be an area critical for the learning and execution of fine motor tasks.[98] Both lesion studies[99] and function explorations of the motor cortex, first in primates[100] and subsequently in humans,[101] provide convincing evidence for the critical role it plays in this regard. There is some evidence to suggest that the caudal region of M1 has evolved in higher primates to facilitate complex patterns of motor activity required for extremely dexterous fine movement patterns[102] because of the relatively high density of fast conducting pyramidal tract cells that originate from layer 5 in this area.[102] Fast pyramidal tract neurons are more likely to synapse directly onto alpha motor neurons offering a route for rapid monosynaptic control of musculature.[103] Because of the privileged position that primary motor cortex appears to play anatomically and physiologically in movement it is commonly thought of as a "final common pathway" for the volitional control of movement and hence an area of significant interest in conditions such as PD where volitional control of movement is compromised.

M1 is known to derive significant inputs from contralateral M1,[104] primary sensory cortex,[105] and secondary motor cortices.[106] In addition to these cortical inputs it receives subcortical projections from both motor and sensory thalamus.[107] Recent studies indicate that motor thalamic inputs to M1 act mainly to entrain firing rather than modulate firing rate per se.[108] Studies of excitatory flow within motor cortex microcircuits has found that excitatory spread within cortical laminae is relatively weak whereas excitatory transmission between laminae, particularly from intratelencephalic neurons of layer 2/3 to the pyramidal tract neurons of layer 5, is comparatively strong.[109]

Debate over what kind of information is encoded by motor cortical cells persists even after half a century of ongoing investigation since initial incursions into the field.[110] These initial studies identified that pyramidal neurons in primary motor cortex modulate their firing during naturally-evoked upper limb movements. The field has since become replete with claims that the firing of pyramidal cells correlates with, and by implication, encodes, movement direction,[111] force,[112] speed,[113] acceleration[114] and position.[115] To complicate matters, evidence has come to light that the feature tuning of pyramidal neurons can be dynamically modulated throughout the evolution of a movement leading some to suggest that the firing rate represents more abstract parameters such as the intended goal or pattern of the resulting movement.[116]

Work using macroelectrode recordings of local field potentials generated by motor cortex has identified the beta range of oscillations as a promising candidate for PD pathology (see subsection 1.4 above for a more extensive treatment of beta oscillations in PD). Studies of STN have identified that levels of beta oscillations at this subcortical site correlate with bradykinesia and rigidity components of PD as recorded by the UPDRS-III scoring system.[13] Beta oscillations have come to prominence in the motor cortex as feature of motor cortex electrophysiology that is movement-modulated,[86] and suppressed bilaterally in sensorimotor cortices by unilateral DBS of the STN,[117] making them the subject of intensive research efforts. One such line of inquiry has focused upon the synchrony of beta oscillations across cortical areas and the relationship between this and the clinical features of PD.[118] Silberstein et al found that EEG recordings from PD patients showed correlations between the coherence in beta oscillations across scalp contacts and the clinical severity of PD. Moreover, the same study identified that the reduction in magnitude of coherence, as a result of either therapeutic DBS or levodopa treatment, was correlated with the improvement seen in clinical symptoms.[118] Such studies formed the

cornerstones of hypotheses that the underlying pathology of PD lay in the hypersynchronization of basal-ganglia-cortical loops particularly in the beta band.[119]

The motor cortex has shown some promise as a potential target for neuromodulation. Due to the superficial location, it is amenable to less invasive modulation approaches than the basal ganglia. Several candidates for neuromodulation of the motor cortex exist including repetitive transcranial magnetic stimulation (rTMS), transcranial direct current stimulation (tDCS) and optogenetic approaches.[120] All the foregoing techniques except optogenetic intervention involve macro-scale interventions in cortical function and without the ability to reliably target specific cell subtypes or populations. Optogenetics has the promise of a more targeted and precise approach to modulating circuit activity but carries with it significant concerns for use in humans and the barriers for entry into the clinic are significant.[121] Hurdles include, but are not limited to, immunogenicity of light sources, viral vectors and opsins (light activated ion channels) themselves as expressed transmembraneously by mammalian cells, many of which have proved problematic in the application of the technology to non-human primate models.[122]

Proof of principle has been obtained with rTMS in PD. Studies applying rTMS to the primary motor cortex of PD patients prior to movement have shown a 20% decrease in subsequent UPDRS-III scores compared to sham stimulation protocols and this effect was apparent for both primary motor cortex applications and SMA applications of rTMS.[123] Interestingly, application of rTMS to either hand or foot regions of primary motor cortex in this study (ventral or dorsal areas respectively) yielded improvement in the UPDRS-III scores attributed to both regions regardless. This could be due to spreading plasticity changes as result of rTMS application but may also be due to striatal release of dopamine, a phenomenon demonstrated to result from rTMS of primary motor cortex in PD patients.[124] Results from rTMS

studies have been somewhat inconclusive likely due to the widespread and relatively difficult to predict subcortical effects of cortical rTMS.[123] Results from experiments using tDCS have also been inconclusive with some studies suggesting a mild benefit from primary motor cortex tDCS in PD,[125] and others suggesting no benefit.[126]

The foregoing studies are among the reasons that some authors have been led to propose that PD symptoms, in particular bradykinesia and rigidity, arise as a result of hypersynchrony of beta oscillations in the basal-ganglia-cortical loop.[119] However such authors are also quick to point out that the relationship between the hypersynchronized beta oscillations and the parkinsonian symptoms is mainly correlative in nature and not causative. It could be, for example that hypersynchronized oscillations occur as a result, rather than a cause, of reduced movement seen in PD. Indeed, some studies have suggested that contrary to the model of hypersynchrony causing PD symptoms, deficits of action selection occur at an earlier stage of dopamine depletion and increased synchronicity of oscillations arises once dopamine depletion has progressed to a more severe pathophysiological stage.[127] We must bear in mind that the latter study is a modeling study with numerous assumptions underlying the characteristics of the basal-ganglia-cortical network, and the predictions of which have yet to be validated *ex silico*. One way in which the hypothesis of network hypersynchrony can be directly tested is through extrinsic synchronization of the network. Initial studies looking at the stimulation of the STN with beta oscillation frequency stimulation (10-20 Hz) trains have shown that exacerbates bradykinesia albeit to a moderate extent.[128, 129]

The foregoing literature leaves little room for doubt that the motor cortex is performing an important role in the execution of voluntary movements and strongly argues that beta oscillations occupy a prominent role within this cortical region. We have seen that the region

itself is densely interconnected with other cortical areas as well as deep brain structures however the role that the motor cortex plays as a site for the cortico-spinal projections of pyramidal neurons makes it an attractive area for study in any attempt to elucidate the underpinnings of voluntary movement in humans. For these reasons we elected to test our hypothesis of PD pathophysiology in the cortical oscillations of the motor and premotor cortices.

1.7 PD and DBS as a Research Model

The application of DBS to PD has resulted in an invaluable human research model permitting the study of a common neurodegenerative disorder in conscious behaving individuals. While conditions such as epilepsy and Montreal Procedure also permit the recording of local field potentials in humans, the situation in PD is relatively unique as it allows researchers to make perturbations to system using stimulation, and to measure the effects, both symptomatically and electrophysiologically, in real time. In this section we describe the PD/DBS research model and touch upon some of the insights it has yielded regarding the cortico-subcortical circuits of the basal ganglia. We will conclude the section with a brief discussion of the drawbacks of the PD/DBS model.

The effect of DBS on PD is often noted to be somewhat paradoxical according to standard theories of basal ganglia function[130] as ablation of the GPi and STN has similar symptomatic benefits to patients when compared with stimulation of the same areas.[131] It has been argued that this can be reconciled by viewing stimulation as a functional ablation of basal ganglia nuclei, replicating the effects of anatomical inactivation.[130] This hypothesis is challenged

by findings that suggest stimulation of basal ganglia nuclei at frequencies within the beta band can enhance bradykinesia,[129] and that stimulation of the GPi at higher therapeutic frequencies can enhance motor cortex excitability.[132] The use of optogenetic interventions in animal models has shown that inhibition of STN activity is alone insufficient to improve the movement symptomatology in mice treated with 6-OHDA to render them parkinsonian. Neither was driving the STN neurons at 20 Hz or 120 Hz sufficient to alleviate parkinsonian symptoms. Driving afferent axons originating in layer V of the motor cortex and projecting to the STN did, however, quickly reverse the motor impairment of 6-OHDA rats suggesting that DBS may be operating via modulation of inputs to the STN.[133] Indeed, studies of cortical excitability during STN stimulation suggest that DBS targeting of this nucleus increases motor cortex excitability in a manner distinct from GPi stimulation, raising the possibility that STN stimulation is exerting circuit level effects to enhance the frequency of afferent activity arising from the cortex.[134] These findings suggest that DBS could be eliciting a response above and beyond mere physiological ablation and that stimulation of different regions in the basal ganglia could be acting on distinct cortico-thalamic circuits to exert a therapeutic benefit.

The PD/DBS approach to researching basal ganglia function suffers from several limitations and challenges. First, and perhaps most significantly, DBS is usually only performed in individuals with advanced stage disease. Healthy individuals are not implanted with electrodes forcing us to compare the findings from PD brains with “controls” in the form of other neurological indications for DBS. Conditions used as controls are often essential tremor (ET) or dystonia, diseases that are expressed in the motor system but lack the dopamine-depleted state characteristic of PD. These conditions are themselves unlikely to represent normally functioning cortico-basal ganglia circuits. Second, although single-cell level studies have been conducted

intraoperatively,[135] the need to make recordings in conscious and acting individuals renders single-unit recording extremely challenging, resulting in a focus upon more stable population-scale recordings via local field potentials. Third, in the absence of post-mortem tractographic analysis, researchers rely on imaging-based measures of structural connectivity between nuclei or between deep brain structures and the cortex when ascertaining how electrode location might be influencing activity in remote structures.[136] Although this approach yields insightful findings, it is limited in terms of ascertaining directionality of tracts while inaccuracies in techniques determining precise anatomical electrode placement can limit the conclusions we are able to draw from such studies. Fourth, despite the fact that patients can be conscious during insertion of DBS leads and recording of LFPs, they are often drowsy from anesthesia given early in the procedure while gaining intracranial access. Acute "stun effects" from electrode insertion can also hamper interpretation of intraoperatively acquired recording results.[137] Fifth, the interpretation of the effects of stimulation is complicated by wash-in[138] and wash-out[139] effects of DBS. Wash-in refers to the delay observed between initiation of stimulation and the observable symptomatic benefit, whereas wash-out applies to the continued symptomatic benefit observed after cessation of stimulation.

In spite of these limitations, DBS for PD has been a hugely informative means by which to study the functioning of the basal ganglia and the relationships of neural oscillations over the network level. Indeed, the surgical procedure of implanting DBS leads is one of only a handful of medical procedures that offer the opportunity to study the electrophysiology of the human brain directly and in awake, behaving individuals. The objective of this research project is to use the opportunity afforded by DBS to gain direct access to the local field potentials generated by the human brain in order to build a more complete picture of electrophysiology of motor circuit

function and dysfunction. The approach detailed below will draw on many of the methods outlined in foregoing sections to test the hypothesis that PD is primarily a disorder of cortico-basal ganglia synchrony driving disordered beta bursting. Work referred to in the previous sections has led to an emphasis upon abnormalities of the beta band as a critical feature of the PD pathophysiology, and so it will be primarily this region of the frequency spectrum that the subsequent analyses will focus upon.

1.8 Phase-Amplitude Coupling in Parkinson Disease

Phase amplitude coupling (PAC) refers to the phenomenon whereby the amplitude of a high frequency oscillation is linked in a statistically significant manner to the phase of a lower frequency oscillation in the same signal.[140] The phenomenon is thought to assist in the coordination of high-frequency processing phenomena across large spatial and temporal scales.[141] PAC in the cortex has been found to vary in a task dependent manner,[44] and has been identified as abnormal in patients with schizophrenia[142] and PD,[26] and is reduced in the motor cortex by therapeutic DBS of both the STN[27] and the GPi[50]. Interestingly, beta to low gamma PAC in the pallidum correlates inversely with severity of PD bradykinesia and rigidity suggesting that it is a normal neurophysiological signal with disrupted levels in PD.[70] In support of this assertion, beta band PAC has also been observed to diminish during states of decreased consciousness[143] which may also indicate that it is an integral aspect of normal brain function. These findings may also support hypotheses identifying a role for PAC in binding the spatially large-scale and distributed low frequency oscillations with more locally generated fast

oscillations proposed to have a role in computation at the cortical level.[141] One such hypothesis proposes that long-range cortical communication is modulated by varying the gain of communication channels, with synchrony of low frequency oscillations in distinct cortical regions either facilitating or inhibiting communication between those regions.[61] The concept of communication through coherence has been developed and advocated by Fries et al[59] and has implicated in processes as diverse as attention and synaptic plasticity.[144]

Alternative hypotheses from Cole et al suggest that statistical PAC can be generated from the asymmetrical waveform shapes of low frequency oscillations[58] and in vivo studies have suggested that this does indeed take place in the human brain.[145] Furthermore, the studies by Vaz et al suggest that both forms of PAC, nested oscillations (correlations between independent oscillators) and sharp waveforms (sometimes referred to as 'spurious PAC'), occur in the human brain in a spatially distinct fashion and that increased PAC (of both varieties) is associated with poorer memory recall on a word pair task.[145] The latter suggests that PAC in word association tasks could be serving as a computational tamponade and that lower levels of PAC are required for accurate memory recall. Some authors have gone further in suggesting that PAC and disorders of PAC can account for age-related cognitive decline, depression and anxiety amongst a host of other neurological disorders. These results invite direct comparisons to research demonstrating increased PAC in the primary motor cortex of PD patients[26] and the suggestion that this phenomenon may represent an over-coupling pattern that inhibits cortical processing required for coordinated movement.[48]

The hypothesis tested here postulates a role for PAC in the tamponade of movement. Findings that beta bursting is prolonged in the basal ganglia nuclei of PD patients could fit well with a model of beta bursting as a state of high PAC acting as a computational tamponade on

processing in cortico-basal ganglia motor circuits. According to this model an analysis of beta bursting would be expected to show that there is a concentration of beta-phase to broadband gamma PAC in the motor cortex of PD patients and ET patients alike. It would thus be the extended duration of beta bursting that explained the pathological state of bradykinesia and rigidity manifested as part of the PD pathology.

Chapter 2. Methods

2.1 Cohort, Task, Recording Parameters

2.1.1 Cohort

DBS is most often undertaken to ameliorate the symptoms of PD or essential tremor (ET). ET is a common movement disorder of uncertain etiology in the majority of cases that is characterized by progressive and often severely debilitating postural and intention tremor of the limbs, typically the arms. While it has the element of tremor in common with PD it also stands as distinct from PD in that the tremor is a kinetic tremor, and is exacerbated by action. We took advantage of the differences between these pathologies to attempt to understand the electrophysiological changes peculiar to the parkinsonian symptomatology. Neurologically normal people do not undergo deep brain stimulation and so the optimal substitute as a control is a patient cohort showing little or no clinical overlap with PD. This study focuses upon the bradykinesia and rigidity components of PD in order to attempt to draw out the electrophysiological changes specific to PD. We used a total of 32 patients (10 ET patients and 22 PD patients) undergoing thalamic DBS in the case of ET and GPi/STN DBS in the case of PD. In our cohort all patients were selected on the basis of clinical need alone and provided written informed consent for research according to a standard protocol agreed with the UCLA Institutional Review Board.

The ages of the ET cohort were not normally distributed by Anderson Darling (AD) testing (AD test statistic = 0.81, p = 0.022). Accordingly, a non-parametric Mann Whitney U test was used to compare the ages of the PD and ET cohorts. There was no significant difference in the ages of the two cohorts (Mann-Whitney U test z-value = 0.77, p = 0.44). Table 1 details patient demographics. Our PD cohort included 4 tremor dominant individuals (subjects 13, 15, 20 and 30, see Table 1) and 18 akinetic-rigid individuals as defined by scoring systems published previously.[146]

Subject Number	Age (Years)	Sex (M/F)	Handedness (L/R)	Disease State	Implantation Site	UPDRS-III Score
1	76	M	R	ET	Bilat. Thal.	N/A
2	37	F	R	ET	Left Thal.	N/A
3	67	F	R	ET	Left Thal.	N/A
4	60	F	R	ET	Left Thal.	N/A
5	67	F	R	ET	Left Thal.	N/A
6	77	M	R	ET	Left Thal.	N/A
7	36	F	R	ET	Left Thal.	N/A
8	73	F	R	ET	Left Thal.	N/A
9	64	F	R	ET	Right Thal.	N/A
10	76	M	R	ET	Bilat. Thal.	N/A
11	78	F	R	PD	Bilat. GPi	16
12	65	M	R	PD	Bilat. GPi	16
13	63	M	R	PD	Bilat. GPi	51
14	76	F	R	PD	Bilat. GPi	29
15	72	M	R	PD	Bilat. GPi	54
16	67	F	R	PD	Bilat. GPi	42
17	58	M	R	PD	Bilat. GPi	72
18	57	M	R	PD	Bilat. GPi	6
19	60	M	R	PD	Bilat. GPi	23
20	70	M	L	PD	Bilat. GPi	42
21	61	F	R	PD	Bilat. GPi	37
22	71	F	R	PD	Bilat. GPi	9
23	57	F	R	PD	Bilat. GPi	32
24	64	F	R	PD	Bilat. GPi	34
25	61	M	R	PD	Right GPi	16
26	63	M	R	PD	Bilat. GPi	55
27	72	M	R	PD	Bilat. GPi	31
28	59	M	R	PD	Bilat. GPi	29
29	60	M	R	PD	Bilat. GPi	35
30	52	M	R	PD	Bilat. GPi	57
31	69	M	R	PD	Bilat. GPi	52
32	61	M	R	PD	Bilat. GPi	37

Table 1. Patient demographics.

2.1.2 Clinical Scores

UPDRS-III scores were collected preoperatively by trained individuals after at least 12 hours of PD medication withdrawal. Clinical scores used in this study were the contralateral upper limb rigidity score (UPDRS 3.3), or aggregated scores calculated by taking the sum of bradykinesia and rigidity scores for the upper limb contralateral to the ECoG strip (UPDRS 3.3-3.6), giving a limb-based measurement of bradykinesia/rigidity. We also employed a 'hemibody score' by aggregating the neck, upper and lower limb bradykinesia and rigidity scores for the contralateral limbs (UPDRS 3.3-3.7). Measures of PD symptomatology were correlated with mean burst duration for each subject using a non-parametric Spearman's rho test.

2.1.3 Task

We opted for a simple finger-tapping task to study the cortical electrophysiology of with PD. This was motivated both by methodological considerations and the necessity for a low-effort task that patients could complete easily in the intraoperative environment. One further advantage of our task is that the minimal cognitive planning in our task is likely to minimize the influence of higher order movement-planning related cognitive effects.

Patients were woken from anesthesia after burrholes had been formed in locations determined according to preoperative clinical stereotactic planning. DBS leads were sited either unilaterally or bilaterally and patients were allowed to recover from the anesthesia for a minimum of ten minutes before clinical testing of stimulation parameters was conducted with a clinical neurologist and technical team. Following DBS lead placement an ECoG strip was

inserted through the burrhole and passed subdurally with saline wash to cover the region of the precentral gyrus and central sulcus. Once satisfactory ECoG strip and lead placement was confirmed both physiologically and clinically, consent was once again obtained by verbal confirmation from the patient. Recordings were then conducted in a quiet resting state with eyes open and the operating neurosurgeon present at all times. Patients were recumbent on the operating table with their head fixed in a stereotactic frame. The operating surgeon provided verbal cues to initiate finger tapping with the hand contralateral to placement of the ECoG strip. Directions were given to maintain a constant rate of finger tapping until directed to cease. Rest and movement blocks were of 30 seconds each and patients were completed a minimum of 3 movement blocks (mean 4.6, standard deviation 1.4, range 3) and 4 rest blocks (mean 5.6, standard deviation 1.4, range 3). Stimulation experiments were also undertaken on patients in our experimental protocol however these are not included in the current analysis.

2.1.4 Recording Parameters and Electrode Locations

Recordings were made at a sampling rate of 2400Hz, bandpass filtered at 0.1Hz and 1000Hz using two designated recording g.USBamp2 amplifiers (GTech, Aus.) and stored using BCI2000 software. A single scalp reference was used for all electrodes. All analysis was performed offline using Matlab 2016a (Mathworks, Natick, MA) in conjunction with the Chronux toolbox. Statistical analysis was performed using Matlab's built-in Statistics and Machine Learning Toolbox.

Our final experimental setup involved two cortically located electrodes from which we obtained local field potential recordings. Both electrodes were sited anterior to the central sulcus, a readily identifiable anatomical landmark considered to delineate the boundary between primary sensory and primary motor cortices.[147] Recordings were obtained simultaneously from all electrodes on the subdurally located electrode strip and from the electrode contacts located on the DBS leads however only the electrodes considered to lie over primary motor cortex and premotor cortex were considered in the following analysis. In each subject these electrodes were identified using techniques detailed below. A schematic representation of our recording setup is shown in Figure 2 below.

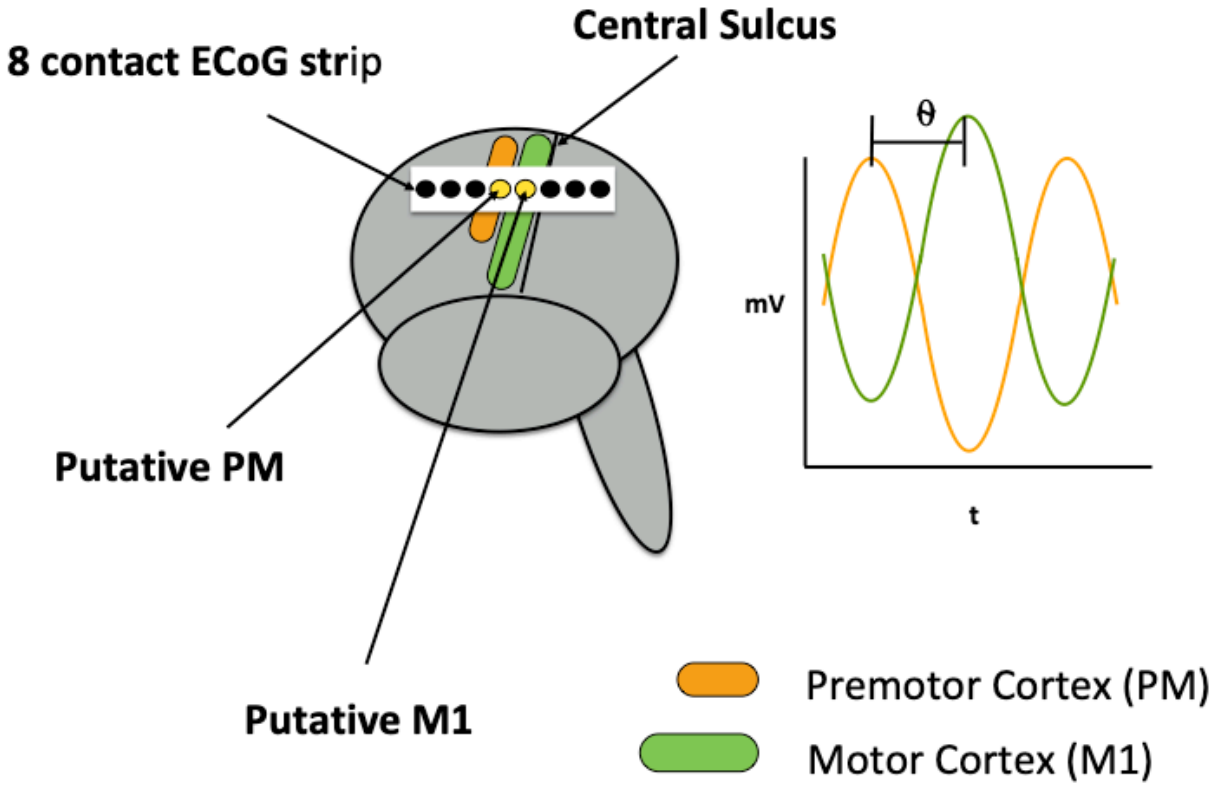

Figure 2. A schematic diagram of the recording setup.

The brain is represented here in grey. An 8 contact ECoG strip was passed through the burrhole to lie subdurally on the cortex. Offline analysis of the strip position was used to determine which contacts overlay the motor cortex (M1, here represented in green) and the premotor cortex (here represented in orange) based on the relationship of the electrode contacts to the central sulcus (straight black line). Recordings were made simultaneously of oscillations recorded from PM and M1 (graph to the right) from which information such as the phase angle difference (θ) could be extracted.

Electrode locations were determined post-operatively using preoperatively obtained MRI and CT, intra-operative fluoroscopy and postoperative CT using a technique described in depth previously.[148, 149] Briefly, the cortical surface was reconstructed using Freesurfer,[150] while OsiriX software was used to build a reconstruction of skull and stereotactic frame reference points.[151] DBS leads and ECoG contacts were then mapped onto the model manually using the intraoperative fluoroscopy and postoperative CT in a purpose-built Matlab GUI (see Figure 3, A and B). The first contact to be sited clearly anterior to the central sulcus was considered to lie over the primary motor cortex (M1), and premotor cortex (PM) was determined to be the contact immediately anterior to that.

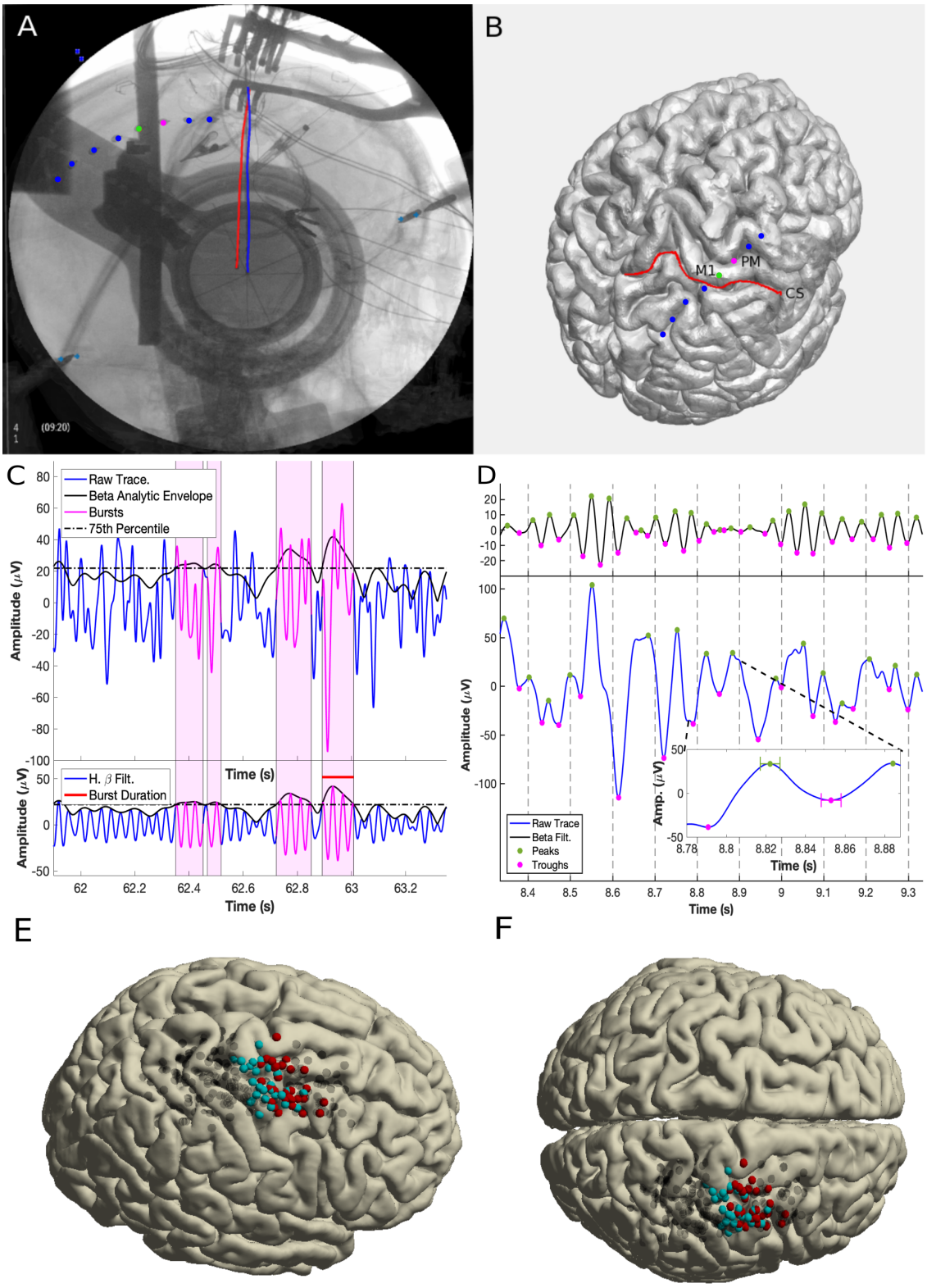

Figure 3. Electrode localization and analysis approaches.

A) Using postoperative CT and intraoperative fluoroscopy, the locations of the ECoG contacts (M1 = green dot, PM = magenta dot, blue dots = unused contacts) are mapped onto a reconstructed cortical surface as shown in panel B). The first contact immediately anterior to the central sulcus (CS, red line) was taken to be primary motor cortex (M1 = green dot) and the contact anterior to that was taken to be premotor cortex (PM = magenta dot). Blue dots indicate unused contacts on the ECoG strip. C) Raw trace from one subject (blue top trace), with the high β filtered trace below (blue bottom trace). Episodes of β bursting when the β analytic envelope exceeds the 75th percentile (black dotted line) are highlighted in magenta on both traces. Burst duration shown in red. D) Waveform analysis. Top black trace shows the filtered signal with green and magenta dots indicating peaks and troughs, respectively. The peaks and troughs are assigned to corresponding locations on the raw signal in the blue trace below. The inset shows a magnified segment of the trace with brackets at the peaks and troughs showing the points used for calculation of peak and trough sharpness measures. E) Lateral and F) superior view of electrode positions across the cohort (blue dots = M1, red dots = PM) projected onto a standard Montreal Neurological Institute (MNI) 3D cortical reconstruction. Electrodes not used in the analysis are faded grey dots. PM electrodes were 1cm anterior to the electrode labeled M1.

2.2 Analysis Approach

The approach to the data analysis was motivated by a desire to obtain accurate metrics for power, synchrony, waveform and PAC parameters. To this end it utilized measures that optimized the balance between noise reduction, frequency resolution and lack of bias. This section outlines the techniques used to quantify the parameters of interest and provides justification for the adopted approaches.

Throughout preprocessing and further analyses a monopolar configuration was maintained in order to preserve the phase of oscillations at spatially proximal sources and prevent possible subtraction of regionally widespread oscillations that may be relevant to our subsequent analysis. This choice may sacrifice a degree of spatial specificity compared to bipolar or common average reference montages as it fails to exclude global signals, however the advantage of preserving phase information was felt to be paramount for the analysis objectives of the experiments. A bipolar montage utilizes frequencies from two cortical contacts and subtracts one from the other whereas in a common average reference montage the 'average signal' taken across the entire array is subtracted from each electrode. Both these methods risk cross-contamination of signals peculiar to each electrode and as we are interested specifically in the interactions between precise cortical regions (M1 and PM) we felt that the cost of averaging would prove too high for our experimental ambitions.

The selected monopolar configuration has two drawbacks worthy of explicit consideration. Detailed below are the means by which analytic techniques have been employed to mitigate these drawbacks. The first disadvantage is that not using a common average reference makes our results susceptible to bias from environmental noise such as 60 Hz line noise. We

relied upon a three-pronged approach to tackle this important consideration. First, it filtered out sources of stable contamination such as the 60Hz line noise using a moving window to fit and subtract significant sine waves at the 60 Hz frequency (Chronux Toolbox, rmlinesmovingwinc, parameters: window = 3s, windowstep = 2s). Second, it utilized visual inspection of time-frequency spectra to attempt to remove regions of artifact-contaminated signal. Artifact was determined to be episodes of high amplitude activity that traversed a wide range of frequencies and was abrupt in both onset and termination. Five recordings underwent artifact removal, Subject 1 (1 episode of 25s), Subject 14 (5 episodes of 7-55s), Subject 23 (1 episode of 38s), Subject 30 (2 episodes of 5s), and Subject 31(2 episodes of 3-14s). A representative example is shown in Figure 4, A and B. Third, the experiments collected of large amounts of data from a large cohort on the assumption that noise effects would be transient and average out over longer durations of signal collection.

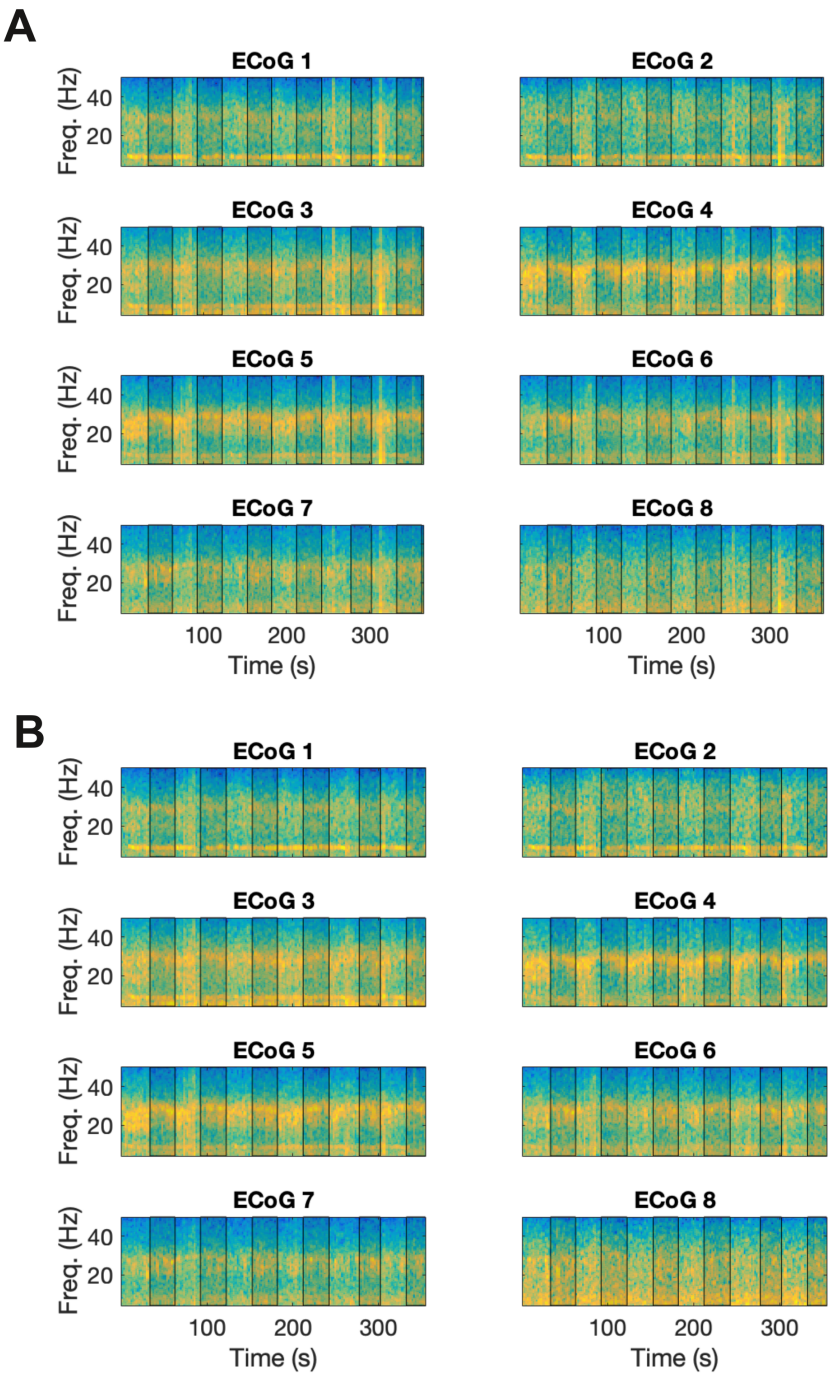

Figure 4. An example of artifact rejection.

Artifact removal for Subject 30. A) ECoG time-frequency spectra show widespread power increase episodes at 254-259 seconds and 310-315 seconds that are present in all electrodes

and span a wide range of frequencies. These were segmented from the time series. Shaded areas of the time-frequency spectra show movement episodes. B) The same time-frequency spectra with artifact removed.

2.3 Measuring Power

This study used two different approaches to calculate power spectra. Results did not differ significantly between the two methods. The first approach was to generate power spectra using Welch's estimate[152] using a 1 second window with zero overlap. Power spectra between 8-50 Hz were normalized using division of each frequency by the total sum of the power spectrum. This accounted for variation in the total power across individuals and provided for a more standardized comparison across the individuals. Powers calculated using Welch's estimate were used to compare power differences between predefined frequency bands.

The second approach to generating power spectra aimed to characterize oscillations in a manner that neutralizes assumptions inherent in the study of predefined frequency bands. The multitaper method uses orthogonal discrete prolate spheroidal sequences (DPSS) to generate estimates of the power spectrum. The approach holds the advantage of being well suited to unbiased exploratory testing of power spectra between groups of differing size using a jackknifing statistical approach.[153]

Defining regions of the signal with transient increases in high beta power ('beta bursts') required an instantaneous measure of power that could give a precise indication of when these transients begin and end. To achieve this the filter Hilbert approach was employed.[154] Periods of

beta bursting were identified by filtering each subject's data using a FIR filter (cutoff frequencies, low beta: 12-20 Hz, high beta: 21- 35 Hz), first high-pass and then low-pass. The analysis of the high beta band was chosen on the basis of previously published data showing that this motor cortical sub-band is modulated selectively by therapeutic DBS of the GPi.[50] These studies suggested that beta burst changes related to movement may be most pronounced within its frequency bracket. Analytical envelope was extracted using a Hilbert transform and bursting was defined as any period of oscillation amplitude that crossed the 75th percentile for that subject and persisted for at least 0.05 seconds, see Figure 2, C. For analysis of burst duration characteristics only, all episodes of amplitude crossing the 75th percentile threshold, even those of duration less than 0.05 seconds, were included as bursts. This approach closely replicates the methodology adopted by Tinkhauser et al in previous papers.[84] Periods of beta bursting in the raw signal were identified by indexing back to the unfiltered signal in subsequent analyses. This is an important step in the calculation of our waveform analysis parameters and will be covered in more depth in the following sections.

The rest vs. movement analysis sought to characterize in depth the changes affecting high beta bursts across conditions. Burst durations across the frequency spectra were calculated using the methods outlined above. The calculation of burst incidences used a similar approach of filtering each signal across the spectra (filter-Hilbert approach, filter width 5Hz centered on frequencies 4-40 Hz in 1 Hz steps). For burst incidence the total number of bursts during the rest or movement condition were identified and this was divided by the total amount of time for each condition to produce a burst-incidence spectra. Burst amplitudes were calculated as the area contained beneath the curve of each beta burst and the 75th percentile.

Testing the differences between power spectra during periods of rest and movement surrounding the time-points of movement initiation involved adopting a Monte-Carlo permutation based analysis. Movement initiation points were identified at the transition from resting state to moving state using custom made algorithms analyzing discreet Fourier transforms of piezoelectric glove measurements. 7 second periods prior to movement initiation were compared with 5 second periods after movement initiation. A time-segment of 'baseline' activity was defined as a 1 second interval from 7 through to 6 seconds prior to movement initiation (hereon referred to as -7 seconds through -6 seconds with 0 seconds being the point of movement onset). Logarithmically spaced wavelet analysis of the selected segments was performed to generate a time-frequency representation in methods previously described (Gaussian tapered 1 second wavelets with 38 logarithmically spaced interval frequencies between 5 and 45 Hz with cycle number increasing in 38 logarithmically spaced intervals from 3 to 10).[154] For completeness the wavelet formula is detailed in Formula 1 below.

$$Wavelet_f = \sqrt{\frac{1}{s_f\sqrt{\pi}} e^{2i\pi f t} e^{\frac{-t^2}{2s_f^2}}}, s_f = \frac{n}{2\pi f}$$

Equation 1. **Wavelet formula.**

Where f denotes frequency in Hz, t is the time-point of the wavelet (0-1 second at a sampling frequency of 2400Hz) and n is the number of cycles.

The time-frequency spectral analysis of the motor cortical signal surrounding time points of movement initiation is hereon referred to as the rest/movement time-frequency representation. Time-frequency representations were converted to decibels (dB) by dividing each frequency in

the time-frequency representation by the mean amplitude for that frequency taken from the first second of the signal (-7 seconds through -6 seconds time-points). Group level analyses were performed by taking the average over all movement initiation points for each cohort. To create a null distribution the group-averaged time series was shuffled 500 times around randomly assigned cut-points. Using these shuffled distributions, a z-map of the real data could be generated. Voxels on the z-map were thresholded at the $p < 0.05$ level and a cluster correction applied (by voxel size of clusters derived from 500 permutations), again at the $p < 0.05$ threshold. This approach has the advantage of being a data-driven discovery of time-frequency differences surrounding movement onset, which makes no assumptions about frequency bands, duration of power changes or effect size. Voxel and cluster-based corrections also hold the advantage of being less prone to Type II errors than multiple comparison corrections such as Bonferroni correction.

Statistical analysis of burst probability around movement onset used a binomial distribution with each episode of movement initiation treated as a single trial. The 7 seconds prior to movement onset and 5 seconds after movement onset constituted our time of interest as in the time-frequency analysis above. Our time period of interest was divided into 500 millisecond windows, 14 before and 10 following movement onset. In total the ET cohort had 44 episodes of movement onset (range 3-6) and the PD cohort had a total of 104 episodes of movement onset (range 3-7). The probability of a burst occurring in any 500 millisecond window was defined using the first two seconds of the pre-movement epoch (-7 to -5 seconds where t=0 is the onset of movement). Probability distributions were then calculated according to the number of bursts observed in each time period given our probability of a single burst occurring in a window in any individual trial. Binomial distributions were calculated using the Matlab function “binopdf” and

a family-wise error rate Bonferroni-Holm correction applied to correct for multiple comparisons.[155]

2.4 Measures of Synchrony

The term synchrony covers a broad array of phenomena in the electrophysiology and is used variously to refer to increases or decreases in power[83] or phase alignment between anatomically disparate oscillators.[156] For the following discourse we will be adopting a narrow definition of synchrony with regard to neural oscillations and will be using the term to refer exclusively to the phase synchronization of remotely placed oscillators. In this study synchrony was assessed using two distinct but related techniques, phase synchrony index (PSI) and debiased weighted phase lag index (dwPLI). These two techniques were chosen as both are purely phase-based measures of connectivity and thus relatively resistant to any confounding effects of amplitude that may be peculiar to episodes of bursting. Custom scripts were developed for the calculation of each synchrony measure. PSI was calculated according to standard techniques.[154] The formula for calculation of PSI is as follows:

$$PSI = \left| \frac{1}{N} \sum_{n=1}^{N} e^{i(\theta_{1n} - \theta_{2n})} \right|$$

Equation 2. **Formula for calculation of PSI.**

Where N is the length of samples over which the PSI is to be calculated, n is an individual sample in the set of N, and θ_1, and θ_2 are the phase angles in radians of signal 1 and 2 respectively.

As a purely phase-based measure of connectivity PSI is relatively invariant to the amplitude of the signal except in the complete absence of any signal.[154] This is an important feature for the present study being as it is concerned specifically with regions of the signal defined by their increased oscillatory power in particular frequency bands. Methods of assessing connectivity such as magnitude-squared coherence and imaginary coherence[157] both normalize using amplitude of the signal and thus constitute conflated approximations of oscillatory relationships. This conflation was considered to be overly detrimental given the present attempt to understand specifically how connectivity is modulated under conditions of high amplitude beta activity. Another significant advantage of PSI is that it is invariant with respect to the precise angle of phase alignment between two signals. PSI measures the extent to which phase differences between two signals cluster within the polar plane. We considered this feature of the measurement to be valuable for its assumption-free approach to identifying phase synchrony relationships.

The measurement obtained with dwPLI is similar to PSI but has two significant advantages and one relative drawback. First, as a purely phase based measure of connectivity it holds the same advantages as PSI for our paradigm, however; dwPLI provides an assessment of the extent to which phase relationships occupy a consistent phase-lead or phase lag relationship. Second, the measure is weighted meaning that not all phase angles contribute equally to the overall score. Weighting allocates greater influence to phase relationships that deviate from the real axis with greater deviations having a greater influence on the overall score. This advantage comes with the

relative expense that clustering around the 0 or π phase angle regions of the polar plane are disregarded and in fact a completely uniform clustering at either one of these angles would register as a zero dwPLI relationship. This is a significant price for the present paradigm where there is a particular interest in closely aligned phase relationships such as those described and constitutes a major reason why the complementary dwPLI and PSI measures were both employed.

The dwPLI was also calculated according to standard techniques outlined in previous publications.[158] The formula used is provided below, notation is identical to that of Formula 1 and 'imag' refers to the imaginary component of the figure contained within the brackets:

$$dwPLI = \frac{\sum_{n=1}^{N} imag(e^{i(\theta_{1n}-\theta_{2n})}) - \left(\sum_{n=1}^{N} imag\left(e^{i(\theta_{1n}-\theta_{2n})}\right)\right)^2}{|\sum_{n=1}^{N} imag(e^{i(\theta_{1n}-\theta_{2n})})| - (\sum_{n=1}^{N} imag(e^{i(\theta_{1n}-\theta_{2n})}))^2}$$

Equation 3. Formula for calculation of dwPLI.

This study compared the synchrony during bursting with the period immediately prior to bursting by calculating PSI/dwPLI over the duration of the burst (period in which the amplitude exceeded the 75th percentile of the amplitudes during rest) and a period of matched duration immediately prior to the burst. Bursts in which the pre-burst matched window overlapped with a previous burst were excluded from the analysis in order to ensure that our pre-burst episodes contained only non-burst epochs of the time series. To further explore trial-averaged synchrony (PSI and dwPLI) during bursting onset, the dwPLI and PSI was calculated across temporally aligned burst onsets for each subject. The time-evolving synchrony at the onset of each burst could thus be plotted alongside trial-averaged normalized power. Maximum values of the first

derivatives for each subject's curve were calculated and the time of peak first derivative relative to burst onset was calculated for each subject. To provide assurance that the measures of synchrony increase were not solely due to the threshold adopted (point of maximum derivative) a second pass analysis used an alternative measure as verification. For each subject the mean across the pre-burst and burst period (-50 milliseconds and +50 milliseconds with respect to burst onset at 0 milliseconds) was taken. The time point at which this mean was met or exceeded constituted the alternative threshold.

In order to test whether increased synchrony was merely a result of increasing amplitude during beta bursts, our second pass analysis generated synthetic signals with no inherent synchrony between signals. This approach allowed the exploration of how, if at all, low amplitudes and transient increases in amplitude (as in beta bursting) might compromise synchrony measurements. To perform this *in silico* analysis 400 synthetic signals of 10 seconds duration were generated using sine waves with frequencies in the 1-20 Hz, 21-35 Hz, 36-50 Hz, and 51-150 Hz ranges. Each signal was composed of the 20 sine waves (5 from each of the four frequency bands) randomly selected from the frequency bands. Each sine wave was modified with noise (a vector of randomly generated values on the open interval [0, 0.05]), a randomized phase shift and a direct current offset of -0.5 arbitrary units (a.u.). All other signal parameters and analysis (sampling rate, filter parameters and PSI calculations) were identical to those used in the *in vivo* analysis. Testing was performed upon 200 pairs of signals generated in the above manner. Only one of the signal amplitudes was modulated as the *in vivo* analysis was concerned with episodes of bursting only at the motor cortex (irrespective of amplitudes at the 'premotor' cortex). Signal 2 was thus modulated by taking the dot product of the raw synthetically generated signal with a Gaussian kernel of equal length having 1 at the zenith, a mean of 5 seconds and a

standard deviation of 0.5 seconds. This produced a signal that varied in amplitude over the course of 10 seconds from near zero amplitude to equal amplitude with Signal 1, before decreasing again to near zero amplitude at the end of the 10 seconds. Maximal PSI levels for each iteration were defined as the mean PSI within +/- 0.5s (+/- 1 standard deviation), of the maximal amplitude at the 5 second point in the signal. The time point of synchrony increase (synchrony onset) was defined as the point at which PSI levels between Signal 1 and Signal 2 reached or exceeded the maximal amplitude threshold, the time point of synchrony decrease (synchrony offset) was defined as the time at which synchrony dropped below this level.

In order to test the statistical significance of synchrony changes at the time point of movement initiation this study adopted an approach similar to the analysis of power at the time of movement onset (see preceding section 2.3). The time point of movement onset for each episode of movement was identified for each subject in the ET and PD cohorts. A 12 second window of the raw time-series centered on the time of movement onset was extracted. In total 44 episodes of movement were extracted for the ET cohort and a total of 104 episodes of movement were extracted for the PD cohort. Wavelet analysis was performed on the signal for both motor and premotor cortices using identical parameters to the power analysis (20 logarithmically spaced frequencies between 5 Hz and 45 Hz, Gaussian complex wavelet of length 1 second). Phase information was extracted from the results of the convolution and the PSI was calculated for each movement episode using a 1 second moving window convolved with the angle difference across motor and premotor cortices for each frequency. A 1 second epoch was removed from -6 through -5 and 5 through 6 seconds of the results of the analysis to exclude edge artifacts from the wavelet analysis and PSI convolutions. Statistical significance was determined using a Monte-Carlo permutation analysis for voxels and clusters. For each frequency in turn feature

scaling was achieved by dividing the PSI by the sum of the PSI for that episode. A formula for this normalization is included below.

$$x_{i,f} = \frac{x_{i,f}}{\sum_N^i x_{i,f}}$$

Equation 4. **Normalization of PSI over time.**

Where x is the PSI at any time point, i, and frequency f. Data for each cohort was randomly shuffled 500 times to generate a null hypothesis distribution of PSI values. Z-values were calculated for the unshuffled distribution and a 5% significance level was applied as a threshold first for voxels and then subsequently for clusters. This analysis approach was adapted from approaches described elsewhere.[154]

2.5 Waveform Analysis

Waveform analysis is a constantly evolving field and attempts to characterize the non-sinusoidal features of neural oscillations have been made previously.[159] Here only minor modifications to the procedure adopted by Cole et al have been made and the methodology is illustrated in Figure 3, D, above. First the present approach used a finite impulse response (FIR) filter to bandpass filter the signal (high beta: 21- 35 Hz) and identify the zero crossings corresponding to peaks and troughs. In the raw signal peaks corresponded to the extrema of the signal between two troughs identified in the filtered signal, likewise, troughs were the extrema of

the raw signal between two peaks in the filtered signal. To constitute a valid peak or trough the extrema had to be accompanied by a net positive gradient 0.002 seconds before the peak and a net negative gradient 0.002 seconds after the peak. Likewise, troughs were only defined in regions of the raw trace where a negative gradient preceded the trough for 0.002 seconds and a positive gradient followed the trough for 0.002 seconds. Figure 3, D shows a representative sample of the waveform analysis illustrating where peaks and troughs fall on the raw signal with the high beta and high beta analytic envelope superimposed. Sharpness and steepness values were calculated according to Formulas 5 and 6 respectively. Peak sharpness was defined as:

$$P_{Sharp,n} = \left| \frac{(Peak_t - Peak_{t-0.005}) + (Peak_t - Peak_{t+0.005})}{2} \right|$$

Equation 5. Calculation of peak sharpness.

Where $P_{Sharp,n}$ is the sharpness of the n^{th} peak, $Peak_t$ is the absolute vaule of the raw trace at the extrema of the peak, $Peak_{t-0.005}$ is the absolute value of the trace 0.005 seconds before the peak, $Peak_{t+0.005}$ is the absolute value of the raw trace 0.005 seconds after the peak. Trough sharpness was calculated in a directly analogous fashion using points 0.005 seconds before and after the trough.

Steepness is intended to measure the rapidity with which the extrema of a peak or trough is reached from the previous extrema. We took this to be the maximum or minimum of the

difference between adjacent samples calculated over the raw data between troughs and peaks. The formula is given below:

$$Steepness_{Rising} = max\left(\left|V_{(t+1)} - V_t\right|, t_{Trough} \leq t \leq t_{peak}\right)$$

Equation 6. Calculation of rising steepness.

A similar equation defined falling steepness.

Several approaches to normalizing steepness and sharpness to account for amplitude changes were considered. This was felt to be necessary to compare directly the measures of waveform shape during bursting and non-bursting episodes, that is to say, across periods of different amplitudes. All of the approaches considered suffered from pitfalls. The first technique proposed to normalize sharpness and steepness values by the amplitude of deflection immediately before the peak or trough in question. Falling steepness scores would be normalized by the amplitude deflection of the falling slope. While intuitively appealing because it would directly compensate for increased excursions during amplitude increases and decreases, this compensation would take the form of a linear correction. Neither sharpness measures nor steepness measures will necessarily change in a linear fashion with changes in amplitude, however. On the contrary, simple Euclidean geometry suggests that there are *a priori* reasons to beleive that sharpness and steepness will change in a non-linear manner as amplitudes increase just as the angle at the apex of an isosceles triangle does not increase linearly with increasing leg length.

For the reasons outlined above the analysis used a ratio to characterize steepness and sharpness across bursting and non-bursting conditions. The approach was pioneered by Cole et al and operates by taking the ratio of peak to trough sharpness.[58] In this manner increases in peak sharpness are negated when accompanied by increases in trough sharpness of the same or similar magnitude. Likewise, rising to falling steepness is taken as a ratio for each condition. Thus the ratio measure is particularly sensitive to asymmetrical changes in peak sharpness without accompanying changes in trough sharpness or *vice versa*. Practically speaking this approach makes no attempt to provide a ratio for individual waveforms but instead takes the average peak sharpness for a condition and divides this by the average trough sharpness for a particular condition. Formula 7 details the method for generation of sharpness ratios. A similar operation generates rising to falling sharpness ratios and is detailed in Formula 8 below.

$$Sharpness\ Ratio = \frac{(\sum_{N}^{1} Peak_N)N^{-1}}{(\sum_{K}^{1} Trough_K)K^{-1}}$$

Equation 7. Calculation of sharpness ratios.

$$Steepnss\ Ratio = \frac{(\sum_{N}^{1} Rising_N)N^{-1}}{(\sum_{K}^{1} Falling_K)K^{-1}}$$

Equation 8. Calculation of steepness ratios.

One weakness, which is apparent with this approach, is the fact that it neglects the cycle-by-cycle variability of oscillations in order to generate a ratio across a whole condition. While this corrects for instantaneous changes in amplitude it in one sense collapses waveform measurements over time into a single measurement in a manner reminiscent of a temporally invariant analysis such as Fourier analysis. One compromise between the amplitude normalization and the ratio method may take the form of a cycle-by-cycle ratio taken between adjacent peaks and troughs and adjacent rising and falling phases. This analysis adopted a single-figure approach in order to relate waveform shifts across the entire recording with features such as the clinical status of patients and the degree of PAC observed on a subject-specific level.

In order to study the effects of movement initiation on waveform shape this analysis adopted the above methodology of waveform quantification and applied it to the time series surrounding the point of hand movement onset as determined by piezoelectric sensors from the hand glove. The time series from 5 seconds prior to movement onset to 5 seconds after movement onset was extracted. Episodes of bursting within that region were identified and sorted into 500 msec bins. Peaks occurring within burst periods were considered together with their corresponding troughs, rising and falling phases. Data for a single burst were assigned to a time bin at movement onset if the peak amplitude of that burst fell within the time bin. Peak:trough ratios together with rising:falling ratios were calculated for each burst individually and the values assigned to one of the twenty, 0.5 second bins, spanning the 10 second movement onset epoch described above. Waveform morphology ratios were averaged with subject level medians for each time bin prior to taking group-level medians. Statistical testing was performed on the median values of waveform shape for each subject. Where no burst peak occurred for a subject in a particular time bin this value was ignored for the group level analysis. This process allowed for the mapping of

waveform morphology evolution over time as movement initiation takes place. Statistical testing was accomplished by comparison with baseline values obtained at -7 seconds to -5 seconds prior to movement onset.

2.6 Phase-Amplitude Coupling Analysis

Phase-amplitude coupling seeks to reveal physiological relationships between neural oscillations concentrated in distinct frequency bands. Such relationships between frequency bands have been used to gain insight into the neuropathologies underlying conditions such as PD in the cortex,[26] and subcortical structures.[160] It has also been proposed to play a role in disorders as diverse as autism,[161] schizophrenia[162] and social anxiety disorder.[163] As a relatively novel method for uncovering neurophysiological mechanisms, the use of PAC in neuroscience has proliferated and expanded with few justifications for parameters used to establish cross-frequency correlation relationships. Aru et al address some of the methodological concerns in PAC in a review aimed at dealing with some of the common methodological pitfalls encountered in PAC studies.[140] One concern addressed is the choice of bandwidths used to calculate the low (f1) and high (f2) frequency components of the PAC relationship.

Aru et al point out that many studies either scan through a frequency band taking sub-bands of fixed width (often ~2Hz) and relate the f1 or phase component to the f2 or amplitude component similarly determined by scanning through a band with sub-bands of fixed widths (often ~5Hz). It is important to realize that a signal composed of two distinct frequencies can be decomposed into two mathematically equivalent representations. Thus, we have:

1)

$$x(t) = \big(1 + \cos(2\pi f_1 t)\big) sin(2\pi f_2 t) + sin(2\pi f_1 t)$$

2)

$$x(t) = \sin(2\pi f_2 t) + cos(2\pi f_1 t)\sin(2\pi f_2 t) + sin(2\pi f_1 t)$$

$$= \sin(2\pi f_2 t) + {}^{1}/_{2}\left(\sin(2\pi(f_2 - f_1)t) + \sin(2\pi(f_2 + f_1)t)\right) + sin(2\pi f_1 t)$$

Equation 9. **Equivalent decompositions of a signal composed of two frequencies.**

Where f1 and f2 are our filtered low and high frequency bands respectively and x(t) is the composite signal. The second decomposition demonstrates that a significant amount of the modulating effect of f1 is contained in a band of width 2Δf1 that is centered on the f2 frequency. Failure to scan bands of reduced width can lead to a failure to detect PAC. For this reason we selected f2 frequency bands that increased as a function of the f1 frequency such that Δf2 = 2f1.

Aru et al also point out some interesting interpretative issues in the study of PAC. They suggest that the term cross-frequency correlation is a more appropriate term for PAC relationships. This is because the association between changes in the phase of an f1 band and the amplitude of an f2 band can be due to a third driver having an effect on both signals. The term 'correlation' makes this possibility clear and aids in restraint when interpreting positive findings. One neurophysiologically relevant example of a third driver could take the form of axonal inputs

to a cortical area that have the effect of simultaneously resetting the phase of beta oscillations and prompting an increase in local neuronal cortical firing (resulting in an increased gamma amplitude). Such a scenario would result in consistent f1 phase and f2 amplitude relationships, and hence yield positive PAC findings, even though f1 phase is not directly modulating f2 amplitude. By outlining this scenario Aru et al do not render PAC an unintelligible phenomenon but rather broaden our scope of interpretation when we uncover PAC relationships. We are able as a result, to conceive of PAC as either a local process occurring between neural oscillations within a restricted cortical location, or as an indicator of an input process to that cortical region. Interventions in the form of stimulation could potentially resolve this ambiguity. Indeed, studies looking at the application of 20Hz transcranial alternating current stimulation (tACS) to the motor cortex have demonstrated slowing of movements in the contralateral hand.[164] This would be the expected result if PAC in motor cortex is a local phenomenon and the f1 phase is indeed modulating the f2 amplitude. In the 'third driver' scenario where f1 phase and f2 amplitude are incidentally related this experimental effect would not be observed.

In the forthcoming analyses PAC was calculated according to methods described in detail previously.[136] Here in brief, we used Tort's method to calculate the Modulation Index[165] and parameterized with reference to previous PAC analyses.[166] Data was filtered using FIR filtering (high-pass then low-pass) at frequencies 8-35 Hz in 2 Hz steps with a 5Hz bandwidth for phase and 40-200 Hz in 5 Hz steps with a 5Hz bandwidth for amplitude. We then extracted phases and amplitudes using Hilbert transforms on our phase and amplitude encoding signals respectively. 12 bins of 30° width were used to categorize phase and derive phase-amplitude histograms. After filtering, the phase and amplitude segments of the signals were sorted into burst and non-burst segments. Tort's entropy was calculated over these segments by shuffling the phase component

of the signal 500 times to create surrogate data. The raw MI significance threshold was set at 1.96 standard deviations above the mean MI calculated over the surrogate data. This significance level corresponds to an increased PAC that meets or exceeds the $p = 0.025$ significance level. PAC results were compared in the low and high β bands by calculating a mean MI for each subject over frequency ranges 12-20 Hz (low β) and 20-35 Hz (high β) phase encoding frequencies with 50-200 Hz amplitude encoding frequencies for both bands as used in previous studies.[26] Mean values of MI were compared using a Mann-Whitney U test for differences between cohorts and to compare bursting and non-bursting conditions within each cohort.

Chapter 3. Parameterizing High Beta Bursting at Rest

3.1 Resting Power

This study conducted an analysis of resting power spectra in the ET and PD cohorts to test the hypothesis that PD shows not only increased beta power at rest as has been previously reported,[167] but that this difference is accompanied by increases in the duration of beta bursts in the motor cortex. Analysis of resting data will also provide a baseline for subsequent comparison with data acquired during movement. Correlation with clinical scores attempts to draw a relationship between disordered beta bursting and the expression of parkinsonian symptomatology.

Spectral power analyses confirm prior findings of increased resting high beta power in PD compared to ET subjects (mean ET high beta power = -20.99, 95% CI +/- 1.53, mean PD high beta power = -17.45, 95% CI +/- 0.67, two tailed t-test, $t = -2.33$, $p = 7.6 \times 10^{-6}$, see Figure 5, A). Increased high beta power in the PD cohort was mirrored by increased burst duration for PD compared to ET in the high β band. Anderson-Darling tests of normality found that the burst duration data for the Parkinson disease cohort was not normally distributed (test statistic = 0.87, $p = 0.021$) and so non-parametric testing was therefore used to compare the cohorts (mean high β burst duration Essential Tremor = 143.24 msecs, +/- 8.20, mean high β burst duration for Parkinson disease = 156.34 msec, +/-7.40, Mann-Whitney U test z-value = -2.38, $p = 0.017$, see Figure 5, B).

To further characterize differences in high beta burst duration between the cohorts, we calculated the distributions of burst durations. A preliminary two-sample KS test showed that the burst duration distributions differed significantly between the two groups (two sampled KS test, KS value = 0.18, p = 0.001, see Figure 5, C). We then modeled high β burst durations using a log logistic distribution for each subject to characterize further the differences between the cohorts. This distribution was selected as it is suitable for continuous, non-negative data with positive skew. Burst analysis closely parallels common applications of this distribution in survival and time-to-failure analyses. In this distribution fit μ values (normally the logarithm of the distribution mean) have been transformed by taking the exponential so that they represent the mean of the fitted distribution in milliseconds. Sigma values (σ, the scale parameter of the log logistic distribution) represent the concentration of burst durations either closer to zero (low σ values) or further from zero (high σ values). Fitting of the log logistic distribution for the population yielded a Log Likelihood of -75376.8, estimated μ = 5.21, S.E. = 0.007, estimated σ = 0.457, S.E. = 0.0035. Both the μ and σ values differed for Essential Tremor and Parkinson disease (mean μ Essential Tremor = 88.5 msec, 95% CI +/- 2.03 msec, mean μ value Parkinson disease = 108.4, 95% CI +/- 2.1, Mann-Whitney U z-value = -2.70, p = 0.007, see Figure 5, C, inset. Mean σ for Essential Tremor = 0.42, 95% CI +/- 0.017, mean σ for Parkinson disease = 0.47, 95% CI +/- 0.018, AD test statistic = 1.26, p = 0.002, Mann-Whitney U test z-value = -3.27, p = 0.001) suggesting that the Parkinson disease cohort had a tendency to stay in high β bursts for greater durations compared to the Essential Tremor cohort (increased μ) and that increased mean burst duration was due to a shift towards increased frequencies of higher duration bursts rather than occasional more extreme values (increased σ).

Finally, we compared the μ values (derived from log-logistic fitting) for each subject in the cohort with the contralateral upper extremity aggregate bradykinesia and rigidity score on the UPDRS-III. This showed a positive relationship between ratings of Parkinson disease symptomatology and burst duration (μ) at rest (Bonferroni corrected $p = 0.029$, Spearman's $r = 0.45$, see Figure 5, D). Here we highlight the relationship between μ and aggregated contralateral upper limb rigidity/bradykinesia because our ECoG placement targeted the more medially placed arm area of M1. In total we compared μ with three different measures of hemi-body UPDRS-III scores, all of which showed a trend towards a positive correlation and two of which survived Bonferroni correction. Comparison of high β burst duration (μ) with aggregated hemibody (upper and lower limb) rigidity/bradykinesia scores also revealed a significant positive correlation (Bonferroni corrected $p = 0.048$, Spearman's $r = 0.42$, see Figure 5, E). Our μ scores showed a trend towards positive correlation with rigidity alone (UPDRS-III section 3.3), however this third correlation did not survive Bonferroni correction (Bonferroni corrected $p = 0.054$, spearman's $r = 0.42$, see Figure 5, F).

Mean beta burst duration correlates with clinical scores of symptomatology. This finding is worthy of note as it illustrates that the clinically observable features of PD can be related in a meaningful manner to the fine temporal structure of neural oscillations in the beta band. When placed in the context of altered beta burst distributions in PD, as shown above, a general picture emerges of subtle disturbances in the electrophysiology that could potentially underlie the symptomatology of the disease in question. Subsequent analyses were directed towards outlining a plausible mechanism whereby this might occur and gathering evidence to further support this hypothesis.

High beta power increases in PD compared with ET could be a result of increased duration of beta bursts. This poses at least two significant questions; first, what is driving increases in beta burst duration? This question is of obvious interest as answers to it might provide novel means to interrupt the pathological processes that underlie PD, potentially leading to novel therapies for the condition. Second, if protracted beta bursting can be held responsible for the symptomatic expression of PD then what is the mechanism by which this occurs? This line of thought was suggested by multiple strands of research linking beta oscillations to disorders of movement[130,168,169] combined with evidence suggesting that waveform changes[58] and PAC[26] could be playing important roles in the pathogenesis of movement disorders.

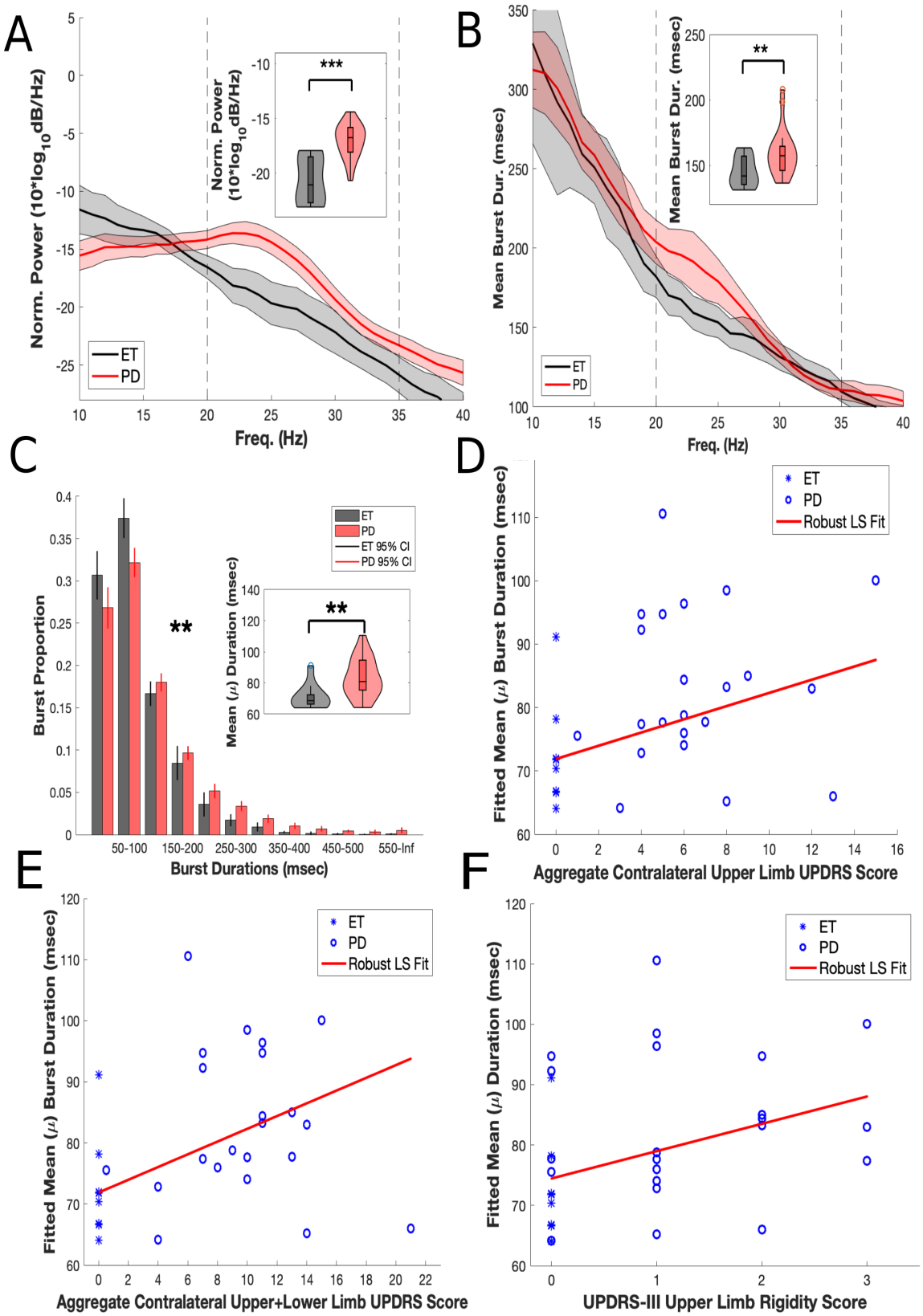

Figure 5. Power spectra comparisons, burst durations and clinical correlations.

A) Power spectral comparisons show that Parkinson disease has a higher resting power in the high beta band compared to Essential Tremor. High beta band demarked by black broken lines and statistical comparisons by cohort of average high beta powers shown in inset. B) The same region of the power spectrum (high beta) also demonstrates higher average beta burst duration. Statistical comparison of cohort mean high beta burst durations shown in inset. C) For each subject the distribution of high beta burst durations can be represented as a log-logistic distribution, where mean cohort distributions are plotted in black (Essential Tremor) and red (Parkinson disease). Fitting a mu value (mean duration) to the distribution allows us to compare the duration of high beta bursting directly across cohorts. Parkinson disease shows a more rightward skew in their distribution when compared with Essential Tremor (higher sigma values, main plot). The inset demonstrates that the parameterized distributions for each cohort (mu values) also differ between the two groups with the Parkinson disease cohort having a higher mean mu value compared to Essential Tremor. D-F) Correlations between mu and three UPDRS-III scores. A total of three different μ/UPDRS-III comparisons were corrected for using the Bonferroni method (D-F). D) Mean high beta burst duration (mu) correlates with severity of Parkinson disease as quantified by the aggregate UPDRS-III contralateral upper limb score (the sum of rigidity and bradykinesia scores for the contralateral upper limb only) and survived Bonferroni correction. E) mu showed a positive correlation with aggregate contralateral hemibody (arm and leg combined) bradykinesia/rigidity scores ($p = 0.016$, $r = 0.42$) which survived Bonferroni correction. F) Although there was a positive correlation between μ and rigidity score for the contralateral upper limb it did not survive Bonferroni correction ($p= 0.018$, $r = 0.42$).

3.2 Power and Synchrony Relationships at Rest

In this section we detail the outcome of our investigations into the phenomenon of beta transients and their relationship to cortico-cortical synchrony. We will show how synchrony and bursting relate to each other on a fine temporal scale and investigate several possible explanations for our findings. Finally, we will relate our results to the current literature in order to clarify the interpretation of these phenomena in the context of the resting motor cortex.

All PSI values met the Anderson-Darling test criteria for normality (all p-values >0.09) and so comparisons were performed using t-tests. Before beta bursting, the PD cohort demonstrates greater M1-premotor PSI compared to the ET cohort (mean pre-burst PSI for ET = 0.7, 95% CI +/-0.027, mean pre-burst PSI for PD = 0.76, 95% CI +/- 0.027, p = 0.0032, see Figure 6, A). In both groups, PSI increased during bursts (mean pre-burst PSI ET = 0.69, 95% CI +/- 0.03, mean burst PSI ET = 0.86, 95% CI +/-0.038, $p = 1.4x10^{-8}$; mean pre-burst PSI PD = 0.76, 95% CI +/- 0.03, mean burst PSI PD = 0.91, 95% CI +/- 0.02, $p = 3.3x10^{-16}$), but most importantly PSI did not differ between the groups during bursts (ET burst PSI mean = 0.86, 95% CI +/- 0.04, PD burst PSI mean = 0.91, 95% CI +/- 0.02, p = 0.23). The pattern of results for dwPLI closely paralleled those for PSI as shown in Table 2, below and graphically depicted in the Figure 6, B.

Comparison	PSI		dwPLI	
	Means (95% CIs)	P-value (Critical p)	Means (95% CI)	P-value (Critical p)
ET pre-burst cf. ET burst	0.69 (+/- 0.03), 0.86 (+/- 0.04)	$1.4x10^{-8}$ (0.0125)	0.50 (+/- 0.02), 0.70 (+/- 0.02)	$9.3x10^{-8}$ (0.0125)
PD pre-burst cf. PD burst	0.76 (+/- 0.03), 0.91 (+/- 0.02)	$3.3x10^{-16}$ (0.0125)	0.55 (+/- 0.02), 0.72 (+/- 0.02)	$1.6x10^{-13}$ (0.0125)
ET pre-burst cf. PD pre-burst	0.69 (+/- 0.03), 0.76 (+/- 0.03),	0.0032 (0.0125)	0.50 (+/- 0.02), 0.55 (+/- 0.02)	0.011 (0.0125)
ET burst cf. PD burst	0.86 (+/- 0.04), 0.91 (+/- 0.02)	0.023 (0.0125)	0.70 (+/- 0.02), 0.72 (+/- 0.02)	0.38 (0.0125)

Note: Critical p-values are corrected for multiple comparisons using the Bonferroni method. Comparisons that meet or exceed the critical p-value are shaded yellow.

Table 2. Statistical comparisons of burst and pre-burst synchrony.

It has been shown that phase synchrony can precede power increases by several milliseconds.[170] Evaluation of the time point of maximum gradient of power and synchrony increases relative to burst onset attempted to discern whether synchrony increases were pre-emptory of beta bursts (see Figure 6, C-E). The results presented here show that the time point of maximal rate of increase in pre-burst synchrony (for both PSI and dwPLI) preceded the time point of maximum rate of power increase (both measured relative to bursting onset, denoted as time 0). Of the three measures compared (PSI, dwPLI and power), PSI showed the earliest increase (-20.7 msecs, 95% CI +/- 4.1 msecs, $p = 5.3x10^{-11}$, Figure 6, C and E), with dwPLI

increasing maximally shortly after PSI and also showing significant anticipation of power increases (mean time of greatest dwPLI increase = -14.2 msecs, 95% CI +/- 5.6 msecs, $p = 3.7x10^{-4}$, mean time of greatest power increase = -3.2 msecs, 95% CI +/- 1.9 msecs, Figure 6, E). Thus, for PSI which shows the earliest rise in synchrony, there is a temporal lead with reference to maximal power increase of -20.7 msec - (-3.2 msec) = -17.5 msec preceding power increase. The temporal precedence of synchrony increases anticipating power increases suggests that these findings could reflect a causal relationship with inter-regional (PM-M1) synchrony increases causing increases in locally measured oscillatory power at M1.

If synchrony is a causal mechanism for transient increases in power, and transient power increases in turn have an inhibitory effect on movement, one would expect burst synchrony to correlate with clinical scores of rigidity/bradykinesia. Average PSI during bursts was positively correlated with contralateral upper limb bradykinesia/rigidity scores across all subjects (Spearman's $r = 0.61$, $p = 1.9x10^{-4}$, see Figure 6, F).

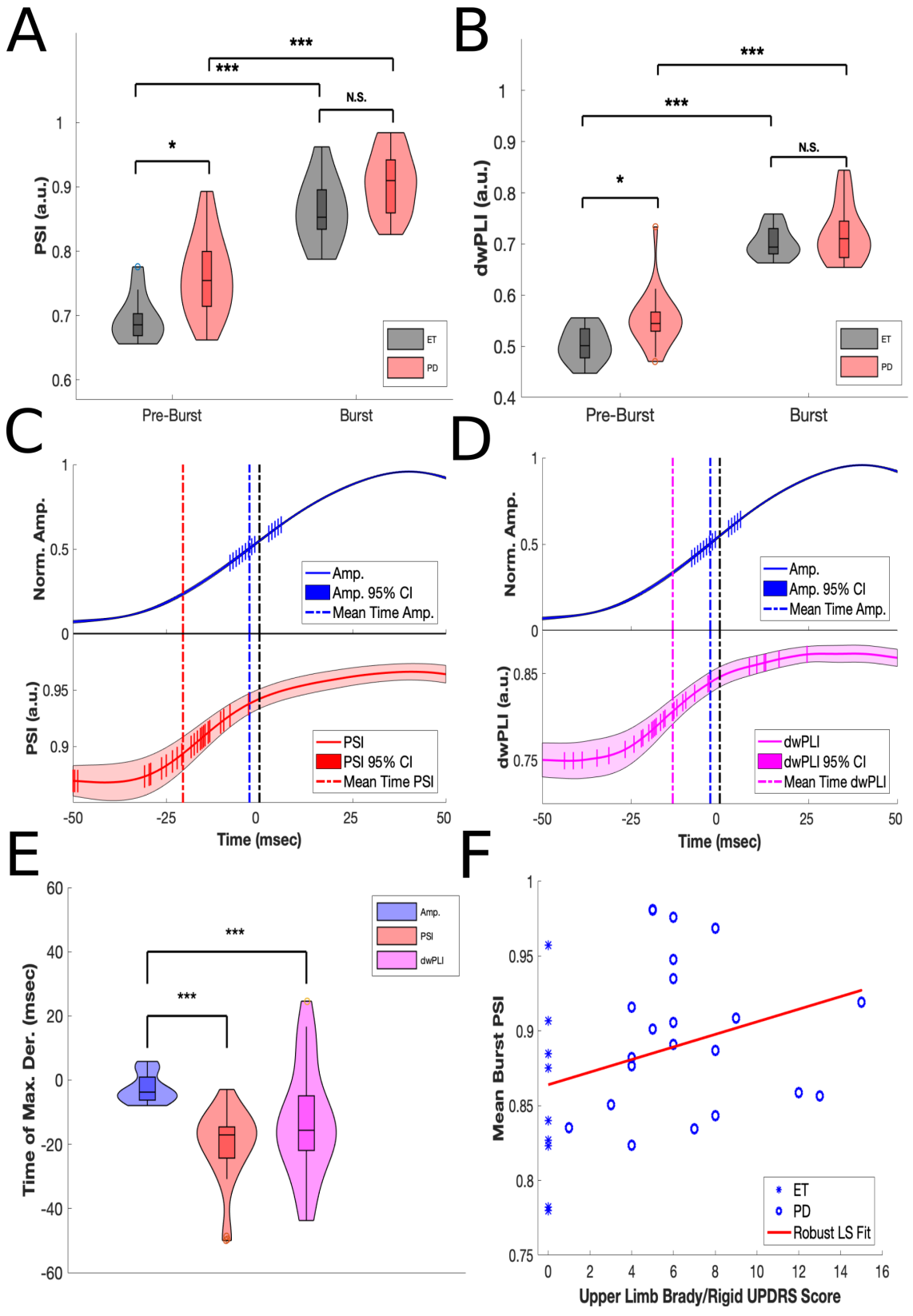

Figure 6. Synchrony increases during beta bursting and clinical correlation.

A) PSI is higher during high β bursting than immediately prior to episodes of high beta bursting. Immediately prior to high beta bursts the PD cohort (red) have a significantly higher PSI when compared to the ET cohort (grey). Both cohorts have significantly higher PSI during high beta bursts compared to immediately prior to high beta bursts however there is no difference between cohorts in the average PSI during bursting. B) An identical pattern of results was identified for dwPLI analysis, see also Table 2. C) Average high beta envelope (blue) and PSI (red) aligned to burst onset (black broken line at 0s). Ticks show the point of maximum derivative calculated for each subject for each measure. D) The same plot as C but for dwPLI (magenta line) showing the temporal relationship between the maximum derivatives of dwPLI and amplitude (blue line). Conventions as in plot C. E) A violin plot comparing average times of maximum derivatives for amplitude (blue violin), PSI (red violin) and dwPLI (magenta violin). Both increases in synchrony measures significantly precede increases in amplitude. F) Scatter plot showing that the mean bursting PSI correlates with symptomatic severity as assessed by UPDRS-III contralateral upper limb bradykinesia/rigidity scores.

Power changes at the level of local field potentials are thought to be underpinned by changes in the synchrony of sub and supra-threshold activity in populations of neurons[171] though it is likely that the contribution of these differs regarding the precise frequency of the neural oscillations in question.[172] Evidence has been presented in the results above that points towards a strong temporal link between synchrony and power increases in the human central nervous system[80, 84] and support the argument that cortical synchrony is promoting episodes of high beta-bursting.

The analysis here is focused upon the phase of beta oscillations in the primary motor cortex and their relationship to the phase of oscillations in the premotor cortex (PM) immediately anterior to M1. Three recent studies have highlighted the important role of synchrony in the electrophysiology of PD. Both have utilized the placement of subcortical electrodes to ascertain changes in phase relationships between subcortical nuclei and each study has suggested a different line of inquiry regarding the current studies of motor cortical electrophysiology. First, Tinkhauser et al demonstrated that inter-nuclear synchrony between left and right STN was greater during overlapping beta bursting in the STN pairs when compared to non-overlapping (shuffled) beta bursting across the nuclei.[84] Interestingly, the authors did not identify any significant difference in phase synchrony of beta bursting when ON and OFF levodopa conditions were compared. This suggests that beta bursting in the subcortical structures represents episodes of network-wide phase synchrony but that the therapeutic effects of levodopa do not modulate the synchronizing effects of beta bursting per se. Instead, the authors suggested that compared to OFF levodopa conditions, ON levodopa conditions represented a shortening of beta burst duration.

Second, using a model of ipsilateral implantation of GPi and STN, Cagnan et al attempted to draw a causal link between power and internuclear phase synchrony.[80] This study revealed that certain 'optimal' phase alignments between STN and GPi had the effect of enhancing beta power within the GPi and STN and that longer runs of phase alignment were associated with greater increases in power. The implication from these findings is that synchrony between nuclei is promoting increases in local power, a well-established pathological finding in many studies of PD.[20] A subsequent third paper by Cagnan et al has taken a closer look at cortico-subcortical synchrony in PD and suggests that beta bursting is anticipated by 'phase

slips' prior to bursting and phase synchrony during beta bursting.[168] In the latter study the authors explicitly state that they feel the burst-associated synchrony increases are not necessarily driving bursting but rather that phase realignments could be providing the conditions required for beta amplification to be propagated throughout the network. We feel that this amounts to a causative role for synchrony and aim to provide some evidence for this with our subsequent findings.

The results presented here validate and extend the findings of Tinkhauser et al and Cagnan et al by showing that cortico-cortical synchrony is increased during motor cortex beta-bursting and that the increase in power of beta bursts is anticipated by steep increases in synchrony between cortical areas. Crucially, there is no difference in the mean burst synchrony between ET and PD cohorts and yet despite this there was a correlation between mean burst synchrony and the clinical bradykinesia/rigidity scores in PD. This is due to the inter-subject variability in rigidity and burst duration, pointing towards a granularity of the data that is easily missed in crude groupwise comparisons.

The data presented above stops short of demonstrating a causal connection between synchrony and power but offers strong circumstantial evidence in support of this by drawing upon the timing of synchrony changes relative to power changes. Likewise, we do not directly implicate synchrony in a causative role with respect to the clinical features of PD however the presence of a correlation between beta burst synchrony and PD clinical features is suggestive that such a relationship might exist. To establish such causal connections with a greater degree of certainty we would need to verify that synchrony has a non-spurious connection with symptomatic expression of PD; that is to say, the relationship cannot be accounted for by other variables in turn linked to synchrony and PD symptoms. Finally, a demonstration that increases

in phase synchrony result in beta bursting and increased PD symptomatology would be strong evidence of a causal link. One means by which such a hypothesis could be tested would be by transiently aligning or disrupting phase synchrony in M1 and PM using alternating current applied via cortical electrodes.

3.3 Verification of Synchrony Findings

The results detailed in section 3.2 appear to suggest that beta bursts are preceded by an increase in the measures of synchrony between cortical areas. It is proposed that this temporal precedence may constitute a causal relationship with cortical hypersynchronicity promoting beta bursting in motor cortex. Because this result forms a key part of the general hypothesis at hand regarding the pathophysiology of PD, means were sought to validate these findings. To this end two distinct approaches were adopted. First, a different method for assessing the timing of increase in synchrony was developed to demonstrate that the results are independent of the criterion used for determining synchrony increases. Second, an *in silico* analysis shows that the observed increases in synchrony are not merely necessitated by an increase in amplitude leading to improved accuracy of phase estimation and hence increased synchrony.

The point of the maximal synchrony increase (maximal first derivative of the synchrony signal) could be a suboptimal means for determining whether synchrony increases precede amplitude bursts. The analysis was therefore repeated using the time point at which synchrony increases beyond the mean synchrony taken across the pre-burst and burst period. The advantage of this approach is that disparate measures such as amplitude and synchrony can be compared

directly in terms of their dynamics during burst epochs. This approach yielded identical results to the initial analysis and full details are depicted in Figure 7, A-C. PSI increased before amplitude (mean time of amplitude increase to threshold = -0.77 msec, 95% CI +/- 2.86 msec, mean time of PSI increase to threshold = -8.57 msec, 95% CI +/- 1.50 msec, Mann-Whitney U test z-value = 6.44, $p = 1.13x10^{-10}$, see Figure 7, A). Similarly, for dwPLI the time point at which the threshold was exceeded temporally preceded the time point at which the threshold was crossed for the normalized amplitude (mean time of amplitude increase to threshold = -0.77 msec, 95% CI +/- 2.86 msec, mean time of dwPLI increase to threshold = -9.28 msec, 95% CI +/- 4.02 msec, Mann-Whitney U test z-value = 5.13, $p = 2.88x10^{-7}$, see Figure 7, B). These results are presented together and summarized in Figure 7, C below.

It is possible that the observed synchrony increases during beta bursting were due to the *a priori* relationship between phase estimation and amplitude. Phases are less precisely estimated at low amplitudes and so synchrony is likely to be underestimated during periods of low amplitude activity (for example, during non-burst periods). In order to show that the synchrony findings were not necessitated by amplitude increases during bursting the next experiment generated 400 synthetic signals composed of random frequencies plus noise and gradually modulated the amplitude of one signal while measuring PSI between pairs of signals (see Figure 7, D). This analysis shows that maximal PSI onset is achieved when the modulated signal reaches 0.4% of maximum amplitude (PSI 'onset' point, 95% CI +/- 0.029%) and synchrony measurement again becomes compromised when the signal drops off to 0.39% of maximum amplitude (PSI 'offset' point, 95% CI +/- 0.027%). These points of the signal corresponded to signal envelope amplitudes of 0.0017 a.u. (mean envelope amplitude for PSI 'onset' point) and 0.0016 a.u. (mean envelope amplitude for PSI 'offset' point). Across the entirety of our *in vivo*

recordings the minimum amplitude of the high beta envelope was 0.0058 μV, which is more than three times the level at which we found PSI was compromised in our *in silico* experiments. This result suggests that low amplitudes alone cannot account for the burst related changes in synchrony we have observed. Furthermore, our burst analyses are conducted using data surrounding the 75th percentile of signal amplitude meaning that our analyses were unlikely to have included epochs of extremely low amplitude. This offers some assurance that our results are not necessitated by the a priori relationships between phase estimation and signal amplitude.

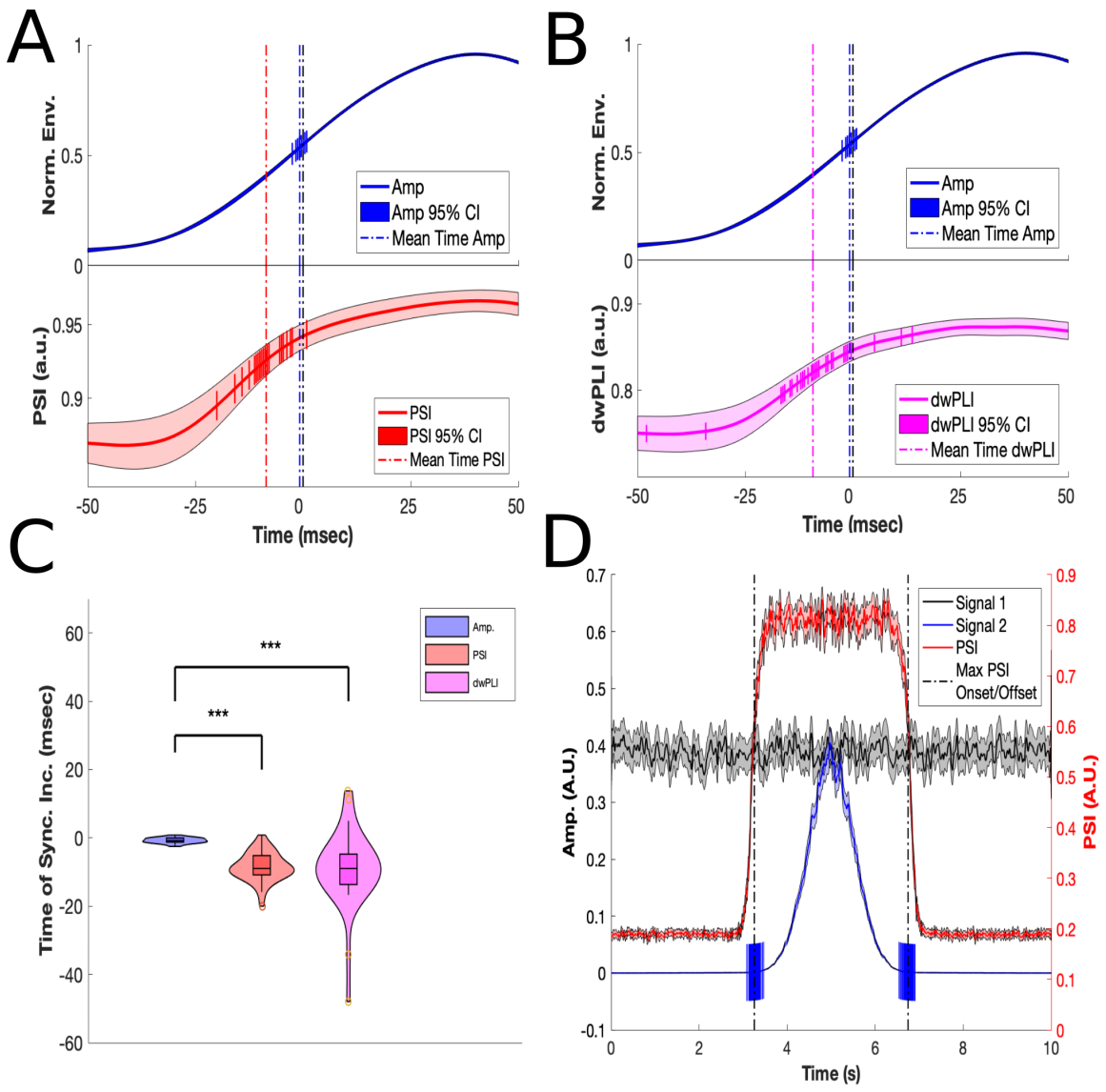

Figure 7. Synchrony increases during beta bursting, control experiments.

A) Using a distinct criterion for PSI increase produces identical results to prior analyses. To check the validity of our burst synchrony analysis (see Figure 6, C-E) we repeated the analysis replacing the criterion for a synchrony increase with an alternative measure. The timepoint of an amplitude or synchrony increase was determined to have occurred when the synchrony or amplitude measurement met or exceeded the mean taken across the entire pre-burst/burst episode. All graph conventions are identical to Figure 6, C-E. This analysis replicated previous findings to show that the measured increases in synchrony

(PSI, red line in Figure 6, C, and dwPLI magenta line in Figure 6, D) preceded the maximal rate of increase in the amplitude (blue line Figure 6, C-D and Figure 7 A-B). Ticks on the graphs indicate the timepoints of amplitude threshold crossings (blue ticks on amplitude traces, Figures 6 C-D, and Figure 7 A-B) and timepoints of synchrony threshold crossings (red and magenta ticks for PSI and dwPLI respectively, Figure 6 C-D and Figure 7 A-B). Figure 7, C shows a comparison of threshold crossing timepoints across amplitude and synchrony measures. Amplitudes (blue trace) superseded the mean close to the burst onset (0 msecs) whereas synchrony measures increased to supersede thresholds several milliseconds before burst onset (red and magenta violins). D) Varying amplitude of one signal has little effect on measurement of PSI above 0.4% of maximal signal amplitude. We generated two synthetic signals (here referred to as Signal 1 and Signal 2) with no inherent synchrony and modulated Signal 2 by taking the dot product of the raw signal with a Gaussian kernel having 1 at the zenith, a mean of 5 seconds and a standard deviation of 0.5 seconds. Our results show that PSI increased and decreased steeply as the amplitude modulated signal (blue trace) reached 0.4% and 0.39% of signal maximum for PSI (red trace, panel D) onset and offset respectively (black dotted lines show the mean timepoint at which PSI reached maximal levels, panel D). Blue ticks on the Signal 2 trace indicate the PSI 'onset' and 'offset' timepoints at which individual iterations of the experiment reached threshold synchrony levels and dropped below threshold levels of synchrony. Threshold PSI levels for each iteration were defined as the mean PSI within +/- 0.5s (+/- 1 standard deviation), of the maximal amplitude at the 5s point in the synthetic signal.

These analyses provide reassurance that the initial findings regarding synchrony and amplitude increases are not merely due to the means by which the time point of synchrony increase was measured. Furthermore, the *a priori* relationship between amplitude and phase measurements cannot alone account for the observed synchrony increases that appear to precede amplitude increases. Proof of causality is hard to obtain in most scientific paradigms and this study is no exception. While the analyses here detailed present results consistent with a causal relationship between synchrony increases and burst increases it must acknowledged that there is a strong possibility the results reflect merely a temporal co-occurrence of amplitude increases and synchrony increases.

3.4 Waveform Shape Changes During Bursting

Novel approaches to time-domain analysis of neural oscillations have shown intriguing relationships between characteristics of waveform shape and established biomarkers of PD such as PAC.[58] Non-sinusoidal features of neural oscillations have captured the interest of neuroscience researchers for many years[173] and there is evidence to suggest that their behavioral relevance is preserved across species.[63] Waveform shape varies with depth of electrode penetration through cortical layers[174] and there is evidence to suggest that waveform shape plays a role in computational processes underlying various behaviors.[175,176,177] Waveform morphology has also been linked to the actions of cortical neurotransmitters such as acetylcholine[175] and glutamate,[178] suggesting that waveform dynamics can be sensitive markers of underlying neurotransmitter profiles. As a new direction for the analysis of neural oscillations in PD

however, waveform analysis is still in its infancy. Many crucial questions remain unanswered in the field. Such questions frequently pertain to the parameters that are most informative with regards to waveform shape. Should the field, for example, be concerned with asymmetries in peak and trough sharpness? Or should it instead be placing more emphasis on the steepness of upstrokes and downstrokes of waveform shapes? To date the main field of interest has been in finding parameters that quantify waveform shapes in terms of steepness and sharpness of oscillations.[58] Other lines of inquiry have placed the emphasis on differences in peak and trough amplitudes in order to characterize waveform shapes.[175] These reflect just a subset of the semi-arbitrary choices about exactly how waveform morphology should be parameterized to offer the most informative insights into neural processing.

The experimental protocol described here involves comparisons of high beta bursts with non-bursting epochs of recordings. For this reason, measures of waveform shape that were resilient to amplitude changes were sought. Plotting peak:trough sharpness (see Formula 7) and rising:falling steepness (see Formula 8) ratios across conditions is one means by which to characterize changes in overall waveform symmetry. Subsequent figures illustrate how waveform shape changes translate into movements in the two-dimensional plane formed by these ratios. Ratio measures has the advantage of negating the potentially confounding effects of power differences between bursting and non-bursting periods as both peak and trough sharpness are expected to be similarly increased by increases in amplitude excursion during bursting episodes. The same argument holds for the ratio measurement of rising and falling steepness. One disadvantage of this approach is that congruent (or symmetrical) increases in steepness or sharpness would not be reflected in changes in the ratio. Because our focus here was on

amplitude-related changes we accepted this penalty to obtain a relatively amplitude-invariant measure of waveform shape.

We first tested whether there was a change in waveform shape in burst compared to non-burst epochs for the entire cohort (see Figure 8, A). Our results demonstrate that there was a significant shift from a relatively steeper rising phase and relatively sharper peak during non-burst periods (black markers) towards a relatively steeper falling phase and relatively sharper trough during bursting (red markers, MANOVA, $d = 1$, $p = 5x10^{-6}$). Figure 8, B-C helps to clarify the method by which waveform changes were further parameterized in this study. Waveform ratios of non-burst epochs were identified (Figure 8, B, blue points) and plotted on a two-dimensional logarithmic axes of sharpness and steepness. This plotting procedure was repeated for waveform shapes during bursting (Figure 8, B, magenta points). Burst and non-burst points for individual subjects were then joined by a solid line colored according to cohort (Figure 8, B, ET cohort in black, PD cohort in red).

Plotting waveform changes thus allowed for characterization of the change in waveform shape for each subject as a vector with a length and direction. The non-burst point was set to be the origin and so the extent and direction of waveform change could be quantified and compared for each subject, this is illustrated in Figure 8, B. Statistical comparison of the angles of waveform change (using the circular Watson-Williams test of equal means) for each group showed that there was no significant difference between the ET and PD cohorts in the direction of burst-dependent waveform change (mean angle for ET = -2.56 rad., mean angle for PD = -2.37 rad., $p = 0.17$) but that the ET cohort changed their waveform shape to a greater extent than the PD cohort (mean Euclidean distance ET = 0.30 a.u., mean Euclidean distance PD = 0.15 a.u., $p = 0.00052$, see Figure 8, C). There was no significant difference between ET and PD cohorts

when waveforms were compared during bursting and non-bursting conditions (see, Figure 8, E). The extent of waveform change (Euclidean distance of waveform change vector) correlated inversely with aggregate upper limb bradykinesia/rigidity scores as measured by UPDRS-III (Spearman's $r = -0.40$, $p = 0.022$, see Figure 8, D). Attempts to replicate previous findings correlating sharpness ratios with contralateral rigidity scores[58] did not reveal a significant relationship in our cohort as a whole (Spearman's $r = -0.11$, $p = 0.55$, see Figure 8, F).

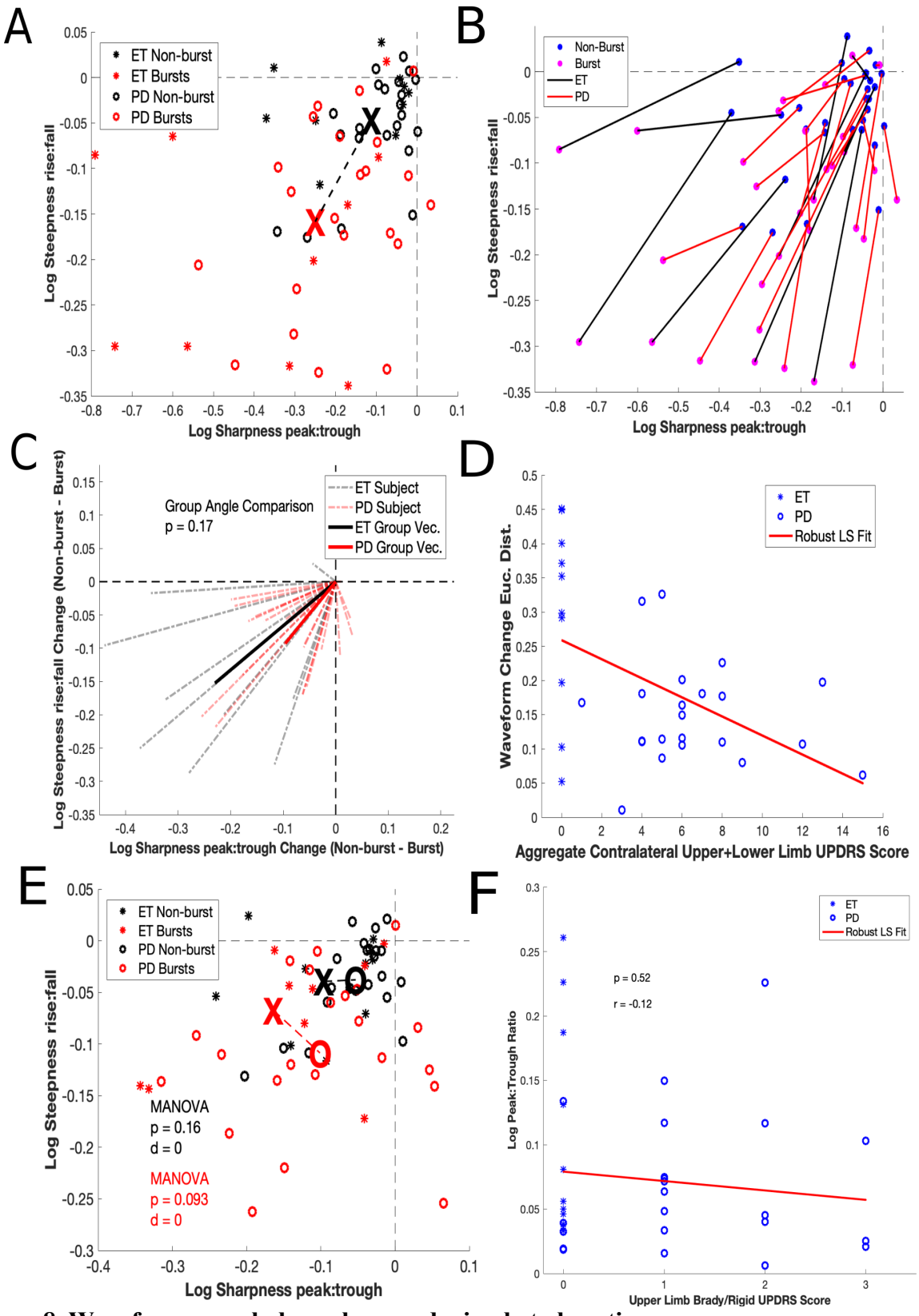

Figure 8. Waveform morphology changes during beta bursting.

A) Waveform ratio plots show that during non-bursting periods (black markers) the waveform is predominantly steeper on the rising phase and has a sharper peak, as evidenced by the concentration at the origin. During bursting (red markers) the waveforms predominantly occupy the lower left quadrat showing a steeper falling phase and sharper trough. B) Each subject had their waveform shift quantified as a directional vector to facilitate comparison of waveform changes in terms of magnitude and direction. C) There was no significant difference between Essential Tremor and Parkinson disease in the direction (vector angle) of waveform shift but there was a significant difference in the vector-based magnitude (vector length) of their waveform change as seen by comparison of solid black (ET) and red (PD) vector lengths. D) Magnitude of waveform change showed a significant negative correlation with Parkinson disease symptomatology. E) There was no significant difference in waveform shape between cohorts in either non-burst (black markers) or burst conditions (red markers). In this diagram the waveform centroid of the Essential Tremor cohort during the non-burst condition is marked with a black X and the waveform centroid of the Parkinson disease cohort is marked with an O. The same markers in red represent the waveform centroids of the cohorts during bursting conditions. F) We found no significant correlation between peak sharpness across the whole recording and contralateral upper limb rigidity scores contrary to findings in previous papers .[84]

The results above demonstrate that high beta bursts are associated with stereotypical changes in waveform shape and that these changes take the form of a deviation away from symmetrical waveform shapes towards asymmetrical waveform traits. The change reflects a shift in waveform symmetry towards a less sharp peak and a less steep rising phase of

the oscillation. One interpretation of this is that during burst epochs there is more synchrony of presynaptic inputs to motor cortical pyramidal cells in the falling phase of high beta oscillations, resulting in an asymmetry of the waveform slopes (shallower upstroke and steeper downstroke) and a delayed peak of the oscillatory cycle. Although speculative, this claim is based upon evidence of the underlying neurophysiological processes that give rise to neural oscillations[179] and computational studies regarding laminar currents capable of generating beta oscillations in pyramidal neurons.[180] A less speculative conclusion to be drawn here is that changes in the amplitude of high beta oscillations are not merely a scaling of the waveform, but instead constitute a quantifiable deviation from lower-amplitude waveform shapes, in particular waveform symmetry, in a stereotypical fashion.

Having established a significant difference between burst and non-burst conditions for the cohort the analytic approach sought to determine whether the ET and PD cohorts differed in terms of their waveform changes. This hypothesis was driven by the supposition that PD appears to be at least in part, a problem related to higher levels of synchrony in cortico-subcortical circuits.[77,78,13,181] Thus, if the hypothesis regarding waveform changes and synchrony of underlying presynaptic activity in M1 pyramidal neurons is correct, one might expect that PD patients are less able to modulate waveform shape between non-burst and burst epochs. Might it be the case for example, that dopamine depletion results in reduced flexibility regarding the modulation of waveform shape, and that this leads to the PD cohort spending a larger proportion of time in bursting states in an effort to increase the extent of waveform change? This would explain previous results demonstrating an increase in burst duration for PD patients coupled with increased power in the high beta band relative to ET patients.

To test this hypothesis the current study parameterized waveform changes in terms of direction (within the two-dimensional plane of steepness and sharpness ratios) and extent (how much the waveform changed in terms of steepness and sharpness ratios. Interestingly the direction of waveform change is remarkably similar for all the subjects, with waveforms becoming relatively sharper in their troughs and relatively steeper in their falling phases during beta bursting. This represents shift towards the left inferior quadrant on the two-dimensional plane of waveform shape could correspond to increased synchrony of inputs at a particularly crucial point in the oscillation. If oscillations are facilitating neural computations as claimed by some researchers[59,61,182] then such specifically timed changes in synchrony might reflect underlying computations for movement parameters.

It is interesting to note that although the direction of change in waveform morphology was the same for both cohorts, the PD cohort seemed to make smaller shifts in the magnitude of their waveform changes. This finding could be hypothesized to represent a deficit in motor cortical computation in PD sufferers, perhaps accounting for some of the defects in movement that characterize the dopamine-depleted state. One hypothesis linking the burst duration findings above with the burst waveform shape changes here would be that increased burst durations are a means of physiological compensation for an inability to shift waveform shapes as efficiently. This notion pictures extended burst durations as an attempt to compensate for decreased waveform shifts but it might also be the case that waveform shape tends to revert to non-bursting profiles during the course of a burst, a phenomenon which would mean that longer burst durations taken as a whole show reduced extents of waveform change.

3.5 Phase Amplitude Coupling

An important part of the hypothesis under consideration in this study is the role for PAC as a physiological tamponade for information processing. This was predicted on the basis of several foregoing results including our earlier findings that beta burst duration is increased in PD, beta bursting was associated with increased beta waveform asymmetry and findings from other studies that PD is associated with increased M1 PAC.[26] This viewpoint proposes that strong coupling between oscillations acts as a 'block', effectively locking closed channels for the development and execution of movement plans across the cortico-basal ganglia circuits. The study of PAC outlined below tests the prediction that beta bursting acts as episodes of high PAC to prevent the interference of competing movement plans with a presently executed movement plan. If non-movement, or rest, is also considered as a movement plan, then beta bursting can be predicted to play a similar role in both rest and movement; that is to say, the prevention of interference from competing movement plans. In this schema a decreased level of beta bursting, and hence PAC, would be hypothesized to allow a movement plan to 'win out' among the competition for it to be enacted.

The following analysis therefore tests whether beta-phase to broadband gamma amplitude PAC is uniformly distributed throughout our recordings or instead is restricted to epochs of beta bursting. Previous studies have not distinguished high beta or low beta in phase modulation and so we examined each sub-segment of the beta band in turn. Our analysis did not explicitly seek to distinguish between nested oscillations and sharp waveforms but were more focused on the presence of these phenomena during beta-bursting

PAC was calculated for bursting and non-burst periods separately. Anderson-Darling tests of normality showed that the data for PD cohort PAC was not normally distributed (low beta PD non-burst MI AD test stat = 2.32, $p = 5.00 \times 10^{-4}$, low beta PD burst MI AD test stat = 2.15, $p = 5.00 \times 10^{-4}$), comparison of the data was therefore made using non-parametric testing. Figure 9, A, shows the group average PAC for non-bursting and bursting segments across all subjects. There were significant burst versus non-burst differences in both the low and high beta band encoded PAC (Figures 9, A-B). Low beta phase encoded PAC increased significantly during bursts compared to non-bursting (mean low beta non-burst MI = 1.20×10^{-4}, 95% CI +/- 6.15×10^{-3}, mean low beta burst MI = 0.0013, 95% CI +/- 5.43×10^{-5}, Mann Whitney U z-value = -4.78, $p = 1.70 \times 10^{-3}$, Figures 9, A-B). Likewise, high beta phase encoded PAC showed similar results with a pronounced elevation in PAC during bursts compared to non-burst periods (mean high beta non-burst MI = 6.96×10^{-5}, 95% CI +/- 4.14×10^{-5}, mean high beta bursting MI = 6.96×10^{-4}, 95% CI +/- 2.88×10^{-4}, Mann-Whitney U z-value = -4.76 $p = 3.93 \times 10^{-6}$, see Figures 9, A-B). There was no significant difference for MI in the Essential Tremor and Parkinson disease cohorts during non-burst or burst periods in the high or low beta-phase encoded bands.

To investigate the relationship between cortical PAC and waveform shape we compared cortical high beta PAC with magnitude of changes in high beta waveform shape. High beta PAC data did not meet the test of normality (Anderson-Darling test statistic = 2.93, $p = 5 \times 10^{-4}$) and so a Spearman's non-parametric test was used to assess correlation. Our data shows a significant positive correlation between the extent of waveform shape change (Euclidean distance on the two-dimensional waveform shape plane) and average high beta phase encoded PAC (Spearman's r value = 0.52, p = 0.0026, Figure 9, C).

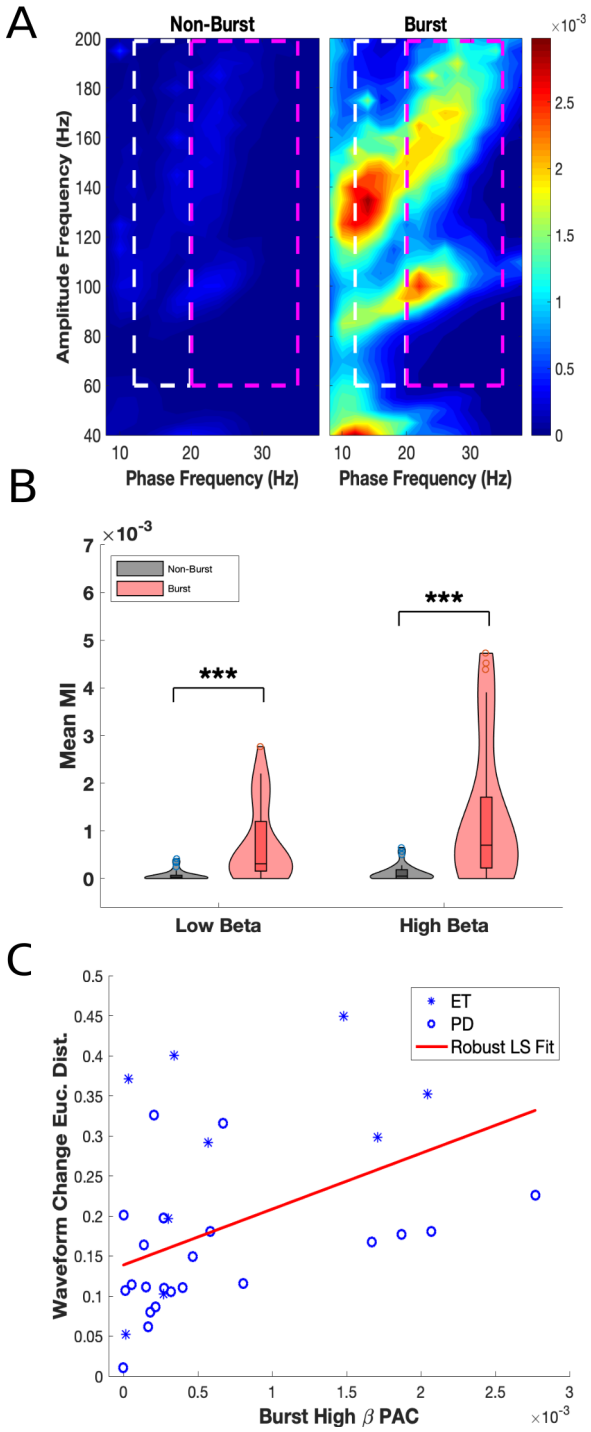

Figure 9. Phase-amplitude coupling during beta bursting.

A) Across the whole cohort PAC during non-burst periods is minimal compared to PAC observed during bursts. White and magenta broken lines indicate the regions of PAC used to calculate statistical comparisons shown in B. B) For both low beta and high beta-

encoded PAC there was a significant increase in MI during bursting compared to non-bursting epochs. C) Average bursting high beta-phase encoded PAC correlated with magnitude of waveform change during high beta bursting.

3.6 Chapter Discussion

The foregoing results demonstrate a temporally dynamic pattern of beta bursting that links dynamic network synchrony with locally observed phenomena of increased high beta power and high beta-phase encoded PAC. Here we have provided evidence linking high beta cortico-cortical synchrony, motor cortex high beta amplitude increases, high beta waveform changes and high beta encoded PAC. Early studies described findings relating time-averaged beta power to symptomatology in the STN.[181] These experiments showed that reduced power in the STN beta band (8-35Hz) was induced by levodopa therapy and positively correlated with improvement in PD symptomatology. Subsequent studies have elaborated on these finding to show that in Parkinson disease, not only is STN time-averaged beta power modulated by levodopa therapy but STN beta burst durations and amplitude are also modulated by levodopa therapy.[84] Furthermore, decreases in burst duration were correlated with symptomatic improvement and the same study showed that longer beta bursts are associated with increases in local and interhemispheric phase synchronization.[84]

These findings are notable for two main reasons. First, they suggest that burst duration, and not just absolute beta power, is associated with motor pathology observed clinically in PD. Second, they imply a role for beta bursting in the hypersynchronous state that is thought to

characterize PD.[20,77,183] How the motor cortex responds to levodopa therapy is less well understood at present. The foregoing results demonstrate that cortical synchrony plays a similar role in cortical beta bursting as it does in subcortical beta bursting; measures of synchrony were elevated across the M1 and PM cortices during beta bursting. Importantly, the present study demonstrates that bursts are preceded by increases in synchrony. This is consistent with Cagnan et al's prior report of amplitude-enhancing phase relationships between the globus pallidus and STN.[80] However, it is now demonstrated that the phenomenon of phase synchronization resulting in amplitude enhancement (or bursting) occurs at other nodes in the motor network and is not specific to the subcortical basal ganglia. This could point to a network-wide pathological hypersynchrony causing the clinical manifestations of PD. In keeping with this hypothesis, this study also shows that higher cortico-cortical synchronization during bursts, and longer duration cortical beta bursts, both correlate with aggregate measures of contralateral Parkinson disease symptomatology. The measures of synchrony used here, burst duration, and waveform shape change all correlated with contralateral upper limb rigidity alone. There was a trend towards scores of contralateral rigidity alone correlating with duration of beta bursting but the correlation did not survive Bonferroni correction (see Figure 5, F).

The increased strength of relationship between synchrony, burst duration, waveform change, and aggregate measures of rigidity/bradykinesia could indicate that these processes play a generalized role in underpinning the clinical features of Parkinson disease. These results taken together suggest that hypersynchrony across the cortico-basal ganglia circuit could be driving increases in beta amplitude, waveform shape changes and motor cortical PAC. Present forms of adaptive DBS stimulate at high frequency only when amplitude of beta rises above a preset threshold, thus effectively shortening burst duration and decreasing burst amplitude.[25] That these

results show PSI increasing more than 17 milliseconds prior to cortical high beta bursts, shines a spotlight on synchrony as an anticipatory biomarker that could be used for adaptive DBS.

Increased beta power, previously reported in the motor cortex of PD patients,[29] may be attributable to the longer duration of beta bursts, which is reported here. Indeed, the mean duration of bursts in the high beta band correlates with the severity of contralateral limb rigidity/bradykinesia, suggesting that prolongation of these transient increases in high beta power is playing a pathophysiological role in Parkinson disease. The results described here could help explain why elevation of beta power in the motor cortex[28] is an inconsistent finding in PD.[29] Total high beta power could remain unchanged despite changes in the underlying dynamics of high beta bursting. Given the dynamicity of high beta bursts, the underlying phenomenon may not always be reflected in grosser time-aggregated measurement of overall power. Intuitively, for power to remain constant while beta bursting alters would necessitate compensatory changes in beta bursting incidence or amplitude. This is a concept explored in more detail in subsequent sections. Of relevance to this idea is the fact that previous studies have found beta bursting in M1 unaltered in terms of duration and frequency when Parkinson disease and dystonia cohorts are compared.[23] Further investigations are necessary to evaluate the relationship between bursts and disease symptomatology across movement disorder diagnoses. It may be the case that increased burst duration is not a feature unique to Parkinson disease pathophysiology, just as PAC is not unique to Parkinson disease.[86]

The experiments above have linked transient episodes of high beta power to both increases in cortico-cortical synchrony and to changes in waveform shape. Waveform shape change has been shown here to relate to beta bursting, Parkinson disease symptomatology and to high beta-encoded PAC in the cortex. Waveform analysis is an emerging field of study but has

already made contributions to the study of Parkinson disease pathophysiology.[58] Cole et al analyzed the motor cortical signal during DBS and found that STN DBS had the effect of 'smoothing' the non-sinusoidal features of beta oscillations in M1 (corresponding to a move towards the origin on Figure 8, A-B). The authors postulated that this reflected a decrease in synchrony of synaptic inputs reflecting reduced coherence in the cortico-basal ganglia circuits. The present study has shown that waveform characteristics do indeed change relative to the bursting state of the underlying signal and cortico-cortical synchrony. Furthermore, the results demonstrate that this change in waveform shape is impaired in the PD cohort and the degree of impairment correlates with clinical symptoms of Parkinson disease. Non-burst epochs appear to favor a higher peak-to-trough ratio and rising-to-falling steepness ratio whereas bursting periods of the signal show the opposite. Waveforms are proposed to be dynamically changing between these bursting and non-bursting states and temporal collapsing of waveform features neglects important features specific to bursting and non-bursting epochs. Cole et al found that M1 sharpness ratio was positively correlated with patient rigidity scores. This finding was not replicated here. The experiments outlined above instead show that synchrony, waveform shape change and mean burst duration are correlated with composite contralateral upper limb rigidity/bradykinesia. On close inspection of previous findings it appears that a large part of Cole et al's previous correlations could have been carried by a small number of data points, possibly representing outliers.[58]

PAC has been strongly implicated in Parkinson disease pathophysiology and is often increased in Parkinson disease despite not being found to be elevated in all Parkinson disease subjects.[26] In their comparison of PD, dystonia and epilepsy patient de Hempetinne et al identified at least some PAC in M1 in all PD subjects however in several of their PD subjects

PAC was extremely limited in the beta-to-broadband-gamma region. PAC has been shown by the analysis above to be largely a phenomenon confined to beta bursts. It has also been related to waveform shape with greater non-burst to burst waveform changes being linked with increased beta-gamma PAC.[58] These findings may explain why not all PD subjects are found to have elevated PAC. Acknowledging that beta-to-broadband gamma PAC is not uniform throughout the recording presents the possibility that certain recording episodes may fail to capture these important epochs of coupling, thus explaining why some patients fail to demonstrate increased PAC. The findings related here establish a correlation between the magnitude of waveform change and levels of high beta-phase encoded PAC. As stated previously the hypothesis under scrutiny is agnostic about the cellular origins of the PAC identified but if the sole contributor to this finding was sharp waveforms (as opposed to nested oscillations) the correlation between waveform change and PAC would be expected to be very close to 1.[145] PAC has been proposed to act as an inhibitor of cortical movement plans,[184] possibly by reducing the informational bandwidth of cellular firing,[185] and so changes in the dynamics of this phenomenon have great potential to act as direct or proximal causes of rigidity observed in Parkinson disease. According to the hypothesis outlined above, and supported by the evidence presented, synchrony across cortical circuits could be driving changes in oscillation amplitude, shape and cross-frequency oscillatory couplings.

Many questions remain unanswered in light of these findings. Attempts must be made to determine whether bursts are modulated in amplitude, waveform or length during movement. The current findings are consistent with predictions that during movement burst incidence will decrease and the dynamics of waveform change will remain unaltered. This would account for the modulatory effect of DBS on PAC observed previously[27] and would be predicted by the

observed correlation between waveform shape changes and PAC. It has been proposed that burst dynamics could also account for the individual differences seen in both power changes and PAC increases observed in Parkinson disease. Further work is required to establish if burst duration is indeed the primary explanatory factor for these inter-subject variations. Finally, it is important to establish how burst duration, synchrony, waveform shape and PAC change during movement.

The hypothesis outlined here proposes that beta bursting plays a central role in the inhibition of voluntary movement by acting to prevent the emergence of competing movement plans via an 'informational tamponade' on cortical processing. The results above suggest that beta bursting is a high-synchrony, high-PAC epoch of the time series driven by increases in cortico-cortical synchrony and featuring stereotyped changes in waveform morphology. Having observed that PD subjects show longer duration beta bursts coupled with reduced magnitude of non-burst to burst waveform change points to these features as salient for the pathology of PD and the present hypothesis proposes that beta bursting duration will remain relatively elevated in the PD cohort during movement. The hypothesis predicts that during movement the waveform morphology for the PD cohort during movement will follow the same pattern as ET, becoming less symmetric during bursting, but that the inability to terminate beta bursting in PD will result in increased duration of beta bursts during movement. Subsequent sections of this dissertation will focus first on the relationship between movement and synchrony-driven beta bursting. In particular, it will investigate whether or not there is a decrease in burst duration during episodes of movement compared with rest and whether bursts themselves are quantitatively distinct during epochs of movement as compared with bursting during epochs of rest. It will also seek to clarify whether PD is related to increased burst duration during movement and whether PD symptoms can be related to the burst duration parameter as measured during movement epochs.

Chapter 4. Rest and Movement

4.1 Background

The cortical electrophysiology of movement has been the subject of a vast literature of scientific study. Only a brief summary of the most relevant literature will be presented here with a focus on the electrophysiological changes in the motor cortex during voluntary movement. The motor cortex is arguably the first cortical area to be studied intensively using electrophysiological techniques.[186] Initial studies by Wilder Penfield outlined the somatotopic maps within motor cortex in human epilepsy patients,[36] several years later, Evarts identified that pyramidal cell firing in macaque monkeys was related to force applied to extensor and flexor displacements of the wrist.[187] Further investigations conducted by Georgopolous et al showed that motor cortical cell firing was often closely linked to direction of wrist displacement, a finding which gave rise to the notion of population encoding.[111] As early as 1979 neural oscillations in the motor cortex were identified at rest and prior to movement initiation being posited as inhibitors of voluntary movements due to their abolition during voluntary movement.[188] Amplitude of beta oscillations and cortico-cortical synchrony have subsequently been linked to symptomatic OFF states in PD patients and are normalized by treatment with levodopa suggesting that symptomatic improvement is related to aspects of the oscillatory profile in the beta range.[189]

Murthy and Fetz were among the first authors to describe the appearance of motor cortical oscillations in the frequency range 25-35Hz during movements made by macaque monkeys in retrieval of raisins from a Klüver board. Their description is prescient in that it clearly describes beta bursting (centered at ~30Hz) in motor cortex, the locking of cell firing to beta oscillation cycles (thought to constitute the basis for at least a portion of PAC), and the synchronization of beta bursts between premotor and motor areas.[190] Interestingly these authors found that oscillatory bursts occurred more often during free arm movements and appeared less frequently in when monkey's performed stereotyped, overtrained ramp-and-hold movements. Oscillatory bursts were found to occur less often when monkeys were quietly resting when compared with free arm or exploratory movement.

More recently, studies have begun to focus on the changes taking place in beta bursting during movement to try to identify a role for beta bursting in voluntary movement.[24] Lofredi et al studied the phenomenon termed the 'sequence effect', a progressive decrement in movement velocity observed in PD patients making continuous hand movements. They recorded from externalized DBS leads with contacts sited in the STN. Over the course of 30 seconds of repetitive movement the authors found that both low and high beta power declined (although not linearly with time) and that decreasing movement velocity was accompanied by reductions in beta burst duration, amplitude and rate. One problem with the methodology outlined by Lofredi et al is that the decrease in beta power observed throughout the movement phases necessitates that bursting will become less frequent, lower amplitude and shorter in duration. This is because the threshold of beta bursting was defined at rest and remained fixed throughout the study. Attempts to define beta amplitude as a mean derived from the 75th percentile of rest data and the 75th percentile of movement data[84] will suffer from the same problem as bursts will potentially

be over-represented in the rest period and under-represented in the movement period (assuming a decrease in beta power between rest and movement). How we might compensate for power changes in order to compare beta bursting during rest with that during movement is non-trivial. Any change in the overall signal amplitude is likely to directly influence the parameters that one is interested in analyzing. Some analysis approaches that may prove invariant to changes in the overall amplitude of the beta band are described below.

A paper by Friston et al (1997) suggests that transient increases in neuronal activity patterns (analogous to beta bursting) are the natural result of sparse connectivity and 'metastable dynamics'.[191] This study proposes that a tendency of neuronal populations to fall in and out of attractor states, short stereotypical excursions of activity, is a natural byproduct of a sparse connectivity and that reductions or increases in connectivity results in decreases in metastability, that is to say, more stable configurations of activity. Friston's approach to quantifying metastability involved looking at the changeability of frequency profiles across windowed segments of the signal. Importantly, Friston's proposals suggested that increases in connectivity resulted in increases in coherence between units, increased stability of attractor states and a reduction in the number and diversity of transients. Continuous movements represent stable attractor states of the type discussed by Friston. Studying the difference between rest and movement can therefore shed light on the predictions of Friston's theory that transients will become less frequent and varied as an attractor state becomes more established. In contrast, periods of rest should be characterized by increased bursting as a means of readying the cortex to enter a novel attractor state. By analogy with our findings, the present study could be looking at a scenario in which dopaminergic depletion during PD is resulting in an increased effective connectivity between nodes in the cortico-sub-cortical loops resulting in more stable and

coherent dynamics. It could be the case that the informational bandwidth discussed in the PD literature[185] is a reflection of the network's inability to occupy a sufficiently 'metastable' state space conducive to local and global processing. Indeed, some preliminary evidence exists to support the assertion that the coefficient of variation (CV) in the high beta band of the STN correlates with UPDRS-III scores off medication.[12] The improvement in clinical scores in this study also showed a correlation with change in the CV of the high beta band in response to treatment with levodopa. Neither correlation was redundant once absolute spectral power was regressed out suggesting that CV is an important feature of the high beta band regardless of absolute high beta amplitude.

Little et al's CV approach provides a plausible and, to some extent, validated measure of variability in the beta band. Furthermore, this measure is explicitly scale invariant and impervious to differences in amplitude between two conditions. This is due to the fact that during the CV calculation, we normalize by the average amplitude of the signal. The CV is calculated as follows:

$$\mathrm{CV} = \frac{\mathrm{Std}\left(\mathrm{Signal}_f\right)}{\mathrm{MeanA}\left(\mathrm{Signal}_f\right)}$$

Equation 10. Equation for the coefficient of variation.

Where CV is the coefficient of variation, Std(Signal$_f$) is the standard deviation of Signal$_f$, the amplitude envelope of the Signal filtered at frequency *f*, and MeanA(Signal$_f$) is the mean amplitude of the signal filtered at amplitude *f*. We would expect from their studies of high beta in the STN, that the CV for high beta in the motor cortex might be similarly reduced in PD.

An alternative approach to quantification of beta variability could measure the

distribution of peak-to peak burst intervals. Intuitively, the intervals between beta bursting will have a log-logistic or skewed-normal distribution. Should there be decreased metastability one would expect the peak-to-peak burst intervals to aggregate around one or more fixed values. This difference would be detectable using either a measure of average interval between beta burst peaks or a direct comparison of distributions using a two-sample Kolmogorov-Smirnov test. Movement data would show both a reduced frequency of beta bursting and more regular burst-interval variability according to the predictions of Friston's model.

While approaches to the complexity of beta oscillations are intriguing, these analytical techniques are beset by two major difficulties. First, the literature involving these analyses is limited, rendering comparison with other studies in PD hard to perform. Second, these approaches are somewhat unintuitive in their implications. Non-linear analyses such as those performed by Friston et al[191] yield interesting results but remain hard to conceptualize and contextualize in the electrophysiological landscape. For these reasons, more intuitive and cognitively graspable concepts such as beta bursting (as defined by amplitude thresholding) have come to dominate the literature. This dissertation's analysis going forward will prioritize these established measures of beta variation while keeping in mind that alternative, albeit less intuitive, measurements could capture important dimensions of the beta oscillation.

4.2 Power and Burst Changes During Movement

Elevated beta power in the STN has been linked to severity of bradykinesia[192] and reductions in beta power in the STN have been related to improvements in UPDRS-III scores for PD patients.[81] Event-related desynchronizations (ERD), reductions in cortical beta power, have also been identified in normal human subjects during simple movement tasks.[71] These lines of evidence suggest that cortical electrophysiology during rest and movement could yield important differences between ET and PD cohorts that sheds light on the pathophysiological origins of PD. Analyses detailed above and performed during rest showed significant differences between ET and PD patients in terms of beta oscillations at rest. High beta power was found to be elevated in the PD cohort compared to the ET cohort and increased burst duration in PD was proposed to explain this difference. Duration of beta bursting was correlated with symptomatic severity on the UPDRS-III scores across the cohort.

By contrast there were few differences between the ET and PD cohorts in terms of synchrony, waveform shape and PAC during bursting. This argues in favor of a hypothesis that attributes the pathological manifestations of PD as being primarily due to the timing of beta bursting episodes rather than their deeper electrophysiological profiles. The central hypothesis tested here proposes that beta bursts are stable electrophysiological features related to changes in cortico-cortical synchrony, waveform changes and phase-amplitude coupling, and this section seeks to develop an evidence base showing that the deficits of PD are associated with changes in the timing of beta bursts rather than their associated electrophysiological characteristics (synchrony, waveform dynamics, PAC). Because the previous analysis has focused upon high

beta due to extended beta burst durations in this region of the spectrum, the movement analysis took the high beta band as our initial frequency band of interest for the rest/movement analysis.

4.2.1 Power remains stable despite reduced burst duration.

ET patients showed no significant change in high beta power during movement compared to rest conditions (data normally distributed by AD, mean ET high beta power at rest = -20.97, 95% CI +/-1.53, ET moving high beta power = -19.70, 95% CI +/- 2.05, , z-value = -3.28, paired t-test p = 0.19, see Figure 9, A), however beta burst duration appeared significantly lower during movement than during rest (data normally distributed by AD test, mean ET high beta burst duration at rest = 122.29 msec, 95% CI +/-5.52 msec, ET moving high beta burst duration = 102.57 msec, 95% CI +/- 9.99 msec, paired t-test p = 0.00071, z-value = -11.16, see Figure 9, B). PD patients also showed no significant change in high beta power during movement compared to rest (data not normally distributed by AD test, p = 0.56 level, mean PD high beta power at rest = -17.49, 95% CI +/-0.66, PD moving high beta power = -17.09, 95% CI +/- 0.69, paired t-test p = 0.418, z-value = -0.81, see Figure 9, C). Similar to the ET cohort, however, the PD cohort showed a highly significant reduction in beta burst duration during movement compared to rest (data normally distributed by AD test at the p<=0.05 level, PD mean high beta burst duration during rest = 122.29 msec, 95% CI +/- 4.49 msec, mean PD high beta burst duration during movement = 102.57 msec, 95% CI +/- 9.47 msec, repeated measures t-test z-value = 17.07, p = 8.37×10^{-5}, see Figure 9, D).

We observed a significant difference between the ET and PD cohorts for high beta power during movement (AD test p = 0.79, mean ET high beta power during movement = -19.70, 95% CI +/- 2.05, mean PD high beta power during movement = -17.12, 95% CI +/- 0.70, Mann-Whitney U test, z-value = -2.74, p = 0.0061, see Figure 9, E). However, there was no significant difference in high beta burst duration for the cohorts during movement (AD test significant at the p<=0.05 level, mean movement high beta burst duration for ET = 102.57 msec 95% CI +/- 9.99 msec, mean PD high beta burst duration during movement 107.13 msec, 95% CI +/- 9.86 msec, see Figure 9, F).

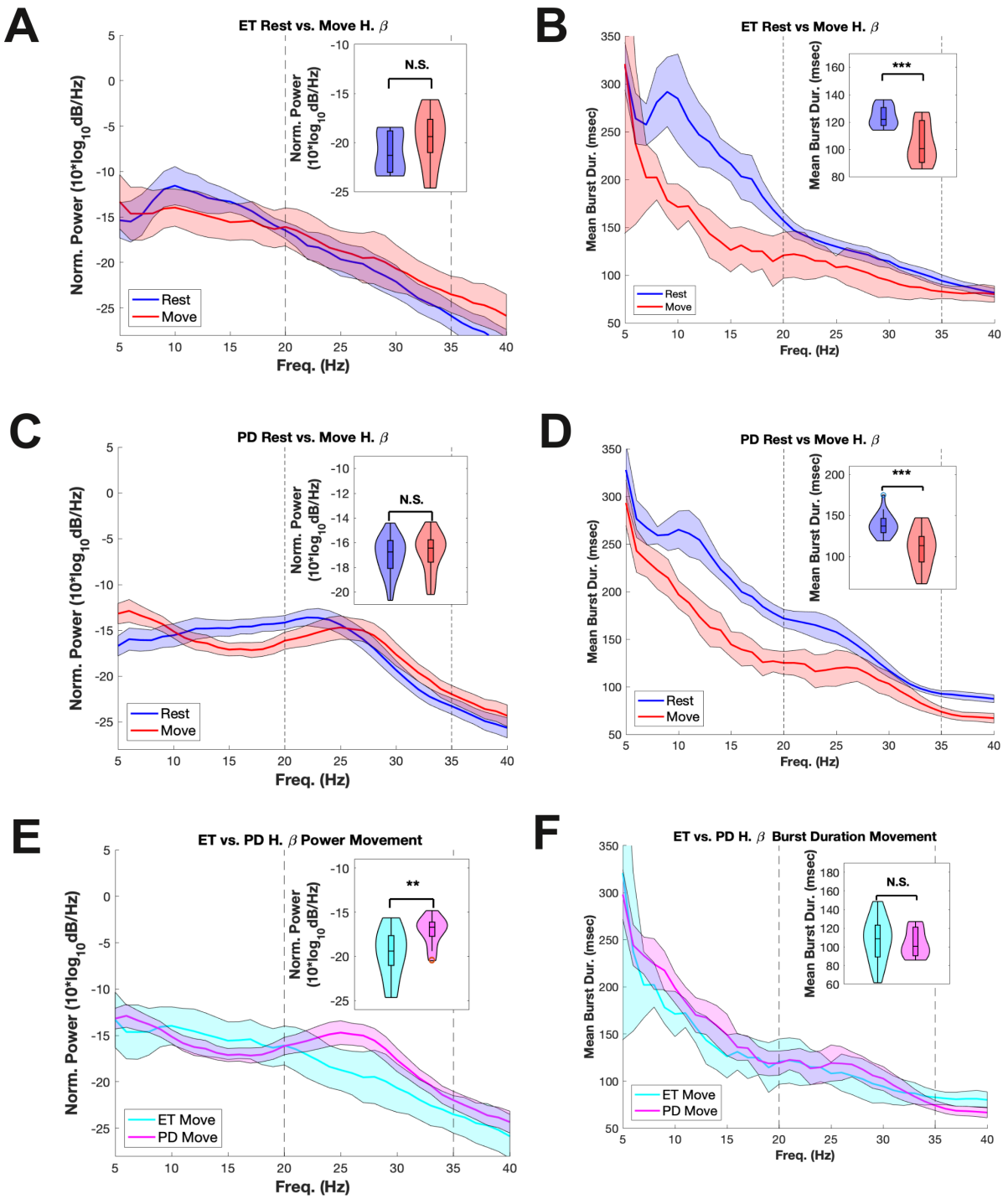

Figure 10. Beta power and burst duration comparisons for rest and movement.

A) ET group power comparison for rest (blue) and movement epochs (blue). Solid lines indicate normalized power averaged across the cohort and shading indicates 95% confidence intervals. For the ET cohort power in the high beta range does not alter during movement (violin plot, inset). B) In the ET cohort there is a significant reduction between rest (blue line) and movement (red line) in the mean high beta burst duration (violin plot, inset). C) PD patients showed the same pattern of results with no change in high beta power between rest and movement epochs but D) a reduction in high beta burst duration during movement compared to rest (conventions the same as panels A and B). E) The PD cohort had a significantly higher mean high beta power during movement when compared to the ET cohort. By contrast there was no significant difference between the mean high beta duration for the ET and PD cohorts during movement (F).

The majority of the literature reports a decrease in motor cortical beta power during movement,[29,86,193] and it may be the case that this was not observed in the current experiments due to our limited analysis of the high beta band. It is surprising however that both the ET and PD cohorts display a decrease in beta burst duration during movement. This finding verifies that the underlying pattern of beta bursting can alter between conditions with no gross impact on overall measurements of power in the same period. For power to remain stable one might expect therefore that the amplitudes of beta bursts are increased during movement (to compensate for their reduced duration) or that the incidence is increased (again to compensate for their reduced duration). These explanations are unlikely in view of previous findings by Lofredi that beta burst amplitude and rate (for clarity we will hereafter refer to the per-second occurrence rate of bursting as the burst incidence) is decreased during continuous movement. Subsequent sections

explore these possibilities in the present data set and the results are presented below. It may be the case therefore that there is a 'flattening' of the high beta signal which attenuates the peaks of the beta oscillation (burst epochs) and increases the troughs of the oscillation amplitude (non-burst epochs), without reducing the overall power.

4.2.2 Burst characteristics during rest and movement

This section outlines results aimed at reconciling the lack of any change in overall high beta power with a reduction in beta burst duration across the high beta band for both ET and PD cohorts. Aspects of beta bursting that are explored include high beta burst incidence, the distribution of burst durations and burst amplitudes. It is important to distinguish burst duration distributions illustrated in this section from the burst durations across the frequency spectra in the previous section. Here the duration distributions represent the proportions of high beta bursts occupying windows of restricted burst durations (0-50 msecs, 50-<100 msecs, 100-<150 msecs…), whereas in the previous section the data represents the average duration of bursts in a particular frequency band. It can be seen therefore, that the latter measurement being an average burst duration, it is easily skewed by extreme values whereas the former is relatively invariant to changes in the frequency of outliers.

The results detailed here show that there was a significant decrease in high beta burst incidence per for the ET cohort (mean resting high beta burst frequency for ET = 2.05 bursts/sec, 95% CI +/- 0.09, mean ET high beta burst incidence during movement = 1.16 bursts/sec, 95% CI +/- 0.32, data normally distributed by AD test, two-sample t-test $p = 1.03 \times 10^{-5}$, z-value = 6.05,

see Figure 11, A). Burst duration distributions differed between rest and movement for the ET cohort (ET cohort KS test, $p = 0.01$, mean ET rest burst duration (μ) = 71.17 msec, 95% CI +/- 5.88 msec, ET move burst duration (μ) = 58.74 msec, 95% CI +/- 8.12 msec, data not normally distributed by AD testing $p < 0.05$, Mann-Whitney U test z-value = 3.06, $p = 0.0022$, see Figure 11, B).

There is also a significant decrease in PD burst incidence during movement compared to rest (mean resting high beta burst frequency for D = 1.9 bursts/sec, 95% CI +/- 0.057, mean PD high beta burst incidence during movement = 0.96 bursts/sec, 95% CI +/- 0.44, data normally distributed by AD test, two-sample t-test $p = 1.2 \times 10^{-6}$, z-value = 5.8, see Figure 11, C). However, despite showing a difference in the distributions of burst durations overall, the PD cohort did not demonstrate significantly different μ values for movement compared to rest (PD cohort KS test, $p = 8.0 \times 10^{-11}$, mean PD rest burst duration (μ) = 83.11 msec, 95% CI +/- 5.46 msec, PD move burst duration (μ) = 72.59 msec, 95% CI +/- 8.80 msec, data not normally distributed by AD testing $p < 0.05$, Mann-Whitney U test z-value = 1.75, $p = 0.08$, see Figure 11, D). The violin plot inset in Figure 11 offers some explanation for this incongruence. It appears that the interquartile range of the PD μ values is larger during movement than rest rendering it less likely that a statistical difference will be detected.

Burst amplitudes did not differ between rest and movement for the ET cohort (ET median resting high beta burst amplitude = 7917.2 a.u. 95% CI +/- 1938.7 a.u., ET median moving high beta burst amplitude = 6590.8 a.u. 95% CI +/- 2029.3 a.u., not normally distributed by AD testing $p < 0.05$, Mann-Whitney U test, z-value 0.79, $p = 0.43$, see Figure 11, E). The PD cohort showed the same pattern of results (PD median resting high beta burst amplitude = 10644.8 a.u. 95% CI +/- 1930.1 a.u., PD median moving high beta burst amplitude = 8761.2 a.u. 95% CI +/-

1555.0 a.u., distributions not normally distributed by AD testing $p < 0.05$, Mann-Whitney U test, z-value 0.93, $p = 0.35$, see Figure 11, E). There was no significant difference between high beta burst amplitudes when comparing ET and PD cohorts in either the resting state (Mann-Whitney U test, $p = 0.36$, see Figure 11, E) or the moving state (Mann-Whitney U test, $p = 0.40$, see Figure 11, E).

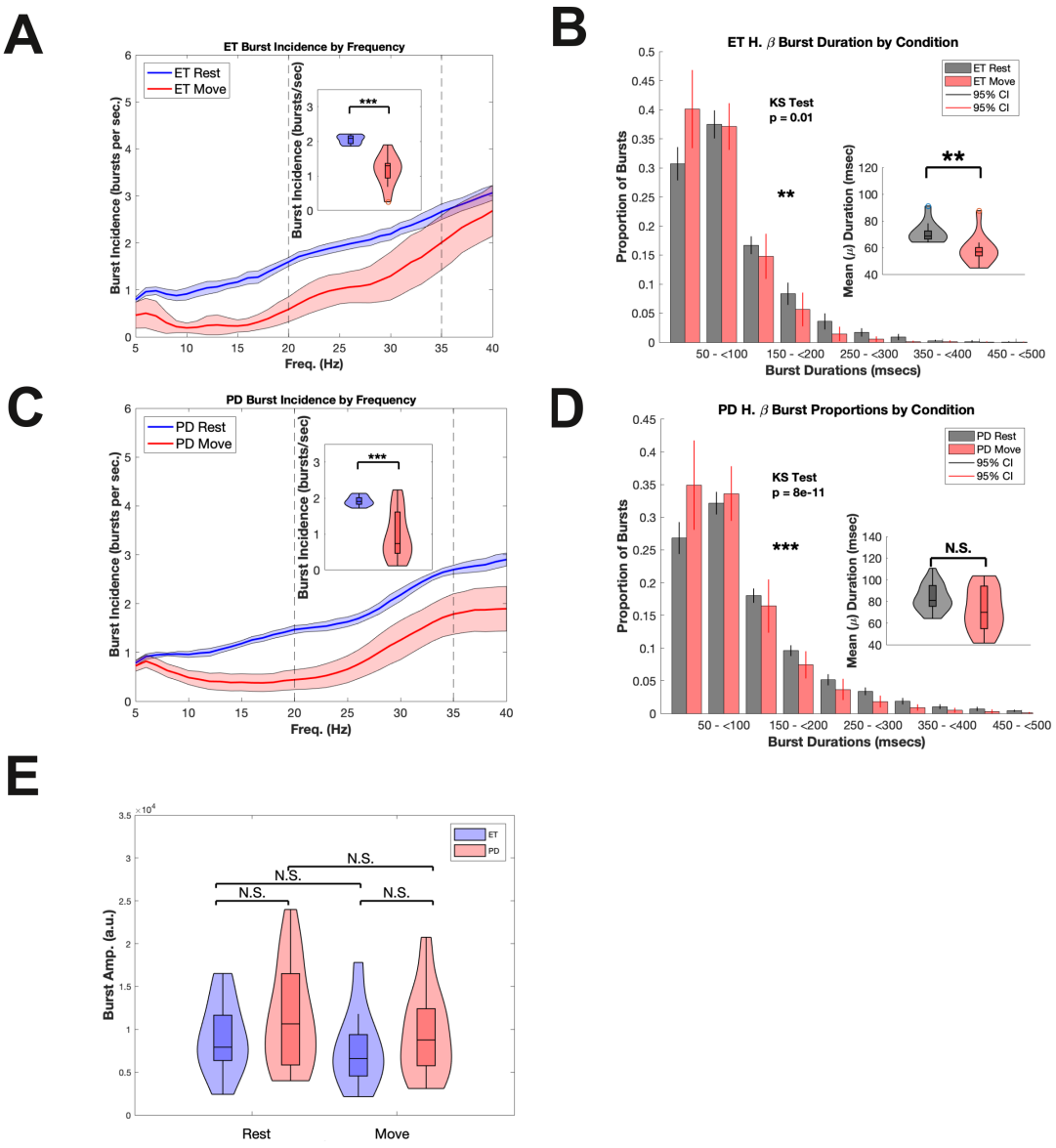

Figure 11. Beta burst incidence, duration and amplitude during rest and movement.

Burst incidence decreases during movement across the whole frequency spectra for both the ET cohort (A) and is accompanied by a significant change in the distribution of high beta burst durations (B) with a reduction in the average burst duration (inset violin plot, panel B). The PD cohort shows a similar reduction in the incidence of bursting across the high beta band (C) and does show a significant change in the distribution of beta bursts during movement compared with rest (D). Despite this the average high beta burst duration (inset violin plot, panel D) does not show a significant change between rest and movement. E) During movement there is no statistically significant change in the burst amplitude for the ET cohort (blue violin plots) or the PD cohort (red violin plots) although both show a weak trend towards a decrease in burst amplitude during movement compared to rest.

4.2.3 Burst Incidence and Burst Duration Cohort Comparisons

This analysis tested for high beta burst incidence differences between the ET and PD cohorts during different conditions of rest and movement. In the resting state there was a significant difference in high beta burst incidence when comparing ET and PD cohorts (data normally distributed by AD testing, $p < 0.05$, mean resting ET burst incidence = 2.047 bursts/sec, 95% CI +/- 0.099 bursts/sec, PD mean high beta burst incidence = 1.91 bursts/sec, 95% CI +/- 0.062 bursts/sec, Mann-Whitney U test z-value = 2.047, $p = 0.0216$, see Figure 12, A). During movement we found no significant difference between the ET and PD cohorts in terms of high beta burst incidence (data normally distributed by AD test $p = 0.47$, ET movement

high beta burst incidence = 1.088 bursts/sec, 95% CI +/- 0.26 bursts/sec, PD movement high beta burst incidence = 0.92 bursts/sec, 95% CI +/- 0.28 bursts/sec, see Figure 12, B).

High beta burst distributions during movement did not differ for the two cohorts significantly (KS test p = 0.4, Mann-Whitney U test z-value = -1.85 p = 0.06 see Figure 12, C). However, the distributions displayed a trend towards elevated high beta burst durations for the PD cohort compared to the ET cohort during movement, so the correlation between movement burst durations was tested against clinical rigidity scores. This showed that there was a significant correlation between contralateral rigidity scores and the mean burst duration (μ) during movement (data not normally distributed by AD test $p < 0.05$, Spearman's rho = 0.41, p = 0.020, see Figure 12, D).

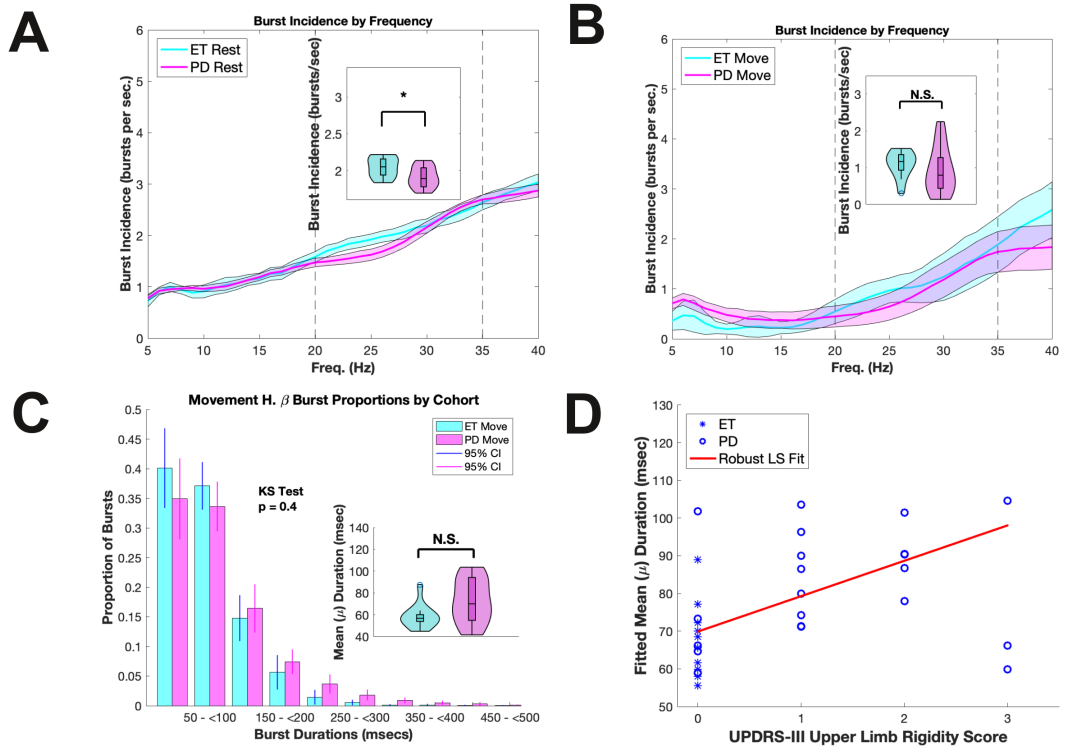

Figure 12. Cohort comparisons of burst incidence, burst durations and clinical correlations.

A) Burst incidence at rest showed that the PD cohort have a significantly reduced incidence of high beta bursting compared to the ET cohort. B) Group comparisons showed no difference between the cohorts in terms of high beta burst incidence during movement. C) Burst duration distributions were significantly difference for the ET and PD cohorts during movement. PD subjects showed an elevated proportion of longer duration bursts during movement when compared to the ET cohort. D) There was a significant correlation between the mean (μ) motor cortex high beta burst duration during movement for the cohort and contralateral rigidity scores on the UPDRS scale.

4.2.4 Power Changes and Burst Probabilities at Movement Initiation

The inability to identify overall decreases in beta power in the motor cortex during movement, as identified in previous literature relating to subcortical structures[24], could be due in part to a concentration of movement related beta suppression in the low beta band but could also be due in part to the temporal pattern of high beta suppression during movement and the nature of the movement task employed here. Indeed, previous studies of motor cortical beta oscillations show a transient decrease in beta power which rectifies over the time course of a prolonged movement.[194,195,196] For this reason our paradigm tested the duration of beta suppression in the motor cortex for each of our cohorts after movement initiation. Wavelet analysis was used to extract the power spectrogram for 7 seconds before and five seconds after the initiation of movement for each subject in each cohort. Power spectra were normalized to the first two

seconds (-7 to -5 seconds where 0 is the point of movement onset) of the extracted time series segments in order to yield a decibel (dB) quantification of power around the time point of movement initiation. A permutation analysis with $p <= 0.05$ threshold for significant voxels and a $p <= 0.05$ cluster analysis was applied to the data for each cohort separately. This data-driven analysis approach revealed that the ET cohort undergoes a short, approximately 2 second decrease in the power spectra centered upon the beta band (see Figure 13, A and B). Likewise, the PD cohort undergoes a short duration beta-band centered power suppression in the motor cortex immediately after movement onset (see Figure 13, C and D), however, this appears to be prolonged in duration compared to the ET cohort with a temporal duration of approximately 3 seconds.

The burst incidence surrounding movement was calculated for each cohort by dividing the time series surrounding movement onset into 500 msec intervals, each constituting a time bin. A burst was counted as occurring in a bin if any part of the burst overlapped with that time bin. A binomial distribution used to calculate probability of burst incidences referenced to probability of burst occurring during baseline, -7 to -5 seconds, and Bonferroni-Holm family-wise error rate correction applied for multiple comparisons. Both cohorts showed a reduction in the probability of high beta bursts occurring after movement (see Figure 13, E and F), however the ET cohort showed a reduction in high beta bursting approximately 1 second prior to movement onset.

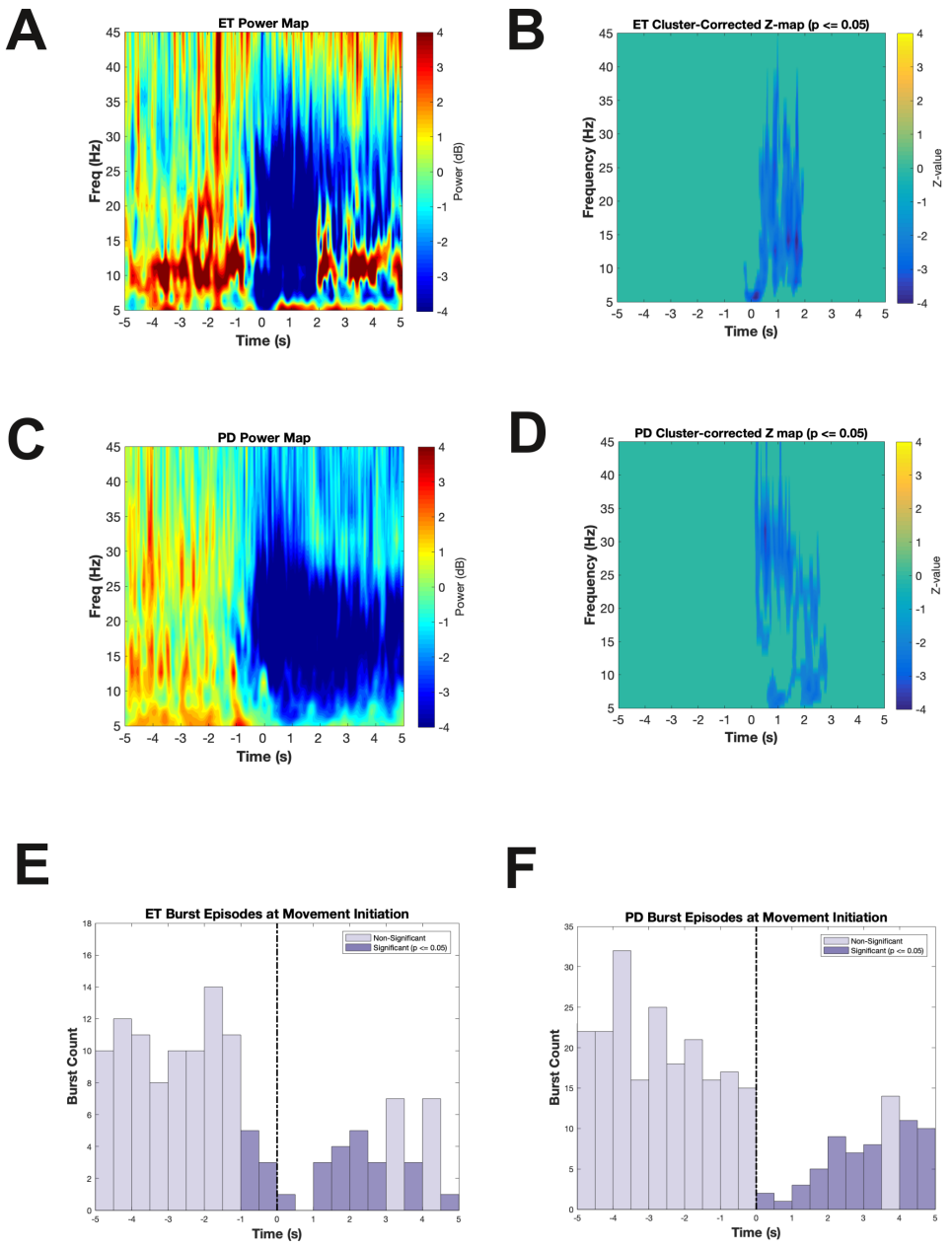

Figure 13. Power changes and burst probabilities at movement initiation.

Time frequency spectrograms of ET and PD cohorts at the onset of movement (0 seconds). A monte-carlo permutation analysis utilizing 500 shuffled time-series (voxel p <= 0.05) was used in conjunction with data-driven cluster analysis (cluster p <= 0.05). This shows that in the ET cohort there is a brief 2 second reduction in power across the entire beta band (12Hz-35Hz) but that this differs for the PD cohort which shows a more prolonged beta depression lasting approximately 3 seconds after movement initiation. In both cohorts any reduction in oscillatory power has disappeared by three to five seconds post-movement initiation. Burst frequency at time of movement initiation was calculated compared to baseline burst incidence (time -7 seconds to -5 seconds). E and F show that in both ET and PD cohorts the burst incidence is diminished immediately after movement onset. In the ET cohort (E) the decrease in burst incidence occurs approximately 1 second prior to movement onset. By contrast the PD cohort (F) does not demonstrate significant burst incidence reduction until after movement has been initiated.

4.3 Synchrony Changes Related to Movement

The exploration of rest and movement synchrony difference takes initial focus on the periods of high beta bursting explored in depth in the rest analysis in Chapter 3. Our resting analysis showed that the PD cohort has higher pre-burst cortical synchrony compared to the ET cohort (see Figure 6, A and B). Chapter 3 also presented evidence that high beta premotor-motor synchrony increases in advance of burst onset (see Figure 6, C and D) and evidence was also

presented there to show that increased cortico-cortical synchrony could be driving motor cortical bursting. Initial investigations in this section therefore focused upon establishing whether similar patterns of synchrony increases preceding beta bursts obtained in the movement phases of the recordings. The general theory of Parkinson pathophysiology proposed in previous sections predicts that high beta bursting characteristics such as synchrony, waveform changes and PAC will remain constant across rest and movement conditions but that bursting will become less frequent during movement, lifting the physiological tamponade on cortical movement plan development and execution. The latter was demonstrated in the previous section where it was shown that movement is associated with a decrease in burst duration and burst incidence for both cohorts. In that section is was also shown that although motor cortex power is unchanged for both cohorts during movement compared to rest, both cohorts display a short-lived decrease in beta power at the onset of movement and this coincides temporally with a reduction in the probability of beta bursts.

The following sections demonstrate that the resting pattern of synchrony preceding burst onset is replicated for movement epochs before proceeding to show test the hypothesis that delayed reduction in burst probabilities for the PD cohort is linked to a reduced capacity for reducing cortico-cortical synchrony prior to movement onset.

4.3.1 Movement Synchrony-Burst Relationships Recapitulate Resting Results

Comparison of the premotor-motor synchrony during burst and duration-matched pre-burst epochs shows that for dwPLI there is an increase in synchrony during bursting compared to non-bursting for both cohorts (data normally distributed by AD test, ET mean pre-burst dwPLI =

0.50, 95% CI +/- 0.025, ET mean burst dwPLI = 0.67, 95% CI +/- 0.025, repeated measures t-test t-stat = -14.26, $p = 1.75x10^{-7}$, PD mean pre-burst dwPLI = 0.54, 95% CI +/- 0.023, PD mean burst dwPLI = 0.70, 95% CI +/-0.031, repeated measures t-test t-value = -15.05, $p = 1.01x10^{-12}$, see Figure 14, A). The ET and PD cohorts showed no significant difference in pre-burst dwPLI (mean ET pre-burst dwPLI = 0.50, mean PD pre-burst dwPLI = 0.54, two-sample t-test t-value = -2.71, p = 0. 11, see Figure 14, A). There was no significant difference between ET and PD cohorts for the cortical high beta dwPLI during bursting (mean ET bursting dwPLI = 0.66, 95% CI +/- 0.025 , mean PD dwPLI during bursting = 0.73, 95% CI +/- 0.031, two sample t-test t-value = -1.15, p = 0.26, see Figure 14, A).

Repeating the analysis with PSI yielded similar results. There was a significant difference in bursting PSI when compared with pre-bursting PSI for both the ET and PD cohorts (data normally distributed by AD test, ET mean pre-burst PSI = 0.70, 95% CI +/- 0.037, ET mean burst PSI = 0.87, 95% CI +/- 0.042, repeated measures t-test t-stat = -20.35, $p = 7.77x10^{-9}$, PD mean pre-burst PSI = 0.76, 95% CI +/- 0.023, PD mean burst PSI = 0.91, 95% CI +/-0.025, repeated measures t-test t-value = -22.39, $p = 4.44x10^{-16}$, see Figure 14, B). For the PSI comparisons there was no significant difference between cohorts for the burst epochs however the pre-burst PSI again differed between cohorts with the PD cohort showing a significantly higher level of synchrony before bursting when compared with the ET cohort (data normally distributed by AD testing, ET mean pre-burst PSI = 0.70, 95% CI +/- 0.037, PD mean pre-burst PSI = 0.76, 95% CI +/- 0.023, two sample t-test t-value = -2.19, p = 0.036, see Figure 14, B).

The previously stated hypothesis asserts that the timing of synchrony changes associated with bursting will remain stable across rest and movement conditions. The following analysis therefore compared the timing of synchrony onset surrounding bursting in movement conditions.

The first derivative of dwPLI increases at burst onset mirrored the results observed during the rest analysis. Taking the data for ET and PD cohorts together the mean time of dwPLI increase relative to burst onset was -20.07 msec, 95% CI +/- 5.0 msec, compared with the mean time of maximal amplitude increase at -2.58 msec, 95% CI +/- 1.07 msec. This yields a temporal precedence of -20.07 – (-2.58) = -17.49 msec, suggesting that dwPLI increases anticipate amplitude increases during bursting by approximately 17.49 msec. This relationship is illustrated in Figure 14, C. PSI demonstrated a very similar relationship (mean time of maximal PSI increase -21.12 msec, 95% CI +/- 4.95 msec, see Figure 14, D). The distributions of amplitude and synchrony increases were significantly different during movement (data not normally distributed by AD test, test statistic = 2.02 , $p = 5.0 \times 10^{-4}$, Mann-Whitney test for amplitude increases versus PSI increases z-value = 6.45, $p = 1.14 \times 10^{-10}$, Mann-Whitney test for amplitude increases versus dwPLI increases z-value = 5.29, $p = 1.23 \times 10^{-5}$, see Figure 14, E). These findings replicate closely the synchrony timing findings observed in the rest condition.

Finally, comparisons were made for the timing of amplitude, PSI and dwPLI increases for rest and movement in order to demonstrate that the relationship between synchrony timing and beta bursting remains unaltered during movement compared with rest. When comparing rest with movement there was no significant difference in the timing of amplitude increases (two sample t-test, t-stat = 0.26, p = 0.80), PSI increases (two sample t-test, t-stat = 0.24, p = 0.81) or dwPLI (two sample t-test, t-stat = -1.25, p = 0.22), again supporting the hypothesis that the characteristics of beta bursting per se remains relatively unchanged across conditions.

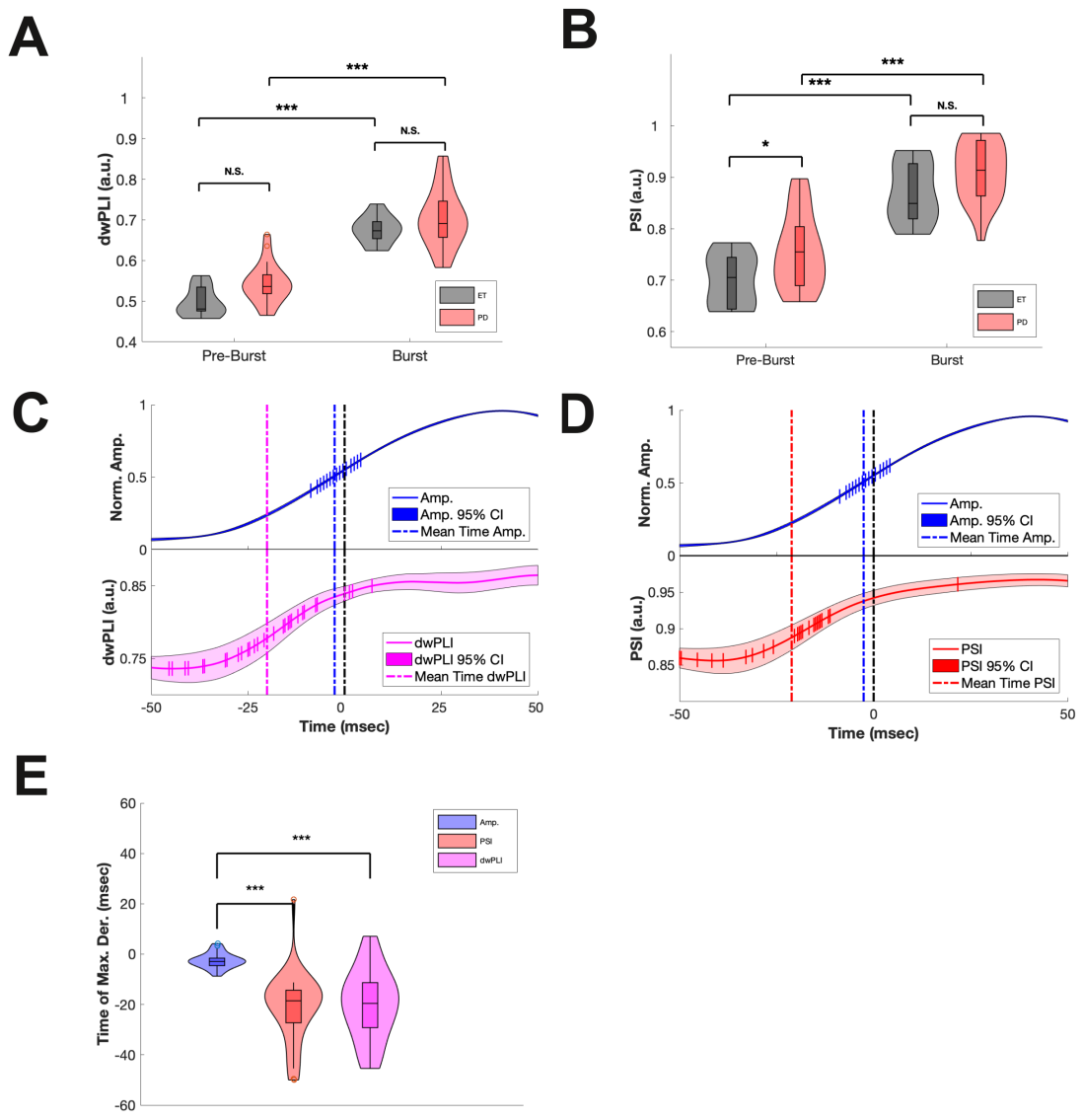

Figure 14. Synchrony changes at beta burst onset during movement.

A) Analysis of dwPLI between motor and premotor cortex for bursts occurring during movement yielded very similar results to the synchrony rest burst analysis. There was no significant difference between the ET and PD cohorts for mean synchrony during the pre-burst (left hand violin plots) and burst episodes (right hand violin plots). For both cohorts the increase in synchrony during bursting compared to pre-burst epochs was robust and highly significant. B) PSI mean burst synchrony showed a similar pattern with the

exception that, as for the resting burst synchrony analysis, there was a significantly higher level of synchrony for the PD cohort (red violin left side) than for the ET cohort (black violin left hand side) during the pre-burst interval. C) and D) show that the timing of synchrony increases for bursts occurring during the movement phase was almost identical to the results obtained for the same analysis performed during rest (see Figure 6, C and D). Both measures of synchrony increased prior to the onset of bursting at -17.49 msec for dwPLI, and -18.54 msecs for PSI.

4.3.2 Burst Synchrony Does Not Differ Between Rest and Movement Conditions

The model of bursting and PD pathophysiology outlined in earlier chapters predicts that there will be no difference in burst synchrony characteristics during rest and movement. To advance the evidence base for this hypothesis, comparisons between burst synchrony for rest and movement epochs were made for both cohorts.

There was no significant difference in burst synchrony for either cohort when resting burst dwPLI was compared to moving burst dwPLI (data normally distributed by AD testing, ET bursting dwPLI during rest compared to movement, t-test t-value = 1.03, p = 0.32, PD burst dwPLI during rest compared to movement, t-test t-value = 1.16, p = 0.25). Neither the ET cohort nor the PD cohort showed a significant difference in burst PSI (data normally distributed by AD testing, ET bursting PSI during rest compared to movement, t-test t-value = -0.39, p = 0.70, PD burst PSI during rest compared to movement, t-test t-value = -0.19, p = 0.85). Pre-burst synchrony also did not differ significantly between the resting and moving conditions for either cohort (data normally distributed by AD testing, ET pre-burst dwPLI during rest compared to

movement, t-test t-value = 0.34, p = 0.74, PD pre-burst dwPLI during rest compared to movement, t-test t-value = 1.04, p = 0.30). No significant differences were observed across conditions for PSI in either cohort (data normally distributed by AD testing, ET pre-burst PSI during rest compared to movement, t-test t-value = -0.33, p = 0.74, PD pre-burst PSI during rest compared to movement, t-test t-value = 0.40, p = 0.69). These results confirm the predictions of the hypothesis that the synchrony aspects of bursting do not alter between resting and movement conditions.

4.3.3 Synchrony Suppression at Movement Onset

The previous section demonstrated that the time point of movement onset is accompanied by a decrease in the probability of beta bursting (1 second prior to movement onset for the ET cohort and immediately after movement onset for the PD cohort). If beta bursting is driven by increases in cortico-cortical synchrony then reduced beta bursting ought to be associated with a suppression of synchrony. The hypothesis at hand would predict that the timepoint of movement onset, when the probability of beta bursting is abruptly reduced, will be accompanied by a reduction in cortico-cortical synchrony, the purported driver of beta bursting. This question was approached in a similar fashion to the movement initiation analysis of power in the foregoing section. Segments of the time series 5 seconds before and after movement were convolved with 20 wavelets covering 5 to 45Hz. Phase information was extracted from the analysis for both motor cortex and premotor cortex. PSI was then calculated between motor and premotor cortices for each frequency. Because absolute PSI levels varied across frequencies the approach feature scaled PSI over the movement initiation period by dividing each time point by

the sum of the PSI values across the 10 second movement initiation period. This allowed for construction of a time-frequency map of synchrony surrounding movement onset. A Monte-Carlo permutation analysis (voxel p <= 0.05, cluster p <= 0.05) showed that the ET cohort transiently decreased their cortical synchrony 1 second prior to the initiation of movement (see Figure 15, A and B). There was no similar statistically significant decrease in synchrony for the PD cohort (see Figure 15, C and D).

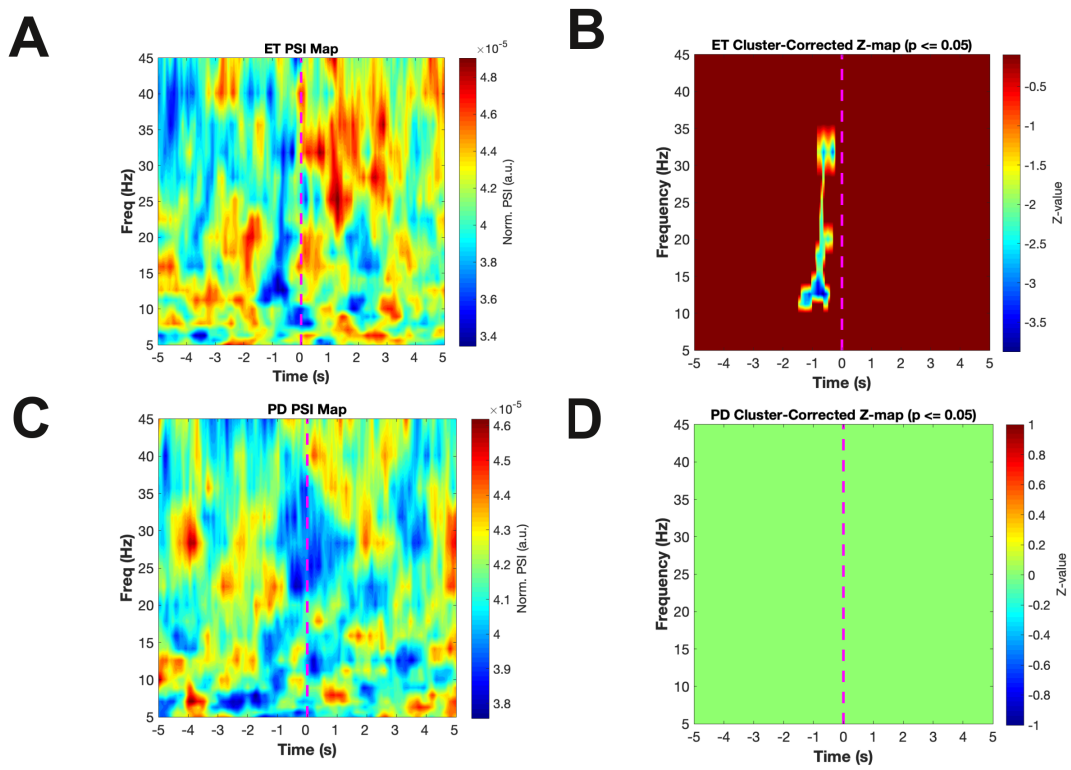

Figure 15. Synchrony changes at movement initiation.

A) Time frequency maps of PSI show the synchrony changes between motor and premotor cortex at the time point of movement onset (t = 0, magenta broken line on figures A to D. B) The results of the Monte Carlo permutation analysis show that for the ET cohort there is a

transient reduction in cortico-cortical synchrony immediately prior to movement. This synchrony decrease takes place in frequencies between 10 and 35 Hz, the beta range. C) and D) The PD cohort do not demonstrate a statistically significant decrease in beta synchrony prior to the moment of movement initiation.

4.4 Burst Waveform During Movement

At rest, waveform changes during burst episodes were found to be stereotyped increases in the ratio of falling steepness and increases in the sharpness of peaks relative to troughs. This can be thought of as a shift in waveform shape away from a symmetrical sinusoidal waveform shape, towards a 'sawtooth' pattern of oscillation (see Figure 8, A). The hypothesis outlined in the introduction states that this change may reflect an increase in the ability of lower frequency oscillations to bind their higher power counterparts via PAC. This has been supported by evidence in the previous chapter that shows PAC is significantly increased during episodes of bursting compared to non-burst episodes. One of the central tenets of this thesis is that high beta bursts are episodes crucial to the regulation of voluntary movement. Previous analyses have helped to depict these episodes of the local field potential as stereotyped episodes of waveform change driven by high cortico-cortical synchrony and characterized by their ability to bind high frequency oscillations to lower frequency phases.

The objectives in this section are therefore threefold; first to demonstrate that episodes of beta bursting in rest and movement are comparable in terms of waveform characteristics and second, to establish that the deficits in PD waveform magnitude change shown at rest are

replicated during movement beta bursting. Finally, this section aims to show that waveform sharpness and steepness ratios remain constant as the probability of beta bursting is modulated around movement intiation.

This study first tested the difference between bursting and non-bursting waveform shapes during movement. The analysis replicated findings obtained during rest and showed that there was a shift during bursting towards a sharper trough and steeper falling phase of the beta oscillation during the burst episodes of movement epochs (analysis for whole cohort, MANOVA with bursting/non-bursting as the independent variable, sharpness and steepness ratios as dependent variables, $d = 1$, $p = 2.0 \times 10^{-4}$, see Figure 16, A). Contrary to the predictions outlined above there was no significant difference between the ET and PD cohorts for movement waveform shape during non-burst (MANOVA, $d = 0$, $p = 0.33$, see Figure 16, B) or bursting episodes (MANOVA, $d = 0$, $p = 0.69$, see Figure 16, B). When the cohorts were taken together as a whole there was a significant reduction in the waveform asymmetry of bursts during movement compared to rest (MANOVA, $d = 1$, $p = 4.11 \times 10^{-5}$, see Figure 15, C). Both cohorts also showed this same result when taken individually (ET cohort burst waveform rest compared to movement MANOVA, $d = 1$, $p = 0.0068$, PD cohort burst waveform rest compared to movement MANOVA, $d = 1$, $p = 0.012$).

The hypothesis as stated previously did not predict significant differences between burst waveforms during rest and movement so the subsequent analysis focused upon the movement initiation epochs when the waveform changes are most likely to be taking place. Movement initiation points were extracted for all subjects and segmented into 0.5 second windows between -7 and 5 seconds, where 0 is the time of movement onset. Peaks were then identified that lay within these windows and simultaneously partook in a burst episode. The corresponding troughs,

rising, and falling phases were also extracted from the time series. For each identified bursting peak-trough complex peak:trough sharpness ratios and rising:falling steepness ratios were calculated in the standard manner described above. Baseline ratios between -7 and -5 seconds prior to movement onset were calculated in order to test the significance of changes in peak:trough ratios and rising:falling ratios a movement initiation. The results are presented in Figures 16, D and E. 16 D shows the temporal evolution of peak:trough ratios as movement is initiated. Testing was non-parametric (AD test $p < 0.05$, single tail Mann-Whitney U test, $p <= 0.05$) and showed that there was a significant increase in peak:trough ratios (indicating a more symmetrical waveform shape) from 3 second prior to movement onset and persisting almost uninterrupted until 3 seconds following movement initiation. The waveform shape assumes a relatively sharper peak compared to trough from one second prior to movement onset. The same result was not observed with rising:falling steepness ratios, as shown in Figure 16, E (AD test $p < 0.05$, single tail Mann-Whitney U test, $p <= 0.05$), in this case a 500 msec increase preceded movement onset by only 2 seconds before returning to baseline for several seconds with another significant period of steepness ratio change at 0.5 seconds following movement initiation. A further period of significant steepness ratio change was observed at 3.5-5 seconds following movement. Again, during these periods the waveform assumes a relatively steeper rising phase compared to falling phase. These results are depicted together in Figure 16, F as a time-dependent shift in waveform shape towards a more symmetrical waveform morphology with sharper peaks relative to troughs. Of note is the fact that although the statistically significant changes in waveform shape emerge as early as 3 seconds before movement onset (see Figures 13, D and E) the change in waveform morphology is led primarily by alterations in the sharpness of peaks increasing relative to the sharpness of troughs.

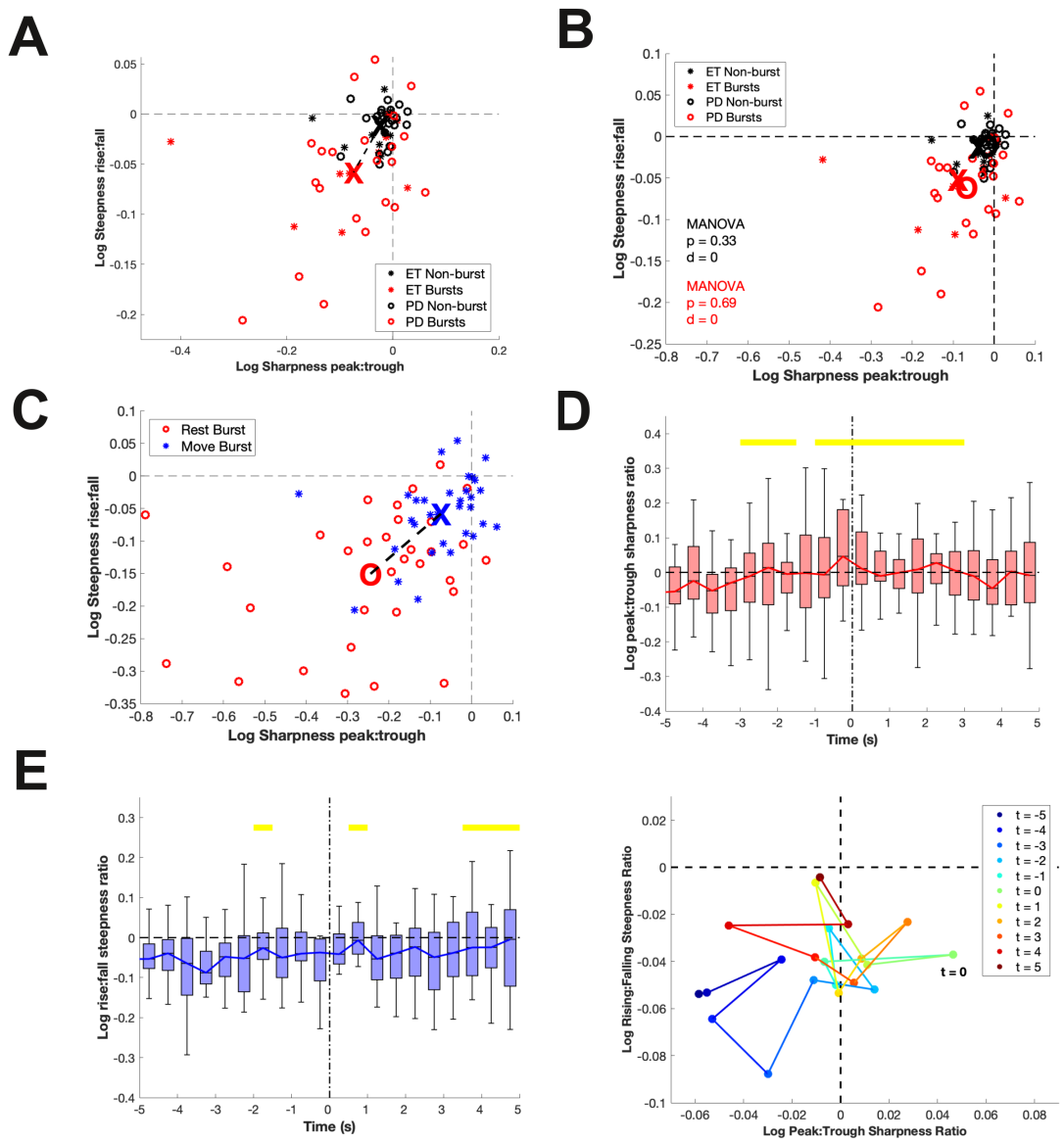

Figure 16. Waveform changes at burst onset and movement initiation.

A) During movement the differences between high beta waveform shape in bursting versus non-bursting mirror those observed at rest. Compared with non-bursts the bursting waveform is more asymmetrical with sharper troughs compared to peaks (negative

deviation on the x axis) and steeper falling phases compared to rising phases (negative deviation on the y axis). Large black 'X' indicates the centroid for the whole cohort non-burst waveforms during movement, the large red 'X' indicates the centroid for waveforms for bursting during movement. B) Similar to resting results, during movement there was no difference between ET and PD cohorts in terms of their high beta waveforms during bursts versus non-bursts. The large black 'X' is the centroid of ET non-burst waveforms, the large red 'X' indicates ET centroid for bursting waveforms, the large black 'O' is the centroid for PD waveform during non-bursts, and the large red 'O' is the centroid for PD burst waveforms. C) We found that there was a significant difference between high beta bursting waveforms at rest (large blue 'X' marks the resting burst centroid) and the high beta bursting waveforms during movement (large red 'X' marks the moving beta burst waveform centroid). We investigated the timing of high beta waveform changes at movement onset. D) Shows that peak to trough ratios change significantly 1 second prior to movement initiation (here denoted by t = 0 seconds). The red line indicates median burst peak:trough ratio and red bars indicate the interquartile range for that 500 msec time window. The yellow bar indicates the times showing a significant change from baseline (-7 to -5 seconds prior to movement onset). E) A similar result obtained for rising:falling steepness ratios (conventions the same as in D) however the increase in rising:falling steepness ratios occurred 0.5 seconds prior to movement initiation and was more short-lived than the changes in peak:trough ratio. F) When depicted on a two-dimensional plane waveform changes can be seen to adopt a trajectory towards a movement-like symmetry almost 2.5 seconds prior to movement onset. Here time is denoted by the colors of the markers, blue indicates resting burst waveform shape, green denotes movement onset, and

red hues denote moving burst waveform shapes. Movement onset occurs at time t = 0 seconds.

4.5 Effects of Movement on Phase-Amplitude Coupling

Following the preceding analysis identifying deflections in waveform shape at the time of movement initiation, the focus of the analysis turned to PAC during movement. PAC has been closely related to waveform shape and in studies investigating PAC in the STN there has been close correlation between waveform asymmetry and PAC.[58] While it is important to note that waveform asymmetry can bias detection of PAC it is incorrect to conclude that PAC does not reflect a physiological mechanism for neural communication. This is because waveform changes can be induced by either statistical coupling of distinct oscillators in low and high frequency ranges or by synchronous synaptic firing of neural inputs causing a waveform asymmetry of a single oscillator.[145,197] In the present scenario we have demonstrated that waveform asymmetry does change during bursting and non-bursting epochs of motor cortical neural oscillations in the high beta range. Both waveform changes or statistical alignment of independent oscillators may reflect important means of communication between cortical areas and so our analysis using PAC is justified on the basis that it aims to reveal significant alterations in cortical physiology that accompany movement, although the conclusions are limited to speculation as to the precise origin of these observed changes. The hypothesis outlined initially predicted that high beta bursting would remain stable during rest and movement however the foregoing section has

shown that burst waveforms alter during the movement period compared with rest. The waveform analysis identified a transition to a more symmetrical waveform shape that begins at 3 seconds before movement initiation. This result gains significance in the light of previous results that show beta burst probability in the ET cohort diminishes significantly 1 second prior to movement onset, this anticipatory effect was not observed in the PD cohort. Similarly, the ET cohort were shown to undergo transient motor-premotor cortex reductions in PSI throughout the beta band occurring one second prior to movement onset. Again, this was not present in the PD cohort.

The previous findings led to an adjustment of the initial hypothesis and a proposal that beta bursts are not invariant with respect to movement. It is still maintained that they are synchrony driven episodes of inhibition that stabilize cortically realized movement routines but they appear to demonstrate some flexibility around periods of transition from a resting to a moving state. This may be for example, due to a reduced amplitude of beta bursts (and so subtler waveform shift) prior to movement onset, in an effect that mirrors the observed reductions in beta burst probability at movement onset outlined previously. The foregoing results therefore do not invalidate the hypothesis that beta bursting is a stable phenomenon in voluntary movement, but rather they can be seen as a special instance of burst variation brought about by subtle shifts in the stochastic nature of beta oscillations.

In the coming section this study sets out to establish first whether burst and non-burst epochs differ in terms of PAC during movement in the same way that PAC has been shown to differ during resting bursts compared to resting non-bursts. Second, the approach aims to test the hypothesis that beta burst PAC levels will not differ between rest and movement as predicted by

a general view of beta bursting as invariant across these conditions. Third, this section tests the proposal that ET and PD cohorts will not differ in terms of burst-related PAC during movement.

The first comparison of non-burst and burst epochs during movement shows that for the cohort as a whole there is an increase in PAC during bursting episodes. This appears to be concentrated in the high beta band and involves a comodulation of high beta phase with gamma amplitude at approximately 80Hz (see Figures 17, A and B). Our analysis shows that there is a statistically significant difference between PAC in the high beta range during movement associated bursting compared to movement associated non-burst episodes when the cohort was tested together as a whole (data not normally distributed by AD test $p < 0.05$, Mann-Whitney U test, mean high beta MI for movement non-burst $= 1.17 \times 10^{-5}$, 95% CI +/- 6.24×10^{-6}, mean high beta MI for movement bursts = 2.58×10^{-4}, 95% CI +/- 1.5×10^{-4}, z-value = -4.12, p = 3.77×10^{-5}, see Figures 17, A and B). This replicates findings from the resting analysis showing a pronounced increase in PAC for high beta bursts compared with non-burst epochs. Contrary to the predictions of the hypothesis our analysis found a statistically significant difference between bursting PAC during movement and bursting PAC during rest for the whole cohort (data not normally distributed by AD test $p < 0.05$, mean MI for high beta burst during rest = 6.75×10^{-4}, 95% CI +/- 2.88×10^{-4}, mean MI for high beta burst during movement = 2.58x10-4, 95% CI +/- 1.50x10-4, Mann-Whitney U test z-value = 2.94, p = 0.0033, see Figures 17, C and D).

The final comparison tested for significant differences in high beta burst PAC between the ET and PD cohorts during movement. We found that there was no significant difference in high beta burst PAC during movement when comparing the ET and PD cohorts (mean ET high beta movement burst PAC = 2.78×10^{-4}, 95% CI +/- 3.29x10-4, mean PD high beta movement burst PAC = 2.45x10-4, 95% CI +/- 1.80×10^{-4}, Mann-Whitney U test z-value = -0.39, p = 0.70,

see Figures 17, E and F). From inspection of our comodulograms in Figure 17, E it was felt that the differences between the cohorts may be restricted to a high beta low-gamma (65- 90 Hz) PAC which appeared more prominent in the PD cohort during movement-related bursting. For this reason a subsequent post hoc analysis was performed for this region of the comodulogram to test the difference between the cohorts. Once again, no statistically significant difference was found between the ET and PD cohorts for high beta burst PAC during movement when testing for high beta (20-35 Hz) coupling to a restricted gamma band of 65-90Hz (mean ET high beta burst PAC during movement = 2.94×10^{-4}, 95% CI +/- 2.85×10^{-4}, mean PD high beta burst PAC during movement = 5.15×10^{-4}, 95% CI +/- 4.15×10^{-4}, Mann-Whitney U test z-value = -0.47, $p = 0.64$, see Figures 17, E, white broken lines, and Figure 17, F, violin plots to the right). To conclude, a correlation analusis between UPDRS-III hemibody bradykinesia/rigidity scores and the levels of high beta to restricted gamma PAC during movement-associated bursting was performed. This too proved non-significant (data not normally distributed by AD testing, $p < 0.05$, Spearman's rho = 0.97, $p = 0.60$).

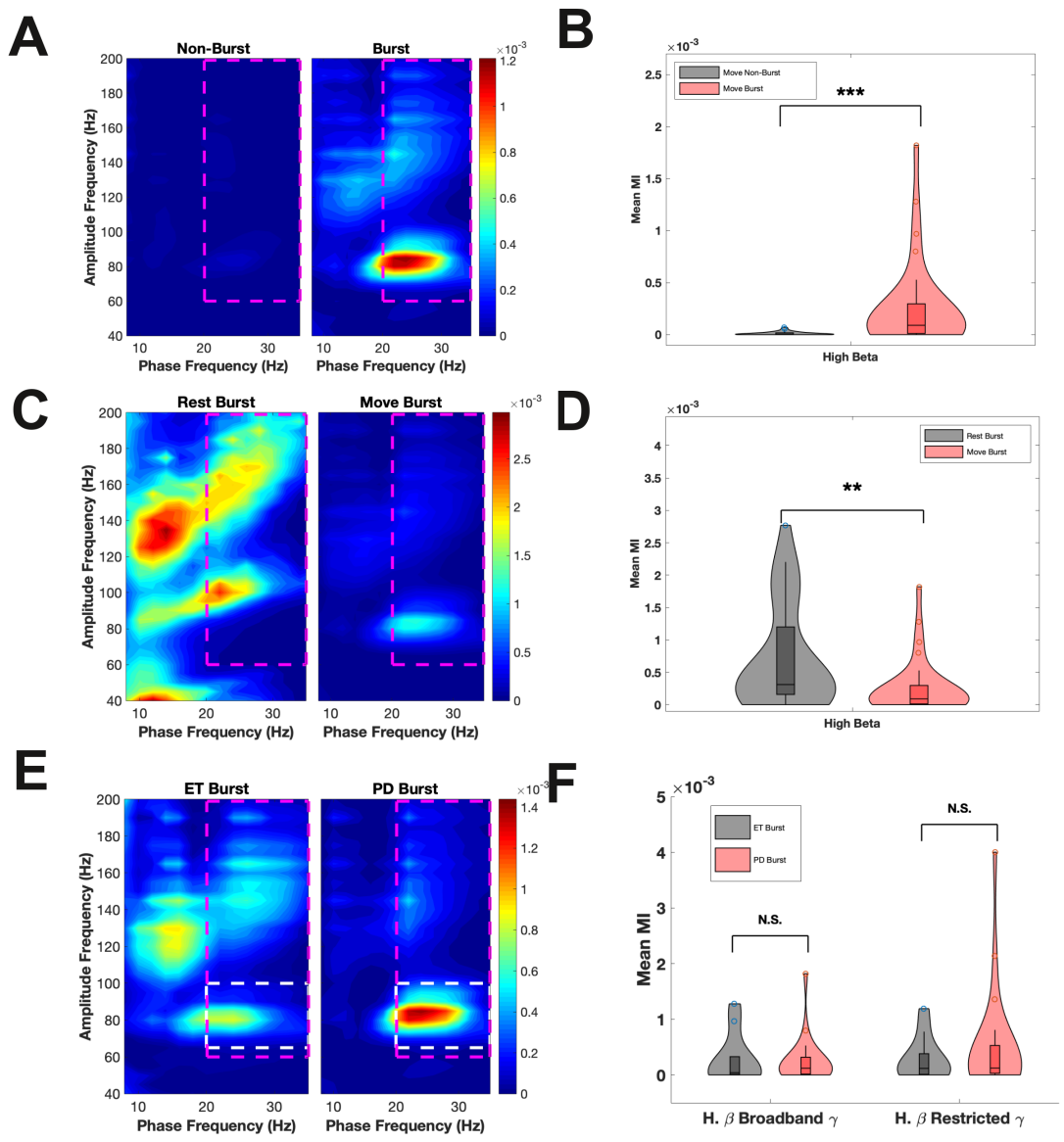

Figure 17. Phase-amplitude coupling changes during rest and movement.

A) During movement an increase in high beta-to-broadband gamma PAC was observed during burst episodes (right comodulogram) compared to non-burst episodes (left comodulogram). This replicated the resting results and proved highly significant as shown in panel B. C) Comodulograms for resting burst and moving bursts adjusted to the same

scales illustrate that resting bursts are characterized by significantly stronger high beta-to-broadband gamma PAC. D) This reduced PAC during movement bursts was statistically significant. E and F) There was no significant difference between the ET and PD cohorts when bursting high beta-to-broadband gamma PAC was compared (magenta broken lines on comodulograms and left hand violin plots), or when high beta-to-narrow band gamma (65-100 Hz, white broken lines on comodulograms and right hand violin plots) was analyzed.

4.6 Chapter Discussion

Parkinson disease is classified primarily as a movement disorder although there are doubtless widespread effects of the condition throughout the nervous system and indeed, some subtle features are frequently evident prior to clinical diagnosis.[198] The central pathological finding in PD is the loss of dopaminergic neurons in the substantia nigra of the basal ganglia that results in reduced dopaminergic input, particularly to the striatum. A large body of literature has linked this dopamine depletion to increased power of beta band oscillations in the STN the reduction of which correlates with symptomatic improvements.[181] Pathological synchronization in PD has also been linked to PD movement symptoms both for synchronization between sub-cortical structures[199] and between cortical areas.[118] Numerous features of neural oscillations in commonly studied anatomical locations have been found to relate to the movement deficits in PD including beta band stability in the STN,[12] absolute changes in STN beta power,[137] cortical somatomotor mu rhythms,[200] cortical network connectivity,[201] and subcortico-cortical coherence

suppression.[202] However, the majority of these findings are circumstantial and lacking in a rationale as to the mechanistic roles for the neurophysiological relationships they uncover. The foregoing chapter has attempted to delve deeper into the questions that underlie some the features of neural oscillations related to PD symptomatology. Cued movements in PD patients undergoing awake implantation of DBS leads was chosen as a model to investigate these phenomena. The analyses have built upon traditional analyses of power[83] and PAC[203] relationships as well as incorporating two relatively recent fields of interest, namely beta burst analysis[25] and waveform analysis.[183] This summary reviews previous studies relating electrophysiological findings to the movement impairments of PD and then proceeds to describe how the findings of this study can be integrated into a broader body of work to augment the understanding of the pathological processes at work in the parkinsonian brain.

4.6.1 The motor cortex and 'idling rhythms'

Early indications that beta oscillations played an important role in the electrophysiological changes of PD used EEG to non-invasively record from patients making wrist and elbow movements on and off levodopa.[83] This study analyzed EEG in 12 patients after overnight levodopa withdrawal and subsequently 1 hour after administration of levodopa. The results identified reduced alpha and beta band power over the motor areas contralateral to movement occurring 1 second prior to movement onset, and furthermore, found that this correlated with improvements in the size and speed of movements resulting from levodopa administration. Interestingly, when wrist and elbow movements were combined simultaneously, there was a correlation between premotor cortex alpha/beta desynchronization and movement

parameters, most prominently for bradykinesia. The authors proposed that the basal ganglia were responsible for releasing the frontal cortices from 'idling rhythms' that were preventing movement selection and execution.

Further evidence was developed in support of the 'idling rhythms' hypothesis by studies employing invasive and non-invasive recording techniques. In a study with non-parkinsonian subjects Cassim et al showed that the power of cortical beta oscillations was reduced at movement onset and returned to baseline within 4-5 seconds of movement initiation for sustained movement paradigms. Kondylis et al used a combination of MEG and recordings from DBS electrodes implanted in the GPi to show that in the motor cortex contralateral to movement there was a decrease in low beta oscillations (13-21 Hz) spatially and temporally coincident with a decrease in frequency matched beta coherence between the cortex and the GPi.[86] Similar to previous studies these changes began at around one second prior to movement onset and were largely resolved by 3 seconds post movement initiation.

Early models of beta oscillations in the motor cortex proposed that 'idling rhythms' exerted their movement-inhibitory effects by impairing the ability of higher amplitude gamma oscillations from becoming coherent during the execution of a movement plan.[204] A landmark study of epilepsy patients with implanted subdural electrodes demonstrated an anticipatory reduction in cortical beta-band power in four subjects making self-paced hand movements. Notably, decreases in cortical beta around movement onset were paired with simultaneous increases in gamma activity at the same spatial locations.[205] A finding which seemed to fit well with the notion of beta suppressing the emergence of spatially localized gamma oscillations.

'Idling rhythms' were also proposed to be exerting a feed-forward influence on cortico-spinal tracts to exert their movement-inhibitory effect. However, several studies investigating the relationship between cortical oscillations and EMG have failed to find PD specific electrophysiological markers in the interactions between muscle activity and cortical oscillations.[206,207] This implied that the electrophysiological deficits associated with PD symptoms were more central in origin. The concept of 'idling rhythms' was also challenged by detailed ECoG studies of the human cortex which found that beta suppression lacked the spatial specificity to fulfil a purely movement inhibitory role as claimed by the hypothesis.[208] The idea that idling rhythms lacked explanatory power for the PD pathological state was suggested by studies looking at the modulation of cortical power bands during the application of dopamine. These have failed to find significant differences in motor cortical power spectra on and off medication.[21] This result raises the possibility that while power changes during movement are an important feature of enacting movement plans they are not instrumental in preventing movement from occurring as has been suggested by some authors.[52]

4.6.2 Alternatives to cortical 'idling rhythms'

Karl Friston was one of the earliest proponents of what he called 'transient coding' as an alternative method by which neuronal communication may be established across spatially remote brain areas.[209] He suggested that the interactions of distinct neuronal populations can be mediated by "reproducible, highly structured spatiotemporal dynamics that endure over extended periods of time". The terminology of 'transients' is borrowed from analysis of non-linear

systems in which a transient refers to a self-limiting structured episode that a system passes through prior to settling into an attractor state. It has been established by prior work that the beta band does appear to display transient bursts of high power and that these phenomena can be related to the symptoms of PD. Vinding et al used MEG in a PD cohort compared to a healthy cohort to show that while off medication PD subjects have a 5-17% lower rate of cortical beta bursting compared to healthy controls. Importantly, the degree to which beta bursting rate was reduced correlated with severity of bradykinesia and postural tremor.[210] Additional support for Friston's proposal has been garnered from MEG studies of healthy individuals making finger movements to a congruent or incongruent cue.[211] This identified that beta bursting decreased in frequency and amplitude after a movement cue was presented and that a high frequency of bursts occurring in the movement preparation phase predicted slower reaction times once the imperative cue was presented. Beta bursting prior to movement and during movement was also topographically more localized than the power-based phenomenon of event related desynchronization in the beta band. These fascinating results embellish upon and provide support for the hypothesis of Friston that transients are performing an important computational role in the control and preparation of voluntary movement.

4.6.3 The Present Results Within the Framework of Beta Transients

The results detailed in this study build upon previous studies of cortical power and beta bursting during movement. The approach used here, targeting electrodes to lie directly over the motor cortex and premotor cortex, allows for the study of precise oscillatory changes that

accompany cued movements. Both ET and PD patients show transient beta power decreases specifically time-locked to movement onset (see Figures 13, A-D) but taken *en bloc,* there is no overall change in the power of the high beta band during movement compared to rest (see Figures 9, A and C). Both cohorts also demonstrated a highly significant reduction in beta burst duration and incidence when movement was compared with rest. A closer analysis of movement onset showed that beta burst probability decreased at movement onset and preceded movement onset by one second in the case of the ET cohort. In the context of Friston's hypothesis this difference in the timing of beta burst reductions between the cohorts could reflect an increased informational fluidity in motor cortical processing of the ET cohort, and may offer an explanatory framework for PD deficits. Congruent with this notion is the finding that beta burst duration at rest is prolonged in the PD state and that the degree of prolongation correlates with clinical scores of PD symptom severity.

The results described here can perhaps also offer some mechanistic insights into Friston's proposal for a framework of 'transient coding'. This study shows that beta bursts are preceded by episodes of high cortico-cortical synchrony, postulated to represent periods of high network synchrony throughout cortico-basal ganglia loops. This synchrony is shown to be subtly disturbed in the case of PD patients compared with the ET cohort, first in that pre-burst synchrony immediately prior to beta bursting, is elevated in PD subjects, and second, in that PD patients fail to show pre-movement synchrony suppression paralleling that of the ET cohort. Additionally, the results show that mean synchrony during bursting correlates with the severity of PD symptoms as measured by the UPDRS-III scores off medication. All of these findings point towards a pathological framework that sees PD as state in which synchrony is

pathologically increased resulting in disruption to the timing of finely tuned methods of neural communication, namely beta bursting.

Little et al[211] have shown that beta bursting in the motor cortex relates to movement planning and movement errors. The finding that ET subjects alter beta burst probabilities one second in advance of movement onset may reflect the selection of movement plans that permits activation of the a relevant movement plan at an appropriate point in time. The suppression of beta bursting in PD lags significantly behind the ET cohort and fails to anticipate movement. This could suggest that beta burst timing impairments are playing an instrumental role in movement initiation deficits and perhaps bradykinesia, observable in the PD state. In support of this hypothesis, Lofredi et al have found that beta bursting incidence predicts bradykinesia during the course of prolonged repetitive movements in blocks of movement.[24]

Running counter to this line of reasoning is the finding that there was no difference between the two groups in terms of high beta burst duration during movement (see Figure 10, F). Likewise, the burst duration distributions during movement were similar for the two cohorts (see Figure 12, C). Despite this, the ET and PD cohorts exhibited high beta burst durations throughout movement that correlated with PD severity (see figure 12, D). These findings are suggestive of an abnormal burst profile during movement that mirrors the pathological burst profile during rest for the PD cohort. It could be the case that subtle exaggerations of burst durations during movement are masked by variability in the severity of symptoms in the PD cohort and that these subtle pathological shifts in burst duration are only brought to light by statistical relation to the clinical severity scores.

4.6.4 Synchrony Changes Drive Beta Bursting

The phenomenon of local cortical synchrony changes has been closely investigated in human motor cortical literature. This section describes several studies that have touched upon the phenomenon of global cortical synchrony and related this to movement parameters in PD. This will form a theoretical framework in which to place the present findings regarding synchrony and the proposed relationship to beta power.

Silberstein et al used EEG in patients implanted with STN electrodes to show that generalized cortical coherence was reduced in a similar manner by both levodopa and stimulation. Reduced inter-regional cortical coherence was correlated with UPDRS motor scores in on and off states for both stimulation and on medication states. This study looked at coherence relationships over extended timescales (seconds to minutes) and as such, neglected to analyze data on the millisecond timescale with respect to movement. Nevertheless, it did identify two prominent frequency groupings of coherence-to-UPDRS score correlations that aggregated around the low-beta (9-18 Hz) and high beta (24-33 Hz) bands.[118] A similar approach was adopted by George et al to show that cortical coherence was abnormally elevated at rest in a PD cohort and that the degree of cortical coherence correlated with clinical impairment.[21]

Studies of propofol-induced anesthesia have demonstrated that although broadband spectral power (2-200 Hz) in sensorimotor cortices is increased during general anesthesia there is a simultaneous suppression of coherence, especially in the beta band.[149] Paradigms similar to this have identified that not only is beta coherence between the motor cortex and STN reduced during anesthesia but STN to motor cortex PAC is also reduced in concert.[143] Using MEG and a task

involving isometric contraction in a PD cohort, Pollok et al have showed increased supplementary motor area (SMA) to M1 coherence that is inversely related to UPDRS-III scores, the correlation was eliminated by treatment with levodopa. The authors proposed that this increased coherence represented a compensatory mechanism in the PD cortex rather than a pathophysiological marker of disease.[212]

Over longer timescales in monkey models Arce-McShane et al have found that learning a tongue protrusion task increased cortical coherence before and after force generation coherence in the beta (15-30 Hz) and gamma bands (30-50 Hz). Coherence between sensorimotor cortices in this model took several days to emerge.[213] Monkey studies have also permitted the simultaneous recording of multiple neuronal populations during hand movements. These paradigms have allow for the use of Granger causality analysis to determine the directionality of beta coherence in the sensorimotor cortex.[214] The results suggest that information flow is primarily from sensory (post-central gyrus) to motor (pre-central gyrus) cortex. This raises the possibility that elevated beta oscillations may reflect the sensory feedback to the motor cortex required to maintain the position and force generated by muscular contraction. These studies of synchrony throughout the cortex and across various timescales, point towards the phenomenon as an important means by which the cortex is regulating computational processes, be it learning, movement, or consciousness itself in the case of anesthesia experiments.

The present analysis aims to understand cortical synchrony in the context of beta bursting. The results show that at rest and during movement, synchrony increases appear to precede increases in beta amplitude by ~17 milliseconds. This temporal precedence was validated using alternative methods of determining the timepoint of synchrony increase as well as an *in silico* analysis of synchrony-amplitude relations. Permutation analysis was used to show

that the ET cohort, but not the PD cohort, exhibited a short period of cortico-cortical desynchronization at one second prior to movement onset (see Figures 15, A-D). This finding agrees well with the hypothesis that synchrony is driving beta bursting. In the framework of this hypothesis one would expect to see a decrease in beta bursting preceded by a reduction in cortico-cortical synchrony. The PD cohort did display a reduced probability of beta bursting at movement onset albeit on that was delayed by comparison with the ET cohort. This was however, present without a concomitantly delayed reduction in cortico-cortical synchrony. There are several potential explanations as to why this study failed to observe a decrease in cortico-cortical synchrony for the PD cohort. One explanation might be that the disordered temporal occurrence of beta bursting (reduced incidence at rest and delayed occurrence at movement onset) could reflect an inability of the cortex to adequately regulate the development of burst episodes. This would imply that synchrony and bursting were less well temporally locked to movement onset with the result that synchrony alterations became less prominent over a trial-aggregated level. This explanation proposes that the deep electrophysiological structure of PD pathology lies in an inability to regulate synchrony changes in a temporally precise manner.

It is interesting to note that although this study found only a trend towards increased movement-associated burst durations for the PD cohort compared to the ET cohort (see Figure 12, C), it nevertheless identified that the mean burst duration, as quantified by distribution fitting, was correlated with bradykinesia scores for the cohort as a whole (see Figure 12, D). It may be the case that disordered cortico-basal-ganglia synchrony manifests itself not only as delayed beta burst suppression at the time of movement onset, but also results in an impairment of beta burst termination once they have been initiated. In support of this idea Yeh et al have used empirical mode decomposition of beta bursts to analyze the changes that evolve over the period of a beta

burst.[64] This approach identified a decrease in the beta to gamma coupling and increased phase slips in the beta oscillations as beta burst amplitude declines over the course of a burst. This could plausibly reflect decreased beta phase synchrony across the cortex as phase slips are likely to reflect either entry to, or exits from, long-range cortical synchrony relationships.

4.6.5 Movement-Associated Waveform Changes

The analyses of waveform changes described above broadly supports the hypothesis that beta bursting waveform changes remain invariant across resting and movement conditions with one important caveat. Our results show that there was a shift in waveform shape between non-burst and burst episodes (see Figure 16, A) that was similar in direction to that observed during rest (see Figure 8, A). There was no difference between the waveform morphologies for ET cohorts in either the non-bursting or bursting states (see Figure 16, B). However, contrary to the hypothesis that the deep structure of bursts is invariant across rest and movement conditions, the results in this chapter show a significant difference in waveform morphology for high beta bursts occurring during rest compared with those occurring during movement (see Figure 16, C). Waveform morphology of movement bursts was less asymmetric than that observed during resting bursts, as shown by a shift in the burst waveform centroid towards the origin during movement (see Figure 16, C). Subsequent analysis of this change showed that there is an evolution towards a more symmetric waveform shape that begins three seconds prior to movement onset in the case of sharpness ratios and two seconds prior to movement onset in the case of steepness ratios (see Figures 16, D and E). Figure 16, F shows how the waveform

parameters change over movement onset in the two-dimensional waveform morphology space formed by peak:trough sharpness ratios and rising:falling steepness ratios.

The transition towards a more symmetrical waveform shape during movement anticipates the reduction in synchrony at the time of movement initiation in the case of the ET cohort, and also anticipates the reduction in beta bursting seen in both cohorts. There is a possibility that these phenomena are linked. Reduced synchrony could be driving a reduced probability of beta bursting at movement onset as described in previous sections. Reduced synchrony could also be reflected in waveform morphology changes.[180] It may be the case that the waveform changes identified three seconds prior to movement onset, reflect an early signal in movement preparation. Arguing against this explanation for the results are the findings outlined above that show no significant differences in the mean cortico-cortical synchrony of bursts when resting bursts are compared with moving bursts. One possibility is that waveform morphology changes of the type described above, reflect changes in the synchronicity of local circuits, afferent inputs or somato-dendritic potentials. Such local changes in synchrony would not be reflected in the interregional measures of synchrony employed in this study (PSI and dwPLI) and could form the basis for the representation of movement plans on a cellular or laminar level.

Because our waveform parameters (peak:trough sharpness ratio and rising:falling steepness ratio) approximate zero as waveforms become more symmetric, we acknowledge that our analyses may neglect important changes such as increased peak and trough sharpness, which if occurring simultaneously and in proportion to each other, will not be reflected in parameter ratios such as those used here. These changes might feasibly reflect important underlying neural processes. This study adopted a ratio-based approach despite this limitation because of concerns

that comparing waveform parameters in periods of differing amplitude (bursts versus non-bursts) could obscure interpretation of changes in waveform shape.

4.6.6 PAC Changes During Movement

Waveform asymmetries of the kind identified here have been linked to PAC in the human motor cortex[58] and the phenomenon of increased PAC has in turn been linked to PD symptoms.[26] This study proposed, on the basis of these previous findings, that high beta bursting acts as a distinct stereotyped episode in the neural time series and that it that has computational import for voluntary movement execution. The results detailed above show that beta bursts display higher levels of PAC than non-bursting episodes (see Figure 9, A) and it has been established by previous work that DBS of the STN reduces motor cortical PAC in tandem with symptomatic improvements.[27] Studies assessing the electrophysiological effects of DBS have sought to establish the cortical ramifications that might correspond to the symptomatic benefits offered by therapeutic stimulation. One such study published recently used MEG to demonstrate that STN stimulation results in a widespread reduction in alpha/beta oscillations across bilateral sensorimotor cortices.[117] This is particularly interesting in light of the study previously outlined[83] that related these oscillation bands to motor deficits in PD. Particularly noteworthy is the fact that the application of DBS was to unilateral STN in this study, yet power changes were observed over the somatosensory cortex bilaterally. This implies that the effects of DBS are capable of propagating widely throughout cortical movement-related regions. Similarly, strong connectivity exists between the bilateral STN and also between the STN and contralateral motor

cortex.[215] Using a very similar model to the one described in this dissertation, Malekmohammadi et al have shown that hand movement and stimulation of the GPi exert similar cortical effects.[50] In patients with GPi DBS stimulators in place, movement reduced power in both low and high beta bands of the motor cortex. These effects were independent for high and low beta bands as demonstrated by using a linear mixed effect model. Furthermore, PAC in the motor cortex was suppressed by movement and similarly by DBS of the GPi. The same effect has been noted during application of levodopa therapy in PD patients. This showed that levodopa therapy normalized motor cortical PAC levels to parity with non-parkinsonian matched control subjects.[216] Almost identical suppression of cortical PAC has been noted for stimulation of the STN as referred to previously.[27]

These studies have all lent support to the hypothesis that PAC in the motor cortex is acting to inhibit the development and execution of movement plans and that pathological levels of coupling between beta and gamma oscillations could be an important element in the producing the movement symptoms of PD. The findings here build upon this literature to show that PAC is not uniformly distributed throughout time in the high beta band but rather, high beta-to-broadband gamma is concentrated in beta bursts and these occur in a dynamic fashion throughout the time-course of cortical oscillations. Contrary to predictions of the hypothesis established at the outset of this study there was reduced PAC during beta bursting that occurred during movement compared to rest. Because beta bursting was constant in terms of amplitude across resting and moving conditions it is hard to ascribe this change to differences in the magnitude of beta bursting. This study did however, identify that beta bursts decrease in duration during movement compared to rest. Yeh et al have shown that PAC during beta bursting decreases as the beta burst terminates and that this is associated with increasing frequency of phase slips in

beta oscillations.[217] This study therefore implies that shorter beta bursts may have less time to develop PAC compared with longer bursts resulting in diminished overall beta to high-gamma PAC over the course of the burst. This might explain the findings related here of reduced burst-related PAC during movement.

Identification of waveform changes occurring early in movement initiation could have significance with respect to PAC. Sharp waveforms can lead to increased estimations of PAC in the absence of true covariation of high beta phase and gamma amplitudes.[179] Although this study does not specifically investigate this caveat here, the finding that PAC remains elevated in beta bursts occurring during movement in spite of significant shifts in waveform sharpness, argues against waveform changes impacting significantly upon the PAC results of the present study. It is interesting to note however, that both PAC and extent of waveform asymmetry are reduced during movement bursts compared with rest bursts. The finding that there is no difference in PAC between the ET and PD cohorts compared here suggests that it may not be PAC per se that is responsible for the symptomatic manifestations of PD.

Another possibility raised by the present findings is that both waveform morphology and PAC are indicators of local processing as opposed to global synchrony. Thus, beta bursting differences observed between the rest and movement states could reflect a modulation of the underlying cortical computations during these states. Such a view of PAC would remain consistent with the overall hypothesis as the overall role of beta bursting as a state of physiological tamponade is not changing but rather the underlying local computational processes associated with it are being modulated.

Chapter 5. Discussion

5.1 Major Findings

This chapter outlines the major findings from the rest and movement analyses and remarks upon their relevance to the hypothesis outlined at the outset of this investigation. To recap, the hypothesis proposed that PD is primarily a disorder of hypersynchronous neural oscillations propagating throughout the basal-ganglia-cortico-thalamic loops. An extensive literature referred to previously has led to the generation of this proposed pathological framework. Novel directions in PD research, namely, beta burst analysis, waveform analysis and PAC, have been described that could potentially link many disparate findings in PD research into a unified theory of PD pathophysiology. The theory proposed describes beta-bursting as being driven by increases in network synchrony and identifies these episodes as periods of exceptionally high PAC driven in part by changes in waveform morphology. The differences in bursting PAC during rest and movement can be explained in terms of PAC comprising a local processing signal and curtailed burst durations limiting the development of PAC during burst epochs. Furthermore, this study proposed that PD symptomatology derived in large measure from a disordered regulation of beta bursting which resultsin the subcortical and cortical changes documented in the PD literature, namely elevated cortical coherence,[21] increased beta burst duration[84] and increased cortical PAC.[26]

The hypothesis presented here takes as its core pathophysiology a postulated hypersynchrony of cortico-subcortical circuits in PD. The degree of synchronization during motor cortical high burst episodes was found to be related to UPDRS-III scores of PD severity. The analyses show that high beta waveform morphology is not static throughout the duration of motor cortical oscillations but varies with beta bursting in a stereotyped fashion. Waveforms become more asymmetrical during bursting for both ET and PD cohorts however, ET subjects show a statistically greater deflection in waveform shape towards a profile with a sharper trough and steeper falling phases when compared with waveform morphology changes in the PD cohort. It has been argued that this has import due to the fact that waveform morphology can reflect underlying synchrony of neural inputs[218] and neurotransmitter profiles.[175] Previous studies have linked waveform morphology tightly to PAC, a phenomenon strongly implicated in the pathophysiology of PD. Congruent with these previous reports, in this study the degree of stereotyped waveform change during bursting was correlated with UPDRS-III scores and similarly, correlated with the extent of burst-related PAC present at rest. This makes a direct link between three previously disparate neurophysiological entities, beta bursting, waveform dynamics and PAC, tying them all to clinical measurements of PD severity and providing support for the unified hypothesis of PD that was set out in the introduction.

This study identified several important findings during movement that also bear upon the hypothesis outlined in the introduction. The results show that there was no significant difference for resting compared to moving high beta power in either cohort when we took aggregated resting epochs for each subject and compared them with the aggregated moving epochs for each subject. Despite this our approach identified significant movement-related suppression of the entire beta band when the five seconds before and five seconds after movement initiation were

analyzed (see Figure 13, A-D). The temporary nature of this movement-related beta suppression (less than three seconds post-movement initiation for both cohorts) suggests that the period surrounding movement onset could represent a time of dynamic cortical attractor shift from a state inhibiting movement and preventing the instantiation of movement plans, to a state of attractor instability whereby movement plans can be enacted, developed and updated real time. If the hypothesis described is correct and beta bursting is transiently preventing these attractor shifts from taking place, then we would expect to see a reduction in the burst frequency when the updating of computations is required, and especially prior to the onset of a movement. Accordingly, this study investigated the incidence of high beta bursting and found that during movement there is a significantly reduced incidence of beta bursts as measured by bursts-per-second (see Figures 11, A and C). This would be predicted by the hypothesis under study if movement is seen as a state in which movement plans require continuous updating and modification by the motor cortex. The PD cohort showed a slightly more reduced high burst incidence at rest when compared to the ET cohort (see Figure 12, A) but there was no significant difference in burst incidence between the cohorts during movement (see Figure 12, B). Interestingly, while the duration distributions of high beta bursts changed for both cohorts during movement, only the ET cohort showed a significant decrease in the mu parameter (approximating mean high beta burst duration) when the distribution fitting models were compared. This was despite the PD cohort appearing to show a more significant shift towards an increased proportion of short duration high beta bursts during movement. The greater spread of mu values for the PD cohort during movement prompted testing of the correlation between mu and UPDRS-III scores. This showed significance and suggested that burst duration both during

rest and during movement can be related to PD symptomatology (see Figures 5, D and E for resting correlations, and Figure 12, D for movement correlation).

One interpretation of these findings is that the increased high beta burst duration during rest seen in the PD cohort, reflects an inability to develop the requisite movement plans required for the initiation of movement. This would result in poor movement initiation and arguably, bradykinesia due to continued inhibition of cortically generated movement plans. If Friston's notion of coding through transients is correct, then extended duration of transients would compromise the metastable state required for movement plan updating and execution. The inability of this study to identify extended beta burst durations compared with ET during movement might be supposed to be due to the fact that, during continuous movement, the movement plans have by definition already been developed, updated and executed, their maintenance placing a less computationally onerous burden on the cortex. Alternatively, if the generation of appropriate movement plans developed at rest is compromised by extended burst durations in the PD cohort, then bradykinesia and rigidity during movement can be seen as the downstream consequences of previously misconceived movement plans.

Having identified that beta bursting appears to change dramatically during movement despite no significant overall decrease in beta power this study attempted to clarify exactly how beta bursts change during movement. The analysis revealed that while the incidence of beta bursts decreases they remain similar in terms of their amplitude (see Figure 11, E). The combination of reduced burst incidence and static burst amplitude might be expected therefore to result in a reduction in high beta power which was not observed. One solution that could reconcile these seemingly contradictory results proposes that beta oscillations undergo a 'flattening' during movement with peaks and troughs becoming less prominent. This would

allow for decreased beta burst incidence (as peaks reaching the 75th percentile become less frequent) and permit overall beta power to remain unchanged, as troughs become shallower to compensate for the reduced number of beta peaks. This possibility could be investigated with a measurement such as the coefficient of variation, as described in the foregoing chapters.

The resting analysis showed convincingly that high beta bursting was preceded by increases in cortico-cortical synchrony between M1 and PM. This study developed and tested the hypothesis that synchrony changes in PD reflect a network level synchrony increase leading to disordered burst termination and resulting in the symptomatic features of PD. The results described have shown that synchrony does indeed appear to by dysregulated in the PD cohort. These patients failed to show a suppression of cortico-cortical synchrony prior to movement onset and at rest demonstrated higher pre-burst levels of synchrony on PSI and dwPLI measurements. The latter is sufficient to explain prolonged burst duration for this cohort during rest and would be predicted by the hypothesis at hand. The relationship between mean beta burst synchrony during rest and clinical scores of PD severity, again points towards a disordered synchrony drive in this cohort and relates it directly to the pathological expression of the disease state. Given the finding that synchrony increases precede those of beta amplitude it is natural to assume that the causal arrow, if there is one, points from synchrony towards beta power rather than vice versa. As stated previously, this is a finding in concert with several other investigations of phase and amplitude in the field.[168,80]

Waveform analysis in this study shows that beta bursts during rest and movement adopt a similar morphology with a tendency to become less symmetric during bursting compared to non-burst episodes (see Figure 8, A and Figure 16, A). Rest and movement beta bursts show significant differences in their degree of asymmetry however, with movement bursts being more

asymmetric than resting beta bursts in terms of their waveform morphology. Previous discussion has suggested the relevance of this finding for underlying synchrony of cortical inputs and the neurotransmitter profiles giving rise to these episodes. It has been proposed that the finding of increased waveform symmetry and decreased PAC during movement-associated bursts represents local processing changes allowing greater information flow as movement plans are updated and executed. Mapping out the time course of the two-dimensional change in waveform morphology shows that there is a deflection towards a more symmetrical waveform shape that appears to begin three seconds prior to movement initiation. The timing of this anticipatory change is most consistent with the development of a movement plan or 'model' in the motor cortices and supports our hypothesis as here stated. Alternatively, burst associated waveform changes could represent the development of a readiness potential, increasing as competing movement plans develop in the cortex and acting as a selective pressure to promote the most effective movement plan in a 'winner takes all' scenario. The previous possibility is more likely in light of the current results as burst-associated waveform symmetry appears to persist throughout movement epochs. A feature which would not be found with a 'readiness potential'.

Our findings are aimed at detailing the high beta burst changes in rest and movement for the motor cortices of two cohorts, one affected by PD, and another affected by a tremor condition that does not feature rigidity and bradykinesia amongst its symptomatology. Both cohorts underwent implantation of deep brain structures as a therapeutic intervention for their condition. These comparisons were chosen for their potential to shed light on the pathophysiology of PD, a common neurodegenerative disorder characterized by dopaminergic depletion of the substantia nigra.[219] The results have shown that PD electrophysiology displays several abnormalities when compared to ET under the assumption that ET is a good surrogate for the 'normal' motor cortical

functional state. The results have shown that episodes of transient bursting activity in PD are central to the pathophysiology of the disease and illustrate that high beta transients are a dynamic feature of cortical electrophysiology. High beta transients are preceded by increases in synchrony and in themselves constitute episodes of high synchrony, waveform change and raised PAC when compared to non-bursts. The hypotheses here examined have developed a correlational line of evidence to suggest that the symptoms of PD increase in proportion to the extended duration of high beta bursting in rest and movement. In the second prior to movement the ET cohort display a distinct pattern of changes in synchrony and beta bursting that is lacking in the PD cohort. Movement is proposed to be impaired in the PD cohort as a result of disordered synchrony acting to tamponade normal cortical processing required for the initiation, development and execution of movement plans.

5.2 Implications for Parkinsonian Pathophysiology

Parkinson disease has, for many years, been a field of intense study from clinical,[220] epidemiological[219], biochemical[221] and neurophysiological[185] perspectives. Despite this intense study the etiological origin(s) of the disease have so far eluded discovery. While it is known that PD exhibits widespread electrophysiological abnormalities in the beta range it remains unknown how precisely this relates to the symptomatic manifestation of the disease or how electrophysiological disturbances are precipitated by dopamine depletion.

Beta bursting abnormalities have been strongly implicated in the pathophysiology of PD by studies relating transient increases in beta power following movement offset,[222] dopamine-dependent modulation of beta burst durations,[84] and correlation of burst duration with clinical

impairment.[25] Studies using Go/NoGo tasks and dual coil transcranial magnetic stimulation in healthy subjects have highlighted a potentially important cortico-cortical communicative role for beta transients in the human cortex.[223] The latter study used motor-evoked potentials and simultaneous EEG to demonstrate that effective connectivity between pre-SMA and motor cortex cycled at ~20 Hz and was inhibitory during NoGo trials only. This implies that beta oscillations may be facilitating inhibitory communication between more frontally placed motor cortices and primary motor cortices.

The results presented here not only agree with and bolster the findings of foregoing research, but they suggest a new unified model of PD that reconciles contradictory findings in the field and embeds several strands of research into a framework of synchrony, waveform morphology and beta bursting. This study identifies a movement-associated reduction in beta burst probabilities which appeared to outlast the reduction in movement-associated beta power suppression (see Figures 13, A-F). In the ET cohort but not the PD cohort there was a reduced burst probability in the 1 second immediately prior to movement onset (see Figures 13, E and F). This deficit in pre-movement beta burst suppression may represent a global deficit in the ability of this cohort to terminate bursts or prevent the occurrence of bursts. To the best of our knowledge this phenomenon of pre-movement burst suppression has not been previously reported in the literature. Studies comparing self-initiated with externally-cued movements in PD have however, found that the deficit of movement initiation appears to be related to low beta pallido-cortical coherence suppression that correlates with bradykinesia scores on UPDRS-III scales.[202] The present study complements this finding by suggesting that high beta cortical bursting may be playing a mechanistic role in failure of movement initiation due to the reduced ability of the PD patient to terminate inhibitory cortical signals. It remains to be seen how, if at

all, these two signals are interacting to contribute to the deficits of movement initiation observed in PD.

Our resting analysis showed that PD subjects have both elevated high beta oscillatory power and elevated high beta burst durations at rest. Indeed, the results show that these two phenomena occur at similar frequency points in the high beta power spectrum. The analysis also demonstrated that elevated beta burst durations at rest were correlated with clinical scores on the UPDRS-III scale congruent with the previous studies focused upon this relationship during movement.[25] All subject groups exhibited a widespread modulation of the entire beta band after movement onset (see Figures 13, A-D). The rebound to baseline for both cohorts was 3 seconds post movement onset. The results outlined here did not identify a pre-movement decrease in beta power as has been identified in some previous studies.[224]

This dissertation has presented a convincing line of evidence to suggest that the occurrence of beta bursting in the motor cortex is preceded by increases in the synchrony between premotor and motor cortices (see Figures 6 and 7). This agrees with previous findings showing an increased frequency of phase-slips preceding the onset of bursts and implying that the conditions of synchronization between motor cortex and basal ganglia structures are established before crossing of the beta burst threshold in the cortex.[168] It is notable that the results presented here show a stark difference between the ET and PD cohorts in terms of cortico-cortical synchrony that appears contemporaneously with the reduction in beta bursting probability for the ET cohort. Figures 15, A and B, show that for the ET cohort there is a short-lived reduction in pre-motor-to-motor cortex synchrony 1 second prior to movement onset that is not observed in the PD cohort as shown in Figure 15, C and D. The hypothesis outlined here postulates that the cortical synchrony dynamics seen in ET are responsible for the reduction in

beta bursting prior to movement and that a delayed or disordered instantiation of this effect could help to account for aspects of the movement impairments seen in PD. Of particular relevance may be the deficit of internally-cued movement initiation which is a prominent feature of PD. Evidence exists to suggest that self-initiated movements in PD subjects requires greater degrees of cortical beta suppression than that required for non-parkinsonian subjects[202] and this could represent a compensatory mechanism for the deficit registered in the cohort under study here.

Lofredi et al have studied beta bursting in the STN during continuous movement and found that the percentage of time spent in a beta bursting state was a better predictor of decreased movement velocity than absolute beta power.[24] They also identified a decrease in beta burst rate and duration during movement. Our results broadly agree with those obtained by Lofredi et al. Although we did not look specifically at percentage of time spent in a beta burst as a proportion of movement time, our finding that cortical high beta burst duration decreases for both ET and PD cohorts (see Figure 10, B and D) fits well with their findings in the STN. In contrast to their results in the STN this study found that cortical beta bursting during movement did not show a reduction in amplitude compared to rest. This feature may be explained by the distinct nature of motor cortical bursting. Previous studies have shown that there is phase locking of STN background spiking activity to cortical oscillations in the beta range[69,168] and it could be that the reduced amplitude of beta bursting in the STN during movement is a result of reduced connectivity between the cortex and STN. Alternatively, reduced beta burst amplitude in the STN may reflect a requirement of ongoing flexibility of processing which is less pertinent to the cortex during the enactment of established movement plans. Nevertheless, our results are broadly in agreement with those of Lofredi in our finding of a correlation between high beta burst duration during movement and clinical scores of PD symptom severity (see Figure 12, D). This

congruence underscores the importance of beta bursting in the pathophysiology of the motor deficits of PD.

Waveform analysis shows that the beta oscillations of the motor cortex are asymmetrical in PD and that these waveform asymmetries appear to be reduced by therapeutic DBS.[58] Computational modeling has shown that waveform asymmetry could be induced by increased synchronicity of afferent inputs into a cortical region.[180] Evidence exists to suggest that waveform asymmetry can lead to elevated estimations of PAC as well as reflecting non-sinusoidal features of local field potential fluctuations, leading to some ambiguity surrounding what exactly is denoted by measurements of PAC.[225] This study finds that beta bursting in rest and movement is similar in nature, is driven by increases in cortico-cortical synchrony and appears to represent episodes of increased synchrony for motor cortical areas. Findings related here show that the average amount of synchrony during cortical high beta transients is correlated with the clinical deficits of PD. The results of this analysis failed to replicate previous findings by Cole et al showing that increasing beta oscillation sharpness ratios were correlated with increased UPDRS scores. Instead of a simple correlation between waveform sharpness and clinical scores, the present study found that PD symptoms correlated inversely with the magnitude of waveform change between non-burst and bursting waveforms. This is an important result as it buttresses our unifying hypothesis that beta bursting constitutes periods of exceptional importance in the cortical local field potentials. On the basis of current findings, it is argued that waveform changes during bursting are not a mere reflection of increased synchrony as the PD cohort shows no significant difference in the amount of overall synchrony during beta bursting when compared to the ET cohort (see Figures 6, A and B). Similarly, the two cohorts showed no significant difference in the centroids of their bursting and non-bursting waveforms (see Figure

8, E). Thus, the hypothesis posits that PD pathophysiology constitutes not only increased beta burst durations but a hypersynchronous cortico-cortical state that leads to extended burst profiles and a reduced ability to modulate waveform shape. This could be due in part to an increased resting non-burst cortico-cortical synchrony for the PD cohort (see Figures 6, A and B) however if this is the case then increased synchrony is not reflected in any difference of waveform morphology between the ET and PD cohorts (see Figure 8, E). Comparisons of waveform shape at the onset of movement show that there is a significant shift in waveform ratios well in advance of movement onset. The reduced waveform asymmetry, with peaks and troughs becoming closer in their sharpness values, occurs at three seconds prior to movement and remains in this morphological configuration until three seconds following movement onset. The proposed hypothesis raises the possibility that this trend towards burst waveform symmetry, reduced beta bursting and reduced cortico-cortical synchrony (identified in the ET cohort) represents a shift in cortical processing towards a more relaxed state in which new attractors (movement plans) can become enacted. Our data lacked the power to identify waveform changes in each cohort individually at the onset of movement, but a prediction can be made on the basis of the present findings, that deficits in bursting waveform modulation at movement initiation would also be found in the PD cohort when compared with healthy controls or the ET cohort. Studies of waveform evolution during beta bursting have shown that as a beta burst progresses there is a decrease in waveform symmetry and a reduction in beta-to-gamma PAC.[64] These studies utilized empirical mode decomposition, an approach to time-frequency analysis that has higher temporal fidelity than standard Fourier-based or wavelet analyses, and is less susceptible to bias of PAC. Our findings agree with these results in demonstrating a hypersynchronous cortico-cortical drive preceding beta bursts and an increased PAC during bursting. The presented data are consistent

with a model of burst-related PAC reducing during movement in order to permit development and updating of movement plans.

We show that burst-related PAC is reduced during movement compared to rest however, there does not appear to be a significant difference between ET and PD cohorts in terms of movement-related PAC during bursting in the studies detailed above. Foregoing chapters have proposed that this reduction in burst related PAC during movement could arise as a direct result of the curtailed beta burst durations observed during movement. PAC has been shown to evolve throughout the temporal course of a beta burst and it is likely that reduced beta burst durations will be associated with reduced PAC. Studies have shown that adaptive DBS curtailing beta burst duration in the STN is more effective than continuous or random DBS in controlling symptoms and symptom reduction has been associated with reduction in cortical PAC.[226] It may be the case that prolonged bursts representing extended episodes of PAC prohibit the exit of cortical networks from attractor states representing movement plans. The fact that this study found no significant difference between high beta burst PAC in the ET and PD cohorts suggests that levels of PAC during bursting cannot alone account for the movement deficits associated with PD. This challenges previous paradigms of cortical PAC as a biomarker of PD pathology[27] but also offers an explanation as to why PAC is not elevated universally in the motor cortex of PD cohorts. The concentration of high beta-to-gamma PAC in burst episodes means that overall PAC can appear relatively normal despite intermittent yet extended bursts of PAC episodes. Because PAC did not relate directly to the clinical manifestations of PD the present findings suggest that synchrony and waveform shape are the primary drivers of PD symptoms and observed increases in PAC represent a downstream consequence of this pathological state, related at least in part, to extended burst durations.

The studies here have focused upon the phenomenon of motor cortical beta bursting in PD. Several different approaches have been employed to characterize what is proposed to be a computationally salient feature of high beta oscillations. The foregoing chapters have shown that the PD state involves prolongation of beta bursting in the high beta spectrum and that this can also be associated with subtle deficits in synchrony and beta bursting surrounding movement onset. Several of the derived neurophysiological parameters have been correlated with the clinical symptomatology of PD such as mean burst cortico-cortical synchrony and mean burst duration in the high beta band. All of the factors here investigated have been linked to PD previously and in this thesis we hope to have gone some distance in clarifying how these factors interact and interrelate in a unified manner in the parkinsonian disease state. We have generated many hypotheses in the process that we hope will become the objects of further study in the field.

5.3 Study Limitations

In choosing the current experimental model to study beta bursting in PD we hoped that simplicity of technique and a sharp focus on anatomical location might assist in providing answers to some broad questions about the electrophysiological state of the diseased brain in PD. No doubt this has been successful by some small measure however it has also limited the number of questions this study was able to answer and to some extent, constrained the analysis of questions pertinent to the hypothesis. The dataset described here is deep and there are many questions answerable with it, only a small fraction of which the foregoing chapters have tried to

address. This section will identify limitations of the current approach and attempt to provide some solutions that can assist with experimental design in the future.

The present paradigm made opportunistic use of two cohorts of patients undergoing surgery for DBS implantation. ET and PD, as has been outlined previously, are both disorders of movement in which a tremor component is prominent however ET lacks the bradykinesia, rigidity and impaired movement initiation that is considered as central to PD. Unlike PD, ET is not characterized by a dopamine-depleted nigrostriatal system. The current study opted to explore the nature of PD pathophysiology by comparison with the ET state when it might have been equally justifiable to do the converse. Implicit in the choice of direction here was the assumption that ET is the 'more normal' state. Or at least, the paradigm must be supposing that the changes responsible for causing the symptoms of ET are unlikely to be similar to those causing PD. Furthermore, there are assumptions that the changes in ET are unlikely to influence the conclusions about the pathophysiology of PD in any major way. It goes without saying that the present methodology is entitled to none of these assumptions. The disease state of ET is probably less well characterized than that of PD and indeed there is a limited evidence base that suggests some similarity of dysfunction in these conditions with regards to movement-related power changes and cortical high beta-to-gamma decoupling.[86]

The problem of comparing two pathological cohorts is not insurmountable, though it does limit the kinds of answers that can be provided regarding PD pathophysiology. One way in which to resolve this issue is to seek to identify a 'more normal' cohort such as epilepsy patients. This patient cohort occasionally undergoes implantation of electrode grids as a means of locating epileptogenic foci for potential resection procedures. Following this procedure, they are often alert and able to engage in everyday tasks for several days while data is collected. A cohort such

as this may represent a 'more normal' control cohort than essential tremor patients and indeed there may even be useful lessons to be drawn from a three-way comparison involving all three cohorts. Of note however, is the fact that the epileptic brain is itself distinct from normal brains and indeed epilepsy, like PD, can be seen as a pathologically hypersynchronized state, albeit with hypersynchronous episodes occurring on a more infrequent basis.[227] There is also a recent trend towards viewing epilepsy as a network-level disorder rather than a disease arising solely from a restricted focus of abnormal tissue.[228,229]

The opportunities to record from non-pathological human cortex are few and far between. There are however, options to obtain invasive recordings from non-human primates and indeed a substantial body of literature has been generated from this approach.[169,230] The ethical debates surrounding this approach are in a constant state of flux[231] and the choice to subject sentient creatures to a potentially dangerous, painful and traumatic protocol should never be choice that is taken lightly. When the potential gains to our understanding of a disease such as PD are large, such approaches can be justifiable utilitarian premises. On a practical level, animal experiments can be extremely challenging, often involve low numbers of individuals and can be limited in the conclusions that can be drawn from them. There is no naturally occurring homologue of PD in primates and instead a parkinsonian state must be induced using neurotoxins, to some extent further limiting the conclusions that can be derived from these studies.[232] Non-invasive human studies of local field potentials using methodologies such as EEG and MEG are without doubt highly informative approaches to understanding the cortical pathology underpinning PD however, they too are limited in their spatial resolution and ability to measure high-frequency oscillations that are filtered out by tissues intervening between the cortical surface and the scalp. Although source localization algorithms are constantly improving, the upper limits set by the

laws of physics means that these approaches are unlikely to ever gain the spatial fidelity offered by direct cortical recordings.[233]

The experimental protocol described here is designed to be minimally taxing for patients emerging from anesthesia, easily executed under the restrictive circumstances of the operating room, and unimpeded by the limitations of head constraint in a stereotactic frame. A simple hand opening and closing paradigm in alternating 30 second blocks of rest and movement was deemed to be sufficient to generate enough data for analysis of movement execution while recordings were made from cortical and subcortical areas. The approach has succeeded on many levels however, certain refinements may render the protocol more standardized and facilitate comparisons that are difficult with our current approach. It would be useful for example, to know the exact point in time in which a movement cue was given. This would help ensure that movement preparation was limited to a well-defined temporal region of our recordings. An auditory cue generator may be well suited to use in the operating room. In order to ensure that patients were not able to anticipate movement cues it may be helpful to intersperse movement and rest periods in a semi-random fashion with temporal jitter and variable delays. A larger number of movement onset and offset episodes would assist with analyzing events such as bursting around movement onset. When designing the experimental protocol, the author was unaware of the extent to which phenomena such as bursting might be suppressed around movement onset, rendering statistically significant results hard to achieve by virtue of the small number of movement initiation episodes acquired.

The results have highlighted what are believed to be interesting and informative interrelationships between beta power, beta bursting, synchrony, waveform shape and PAC. The study has attempted to draw links between these features of neural oscillations but there remains

a large amount of work to be done to more precisely clarify the relations between these phenomena. Emerging evidence has closely linked PAC and waveform shape[179,58] while approaches such as empirical mode decomposition are making inroads on the analysis of the fine temporal structure of neural oscillations.[64] There nevertheless remain many questions about the extent to which these phenomena represent computationally important processes in the brain. Modeling of the mechanisms by which neuronal ensembles generate these electrophysiological phenomena[180] can give important insights into how the brain functions and yet we remain relatively unaware of the precise cellular events that give rise to many of these oscillatory features.

The relationship between PAC, waveform shape and synchrony must be explored in more detail with approaches such as empirical mode decomposition, single unit recording and optogenetic approaches to inducing hypersynchronous states. Ultimately the bringing to bear of novel technologies able to rapidly probe massive datasets on multiple dimensions may prove crucial to our understanding of how the brain generates voluntary movement.[234]

5.4 Future Directions

The process of investigating the hypothesis at hand has raised many interesting questions related to the current line of investigation that remain unanswered due to time constraints. Outlined here are some of the questions felt to be of interest and benefit for further study. The focus here will be upon the questions that align most closely with the joint objectives to improve

our understanding of PD pathophysiology and assist in the development of improved efficacy for treatment options.

The results detailed above have highlighted the limitations of time-invariant approaches such as simple power calculations, in the understanding of neural computations underlying movement. This study has shown that on progressively finer timescales, from beta bursting to individual waveform analysis on a cycle-by-cycle level there are important features relevant to pathology and worthy of ongoing study. One large question that arises naturally from these forays into the fine temporal structure of neural oscillations is how one can best analyze and understand them. This study adopted an approach that measured four parameters of the waveform, peak and trough sharpness, and the steepness of the rising and falling phases of the oscillatory cycle. These parameterizations have proved useful in developing an understanding of the contributions that waveform changes might be making to movement computations. It is not clear from the choices made here whether there may be more productive approaches to the study of waveforms. It may be the case for example that an individual cycle of a waveform is a relatively uninformative level on which to perform analysis. Could it be that the most relevant feature of a waveform is the temporal context in which it occurs? Rapid switching from sharp to symmetrical waveforms may also be performing a completely different role in neural computation when compared to a transition in the opposite direction. Indeed this has been suggested by the limited analyses of waveform shape as movement is enacted (see Figures 16, D-F) and by studies showing that waveform shape during beta bursting is itself a dynamic process.[235]

The analysis approach adopted here took the view that the high beta band should be considered as a whole. This was motivated by a desire for simplicity and standardization as well

as evidence that low and high beta bands are differentially modulated by movement in terms of their power and coherence.[50] On a group level the analysis of this band *en bloc* provided some good insights into the nature and timing of beta bursting as well as providing some suggestive findings regarding a computational role for the high beta band. Doubtless this was a benefit to some extent, of the relatively large cohort size and extended temporal durations of our recordings. Nevertheless, a more targeted and individually tailored approach to analysis of the beta band has also been shown to yield important results and may obviate the need for large cohorts and data sets.[80] One way that this can be achieved is through the identification of a salient feature in the power spectrum (although a salient feature in the PAC or burst spectrum may serve just as well) and use of this feature to delineate a band of frequencies for each participant. The drawback of this individualized approach to neural oscillations is that the analysis remains semi-arbitrary. A band of interest still must be pre-determined (in terms of width, frequency band in which it is to lie, and so on). Arguably, the analysis of different frequency bands for each participant also complicates the precise temporal comparisons that may be crucial to downstream analysis. On the other hand, it is unlikely that human brains replicate identical frequency profiles for encoding and computation. Indeed, the methods of processing information employed by each person's cortex are likely to be as diverse as human personas themselves.[236]

The present study found that the PD cohort does not appear to mirror the movement-anticipatory changes in beta bursting and beta synchrony that is shown by the ET cohort and the study has postulated that this reflects an element in the underlying pathological processes of PD. It remains to be seen whether the features here identified are truly representative of the pathological processes this study aimed to characterize. One way in which the data could bring to

light greater significance of the findings would be analyses to relate the temporal structure of neural oscillations to the pace and amplitude of hand movements. This approach holds the promise of providing firmer relationships between specific features of neural oscillations and specific pathological components of the UPDRS-III scale such as bradykinesia. Combined with an auditory cue as proposed previously, it would permit the study of movement initiation, potentially linking this feature to some of the underlying neural processes these experiments have been studying. It would be of particular interest to relate waveform dynamics of beta bursting to speed and amplitude of hand movements. The present hypothesis would predict that more asymmetric burst waveforms (found predominantly during rest) would be correlated with slower hand movements.

One of the elements studied here that would be worthy of deeper consideration is the precise reason for the absence of movement-anticipatory suppression of beta bursting in the PD cohort. This phenomenon may be due to an inability to prevent beta bursts from occurring (as a result of increased cortico-cortical synchrony for example) or it may equally be due to an inability to terminate already established bursts. Increased numbers of movement epochs would permit the study of this phenomenon in more detail and with sufficient quantities of data it may be possible to use the anticipatory beta burst reductions to predict time of movement onset or predict features of movement initiation such as acceleration.

This study has identified and characterized the role of cortico-cortical synchrony as a candidate driver for high beta bursting. This phenomenon was shown to reliably pre-empt the occurrence of a beta burst both in the resting and the moving state, raising the possibility that the standard mode of burst initiation takes place via increases in synchrony similar to those reported here. It may be worthwhile investigating whether synchrony plays a similar role in termination of

bursts. Recent studies have demonstrated that the dynamic evolution of beta bursting features reduced PAC, increased theta and increased phase slips in the beta range.[64] Techniques such as Granger causality analysis or dynamic causal modeling could prove useful in attempting to discern a causal relationship between phase synchrony and beta bursting in the motor cortex.

Finally, this study has hypothesized that beta bursting represents an inhibitory influence on the processing and updating of movement plans in the motor cortex. One hypothesis is that reductions in beta bursting at movement onset reflect a need for the motor cortex to implement novel movement parameters that can be thought of as an attractor state in the case of continuous movements. The current hypothesis predicts that movements requiring frequent updates in movement parameters throughout the movement (such as finger tracking of a moving target on a screen) would necessitate greater suppression of beta bursting during the movement. It would be of great interest to compare neural oscillations during this type of movement with similar tasks where movement updates were not necessary.

These investigations have certainly generated more questions than they have answered, and it will be the careful selection of future avenues of research that determines the lasting value of these foundation studies. Inspiration for this research has been drawn from a wide variety of clinical and neurophysiological research acting in concert to guide and refine the endeavor, and hopefully to propose some promising lines of inquiry for taking the field forward. The hard work and dedication of researchers in the neurosciences continues to yield extraordinary insights into some of the deepest aspects of human nature. It is with great excitement and anticipation that I look forward to making ongoing contributions to this field.

References

1. Parkinson, J. *An essay on the shaking palsy*. (London Printed by Whittingham and Rowland for Sherwood, Neely and Jones, 1817).
2. de Lau, L. M. & Breteler, M. M. Epidemiology of Parkinson's disease. *The Lancet Neurology* **5**, 525–535 (2006).
3. Yang, W. *et al.* Current and projected future economic burden of Parkinson's disease in the U.S. *npj Parkinsons Dis.* **6**, 1–9 (2020).
4. Hornykiewicz, O. & Kish, S. J. Biochemical pathophysiology of Parkinson's disease. *Adv Neurol* **45**, 19–34 (1987).
5. Queen Square Brain Bank (QSBB) criteria for PD diagnosis. *MIMS Ireland* https://www.mims.ie/news/queen-square-brain-bank-qsbb-criteria-for-pd-diagnosis-02-04-2013/ (2013).
6. Jankovic, J. Parkinson's disease: clinical features and diagnosis. *Journal of Neurology, Neurosurgery & Psychiatry* **79**, 368–376 (2008).
7. Ehringer, H. & Hornykiewicz, O. Verteilung Von Noradrenalin Und Dopamin (3-Hydroxytyramin) Im Gehirn Des Menschen Und Ihr Verhalten Bei Erkrankungen Des Extrapyramidalen Systems. *Klinische Wochenschrift* **38**, 1236–1239 (1960).
8. BIRKMAYER, W. & HORNYKIEWICZ, O. [The L-3,4-dioxyphenylalanine (DOPA)-effect in Parkinson-akinesia]. *Wien Klin Wochenschr* **73**, 787–788 (1961).
9. Samii, A., Nutt, J. G. & Ransom, B. R. Parkinson's disease. *The Lancet* **363**, 1783–1793 (2004).

10. Calabresi, P., Picconi, B., Tozzi, A., Ghiglieri, V. & Di Filippo, M. Direct and indirect pathways of basal ganglia: a critical reappraisal. *Nat Neurosci* **17**, 1022–1030 (2014).
11. Bratsos, S., Karponis, D. & Saleh, S. N. Efficacy and Safety of Deep Brain Stimulation in the Treatment of Parkinson's Disease: A Systematic Review and Meta-analysis of Randomized Controlled Trials. *Cureus* **10**, e3474–e3474 (2018).
12. Little, S., Pogosyan, A., Kuhn, A. A. & Brown, P. Beta band stability over time correlates with Parkinsonian rigidity and bradykinesia. *Exp Neurol* **236**, 383–388 (2012).
13. Kühn, A. A. *et al.* Pathological synchronisation in the subthalamic nucleus of patients with Parkinson's disease relates to both bradykinesia and rigidity. *Experimental Neurology* **215**, 380–387 (2009).
14. Kühn, A. A. *et al.* High-Frequency Stimulation of the Subthalamic Nucleus Suppresses Oscillatory β Activity in Patients with Parkinson's Disease in Parallel with Improvement in Motor Performance. *J. Neurosci.* **28**, 6165–6173 (2008).
15. Lang, A. E. *et al.* Posteroventral Medial Pallidotomy in Advanced Parkinson's Disease. *New England Journal of Medicine* **337**, 1036–1043 (1997).
16. Bergman, H., Wichmann, T. & DeLong, M. R. Reversal of experimental parkinsonism by lesions of the subthalamic nucleus. *Science* **249**, 1436–1438 (1990).
17. Levy, R. *et al.* Effects of Apomorphine on Subthalamic Nucleus and Globus Pallidus Internus Neurons in Patients With Parkinson's Disease. *Journal of Neurophysiology* **86**, 249–260 (2001).
18. Gatev, P., Darbin, O. & Wichmann, T. Oscillations in the basal ganglia under normal conditions and in movement disorders. *Movement Disorders* **21**, 1566–1577.

19. Kravitz, A. V. *et al.* Regulation of parkinsonian motor behaviours by optogenetic control of basal ganglia circuitry. *Nature* **466**, 622–626 (2010).

20. Brittain, J.-S., Sharott, A. & Brown, P. The highs and lows of beta activity in cortico-basal ganglia loops. *Eur J Neurosci* **39**, 1951–1959 (2014).

21. George, J. S. *et al.* Dopaminergic therapy in Parkinson's disease decreases cortical beta band coherence in the resting state and increases cortical beta band power during executive control. *NeuroImage: Clinical* **3**, 261–270 (2013).

22. Chen, C. C. *et al.* Excessive synchronization of basal ganglia neurons at 20 Hz slows movement in Parkinson's disease. *Exp Neurol* **205**, 214–221 (2007).

23. Wang, D. D. *et al.* Pallidal Deep-Brain Stimulation Disrupts Pallidal Beta Oscillations and Coherence with Primary Motor Cortex in Parkinson's Disease. *J. Neurosci.* **38**, 4556–4568 (2018).

24. Lofredi, R. Beta bursts during continuous movements accompany the velocity decrement in Parkinson's disease patients. *Neurobiology of Disease* 10 (2019).

25. Tinkhauser, G. *et al.* The modulatory effect of adaptive deep brain stimulation on beta bursts in Parkinson's disease. *Brain* **140**, 1053–1067 (2017).

26. de Hemptinne, C. *et al.* Exaggerated phase–amplitude coupling in the primary motor cortex in Parkinson disease. *Proc Natl Acad Sci U S A* **110**, 4780–4785 (2013).

27. de Hemptinne, C. *et al.* Therapeutic deep brain stimulation reduces cortical phase-amplitude coupling in Parkinson's disease. *Nat Neurosci* **advance online publication**, (2015).

28. He, X. *et al.* The patterns of EEG changes in early-onset Parkinson's disease patients. *International Journal of Neuroscience* **127**, 1028–1035 (2017).

29. Crowell, A. L. *et al.* Oscillations in sensorimotor cortex in movement disorders: an electrocorticography study. *Brain* **135**, 615–630 (2012).
30. Caton, R. The electric currents of the brain. *British Medical Journal* 278 (1875).
31. Berger, P. D. H. Über das Elektrenkephalogramm des Menschen. *Archiv f. Psychiatrie* **87**, 527–570 (1929).
32. Haas, L. Hans Berger (1873–1941), Richard Caton (1842–1926), and electroencephalography. *J Neurol Neurosurg Psychiatry* **74**, 9 (2003).
33. Loomis, A. L., Harvey, E. N. & Hobart, G. A. Cerebral states during sleep, as studied by human brain potentials. *Journal of Experimental Psychology* **21**, 127–144 (1937).
34. Palmini, A. The concept of the epileptogenic zone: a modern look at Penfield and Jasper's views on the role of interictal spikes. *Epileptic Disorders* **8**, 10–15 (2006).
35. Penfield, W. THE RADICAL TREATMENT OF TRAUMATIC EPILEPSY AND ITS RATIONALE*. *Can Med Assoc J* **23**, 189–197 (1930).
36. Penfield, W., Jasper, H. H. & Penfield, W. *Epilepsy and the functional anatomy of the human brain*. (Little, Brown, 1954).
37. Elias, W. J., Zheng, Z. A., Domer, P., Quigg, M. & Pouratian, N. Validation of connectivity-based thalamic segmentation with direct electrophysiologic recordings from human sensory thalamus. *NeuroImage* **59**, 2025–2034 (2012).
38. Buzsáki, G. & Draguhn, A. Neuronal Oscillations in Cortical Networks. *Science* **304**, 1926–1929 (2004).
39. Viswam, V., Obien, M. E. J., Franke, F., Frey, U. & Hierlemann, A. Optimal Electrode Size for Multi-Scale Extracellular-Potential Recording From Neuronal Assemblies. *Front. Neurosci.* **13**, (2019).

40. Mann, E. O. & Paulsen, O. Role of GABAergic inhibition in hippocampal network oscillations. *Trends in Neurosciences* **30**, 343–349 (2007).

41. Soplata, A. E. *et al.* Thalamocortical control of propofol phase-amplitude coupling. *PLOS Computational Biology* **13**, e1005879 (2017).

42. Gray, C. M., König, P., Engel, A. K. & Singer, W. Oscillatory responses in cat visual cortex exhibit inter-columnar synchronization which reflects global stimulus properties. *Nature* **338**, 334–337 (1989).

43. Sanes, J. N. & Donoghue, J. P. Oscillations in local field potentials of the primate motor cortex during voluntary movement. *Proc Natl Acad Sci U S A* **90**, 4470–4474 (1993).

44. Axmacher, N. *et al.* Cross-frequency coupling supports multi-item working memory in the human hippocampus. *PNAS* **107**, 3228–3233 (2010).

45. Steriade, M. Impact of Network Activities on Neuronal Properties in Corticothalamic Systems. *Journal of Neurophysiology* **86**, 1–39 (2001).

46. Nimmrich, V., Draguhn, A. & Axmacher, N. Neuronal Network Oscillations in Neurodegenerative Diseases. *Neuromol Med* **17**, 270–284 (2015).

47. Uhlhaas, P. J. & Singer, W. Abnormal neural oscillations and synchrony in schizophrenia. *Nat Rev Neurosci* **11**, 100–113 (2010).

48. Voytek, B. & Knight, R. T. Dynamic Network Communication as a Unifying Neural Basis for Cognition, Development, Aging, and Disease. *Biological Psychiatry* **77**, 1089–1097 (2015).

49. Holtzheimer, P. E. & Mayberg, H. S. Deep brain stimulation for psychiatric disorders. *Annu Rev Neurosci* **34**, 289–307 (2011).

50. Malekmohammadi, M., AuYong, N., Ricks-Oddie, J., Bordelon, Y. & Pouratian, N. Pallidal deep brain stimulation modulates excessive cortical high β phase amplitude coupling in Parkinson disease. *Brain Stimulation* **11**, 607–617 (2018).

51. Cagnan, H., Duff, E. P. & Brown, P. The relative phases of basal ganglia activities dynamically shape effective connectivity in Parkinson's disease. *Brain* **138**, 1667–1678 (2015).

52. Brittain, J.-S. & Brown, P. Oscillations and the basal ganglia: Motor control and beyond. *NeuroImage* **85**, 637–647 (2014).

53. Bosboom, J. L. W. *et al.* Resting state oscillatory brain dynamics in Parkinson's disease: an MEG study. *Clin Neurophysiol* **117**, 2521–2531 (2006).

54. Bronte-Stewart, H. *et al.* The STN beta-band profile in Parkinson's disease is stationary and shows prolonged attenuation after deep brain stimulation. *Exp. Neurol.* **215**, 20–28 (2009).

55. Mitzdorf, U. & Singer, W. Excitatory synaptic ensemble properties in the visual cortex of the macaque monkey: A current source density analysis of electrically evoked potentials. *Journal of Comparative Neurology* **187**, 71–83.

56. Bertrand, O., Bohorquez, J. & Pernier, J. Time-frequency digital filtering based on an invertible wavelet transform: an application to evoked potentials. *IEEE Transactions on Biomedical Engineering* **41**, 77–88 (1994).

57. Mitra, P. P. & Pesaran, B. Analysis of Dynamic Brain Imaging Data. *Biophysical Journal* **76**, 691–708 (1999).

58. Cole, S. R. *et al.* Nonsinusoidal oscillations underlie pathological phase-amplitude coupling in the motor cortex in Parkinson's disease. *bioRxiv* 049304 (2016) doi:10.1101/049304.

59. Fries, P. A mechanism for cognitive dynamics: neuronal communication through neuronal coherence. *Trends in Cognitive Sciences* **9**, 474–480 (2005).

60. Sejnowski, T. J. & Paulsen, O. Network Oscillations: Emerging Computational Principles. *J. Neurosci.* **26**, 1673–1676 (2006).

61. Fries, P. Rhythms For Cognition: Communication Through Coherence. *Neuron* **88**, 220–235 (2015).

62. Gastaut, H. J. & Bert, J. EEG changes during cinematographic presentation (Moving picture activation of the EEG). *Electroencephalography and Clinical Neurophysiology* **6**, 433–444 (1954).

63. Trimper, J. B., Stefanescu, R. A. & Manns, J. R. Recognition memory and theta–gamma interactions in the hippocampus. *Hippocampus* **24**, 341–353 (2014).

64. Yeh CH, A.-F. B. Waveform changes with the evolution of beta bursts in the human subthalamic nucleus. https://www.mrcbndu.ox.ac.uk/publications/waveform-changes-evolution-beta-bursts-human-subthalamic-nucleus.

65. Wang, D. D. *et al.* Pallidal deep brain stimulation disrupts pallidal beta oscillations and coherence with primary motor cortex in Parkinson's disease. *J. Neurosci.* 0431–18 (2018) doi:10.1523/JNEUROSCI.0431-18.2018.

66. Whitmer, D. *et al.* High frequency deep brain stimulation attenuates subthalamic and cortical rhythms in Parkinson's disease. *Front. Hum. Neurosci.* **6**, (2012).

67. McCairn, K. W. & Turner, R. S. Pallidal Stimulation Suppresses Pathological Dysrhythmia in the Parkinsonian Motor Cortex. *Journal of Neurophysiology* jn.00701.2014 (2015) doi:10.1152/jn.00701.2014.

68. McCairn, K. W. & Turner, R. S. Pallidal stimulation suppresses pathological dysrhythmia in the parkinsonian motor cortex. *Journal of Neurophysiology* **113**, 2537–2548 (2015).

69. Steigerwald, F. *et al.* Beta-band power: A suitable physiomarker for closed-loop deep brain stimulation in Parkinson's disease? [abstract]. *Movement Disorders* **30 Suppl 1 :616**, (2015).

70. Tsiokos, C., Malekmohammadi, M., AuYong, N. & Pouratian, N. Pallidal low β-low γ phase-amplitude coupling inversely correlates with Parkinson disease symptoms. *Clinical Neurophysiology* **128**, 2165–2178 (2017).

71. Stancák, A. & Pfurtscheller, G. Event-related desynchronisation of central beta-rhythms during brisk and slow self-paced finger movements of dominant and nondominant hand. *Cognitive Brain Research* **4**, 171–183 (1996).

72. Zaepffel, M., Trachel, R., Kilavik, B. E. & Brochier, T. Modulations of EEG Beta Power during Planning and Execution of Grasping Movements. *PLOS ONE* **8**, e60060 (2013).

73. Alegre, M. *et al.* Movement-related changes in cortical oscillatory activity in ballistic, sustained and negative movements. *Exp Brain Res* **148**, 17–25 (2003).

74. Gaetz, W., Edgar, J. C., Wang, D. J. & Roberts, T. P. L. Relating MEG measured motor cortical oscillations to resting γ-Aminobutyric acid (GABA) concentration. *NeuroImage* **55**, 616–621 (2011).

75. Uhlhaas, P. J. & Singer, W. Neural Synchrony in Brain Disorders: Relevance for Cognitive Dysfunctions and Pathophysiology. *Neuron* **52**, 155–168 (2006).

76. Rubchinsky, L. L., Park, C. & Worth, R. M. Intermittent neural synchronization in Parkinson's disease. *Nonlinear Dyn* **68**, 329–346 (2012).

77. Goldberg, J. A. *et al.* Enhanced Synchrony among Primary Motor Cortex Neurons in the 1-Methyl-4-Phenyl-1,2,3,6-Tetrahydropyridine Primate Model of Parkinson's Disease. *J. Neurosci.* **22**, 4639–4653 (2002).

78. Goldberg, J. A., Rokni, U., Boraud, T., Vaadia, E. & Bergman, H. Spike Synchronization in the Cortex-Basal Ganglia Networks of Parkinsonian Primates Reflects Global Dynamics of the Local Field Potentials. *J. Neurosci.* **24**, 6003–6010 (2004).

79. Herz, D. M. *et al.* Dopamine Replacement Modulates Oscillatory Coupling Between Premotor and Motor Cortical Areas in Parkinson's Disease. *Cereb. Cortex* **24**, 2873–2883 (2014).

80. Cagnan, H., Duff, E. P. & Brown, P. The relative phases of basal ganglia activities dynamically shape effective connectivity in Parkinson's disease. *Brain* **138**, 1667–1678 (2015).

81. Cassidy, M. *et al.* Movement-related changes in synchronization in the human basal ganglia. *Brain* **125**, 1235–1246 (2002).

82. Babadi, B. & Brown, E. N. A Review of Multitaper Spectral Analysis. *IEEE Transactions on Biomedical Engineering* **61**, 1555–1564 (2014).

83. Brown, P. & Marsden, C. D. Bradykinesia and impairment of EEG desynchronization in Parkinson's disease. *Mov. Disord.* **14**, 423–429 (1999).

84. Tinkhauser, G. *et al.* Beta burst dynamics in Parkinson's disease OFF and ON dopaminergic medication. *Brain* **140**, 2968–2981 (2017).

85. Oswal, A. *et al.* Deep brain stimulation modulates synchrony within spatially and spectrally distinct resting state networks in Parkinson's disease. *Brain* **139**, 1482–1496 (2016).

86. Kondylis, E. D. *et al.* Movement-related dynamics of cortical oscillations in Parkinson's disease and essential tremor. *Brain* **139**, 2211–2223 (2016).

87. Penfield, W. EPILEPSY AND SURGICAL THERAPY. *Arch NeurPsych* **36**, 449–484 (1936).

88. Spiegel, E. A., Wycis, H. T., Marks, M. & Lee, A. J. Stereotaxic Apparatus for Operations on the Human Brain. *Science* **106**, 349–350 (1947).

89. Gardner, J. A history of deep brain stimulation: Technological innovation and the role of clinical assessment tools. *Soc Stud Sci* **43**, 707–728 (2013).

90. Gildenberg. Fifty years of stereotactic and functional neurosurgery. in *Fifty Years of Neurosurgery: Sponsored by the Congress of Neurological Surgeons y First edition by Barrow, Daniel L., Kondziolka, Douglas S., Laws, Edward R., (2002) Hardcover* 295–320 (Lippincott Williams and Wilkins, 2002).

91. Sem-Jacobsen, C. W. Depth-electrographic observations related to Parkinson's disease. Recording and electrical stimulation in the area around the third ventricle. *J. Neurosurg.* **24**, Suppl:388-402 (1966).

92. Nashold, B. S. & Slaughter, D. G. Effects of Stimulating or Destroying the Deep Cerebellar Regions in Man. *Journal of Neurosurgery* **31**, 172–186 (1969).

93. Shealy, C. N., Mortimer, J. T. & Reswick, J. B. Electrical inhibition of pain by stimulation of the dorsal columns: preliminary clinical report. *Anesth. Analg.* **46**, 489–491 (1967).

94. Fahn, S. & Elton, R. in *Recent Developments in Parkinson's Disease* 153–163 (Raven Pr, 1987).

95. Kisely, S., Li, A., Warren, N. & Siskind, D. A systematic review and meta-analysis of deep brain stimulation for depression. *Depress Anxiety* **35**, 468–480 (2018).

96. Piacentino, M., Beggio, G., Zordan, L. & Bonanni, P. Hippocampal deep brain stimulation: persistent seizure control after bilateral extra-cranial electrode fracture. *Neurol. Sci.* (2018) doi:10.1007/s10072-018-3444-9.

97. Winter, L. *et al.* Acute Effects of Electrical Stimulation of the Bed Nucleus of the Stria Terminalis/Internal Capsule in Obsessive-Compulsive Disorder. *World Neurosurgery* **111**, e471–e477 (2018).

98. Underwood, C. F. & Parr-Brownlie, L. C. Primary motor cortex in Parkinson's disease: Functional changes and opportunities for neurostimulation. *Neurobiology of Disease* **147**, 105159 (2021).

99. Kwakkel, G. & Kollen, B. Predicting improvement in the upper paretic limb after stroke: A longitudinal prospective study. *Restorative Neurology and Neuroscience* **25**, 453–460 (2007).

100. Leyton, A. S. F. & Sherrington, C. S. Observations on the Excitable Cortex of the Chimpanzee, Orang-Utan, and Gorilla. *Quarterly Journal of Experimental Physiology* **11**, 135–222 (1917).

101. PENFIELD, W. & BOLDREY, E. SOMATIC MOTOR AND SENSORY REPRESENTATION IN THE CEREBRAL CORTEX OF MAN AS STUDIED BY ELECTRICAL STIMULATION1. *Brain* **60**, 389–443 (1937).

102. Rathelot, J.-A. & Strick, P. L. Subdivisions of primary motor cortex based on cortico-motoneuronal cells. *PNAS* **106**, 918–923 (2009).

103. Lemon, R. N. REVIEW ■ : Mechanisms of Cortical Control of Hand Function. *Neuroscientist* **3**, 389–398 (1997).

104. Fang, P.-C., Stepniewska, I. & Kaas, J. H. Corpus callosum connections of subdivisions of motor and premotor cortex, and frontal eye field in a prosimian primate, Otolemur garnetti. *Journal of Comparative Neurology* **508**, 565–578 (2008).

105. Mao, T. *et al.* Long-Range Neuronal Circuits Underlying the Interaction between Sensory and Motor Cortex. *Neuron* **72**, 111–123 (2011).

106. Lu, M.-T., Preston, J. B. & Strick, P. L. Interconnections between the prefrontal cortex and the premotor areas in the frontal lobe. *Journal of Comparative Neurology* **341**, 375–392 (1994).

107. Hooks, B. M. *et al.* Organization of Cortical and Thalamic Input to Pyramidal Neurons in Mouse Motor Cortex. *J. Neurosci.* **33**, 748–760 (2013).

108. Sauerbrei, B. A. *et al.* Cortical pattern generation during dexterous movement is input-driven. *Nature* **577**, 386–391 (2020).

109. Weiler, N., Wood, L., Yu, J., Solla, S. A. & Shepherd, G. M. G. Top-down laminar organization of the excitatory network in motor cortex. *Nature Neuroscience* **11**, 360–366 (2008).

110. Evarts, E. V. Pyramidal tract activity associated with a conditioned hand movement in the monkey. *Journal of Neurophysiology* **29**, 1011–1027 (1966).

111. Georgopoulos, A. P., Kalaska, J. F., Caminiti, R. & Massey, J. T. On the relations between the direction of two-dimensional arm movements and cell discharge in primate motor cortex. *J. Neurosci.* **2**, 1527–1537 (1982).

112. Evarts, E. V. Relation of pyramidal tract activity to force exerted during voluntary movement. *Journal of Neurophysiology* **31**, 14–27 (1968).

113. Beloozerova, I. N. & Sirota, M. G. The role of the motor cortex in the control of vigour of locomotor movements in the cat. *The Journal of Physiology* **461**, 27–46 (1993).

114. Georgopoulos, A. P., Kalaska, J. F., Caminiti, R. & Massey, J. T. On the relations between the direction of two-dimensional arm movements and cell discharge in primate motor cortex. *J. Neurosci.* **2**, 1527–1537 (1982).

115. Pasquereau, B., DeLong, M. R. & Turner, R. S. Primary motor cortex of the parkinsonian monkey: altered encoding of active movement. *Brain* **139**, 127–143 (2016).

116. Churchland, M. M. & Shenoy, K. V. Temporal Complexity and Heterogeneity of Single-Neuron Activity in Premotor and Motor Cortex. *Journal of Neurophysiology* **97**, 4235–4257 (2007).

117. Abbasi, O. *et al.* Unilateral deep brain stimulation suppresses alpha and beta oscillations in sensorimotor cortices. *NeuroImage* **174**, 201–207 (2018).

118. Silberstein, P. *et al.* Cortico-cortical coupling in Parkinson's disease and its modulation by therapy. *Brain* **128**, 1277–1291 (2005).

119. Hammond, C., Bergman, H. & Brown, P. Pathological synchronization in Parkinson's disease: networks, models and treatments. *Trends in Neurosciences* **30**, 357–364 (2007).

120. Underwood, C. F. & Parr-Brownlie, L. C. Primary motor cortex in Parkinson's disease: Functional changes and opportunities for neurostimulation. *Neurobiology of Disease* **147**, 105159 (2021).

121. Shen, Y., Campbell, R. E., Côté, D. C. & Paquet, M.-E. Challenges for Therapeutic Applications of Opsin-Based Optogenetic Tools in Humans. *Front. Neural Circuits* **14**, (2020).

122. Galvan, A. *et al.* Nonhuman Primate Optogenetics: Recent Advances and Future Directions. *J. Neurosci.* **37**, 10894–10903 (2017).

123. Yokoe, M. *et al.* The optimal stimulation site for high-frequency repetitive transcranial magnetic stimulation in Parkinson's disease: A double-blind crossover pilot study. *Journal of Clinical Neuroscience* **47**, 72–78 (2018).

124. Strafella, A. P., Vanderwerf, Y. & Sadikot, A. F. Transcranial magnetic stimulation of the human motor cortex influences the neuronal activity of subthalamic nucleus. *European Journal of Neuroscience* **20**, 2245–2249 (2004).

125. Cosentino, G. *et al.* Effects of More-Affected vs. Less-Affected Motor Cortex tDCS in Parkinson's Disease. *Front. Hum. Neurosci.* **11**, (2017).

126. Schabrun, S. M., Lamont, R. M. & Brauer, S. G. Transcranial Direct Current Stimulation to Enhance Dual-Task Gait Training in Parkinson's Disease: A Pilot RCT. *PLOS ONE* **11**, e0158497 (2016).

127. Leblois, A., Boraud, T., Meissner, W., Bergman, H. & Hansel, D. Competition between Feedback Loops Underlies Normal and Pathological Dynamics in the Basal Ganglia. *J. Neurosci.* **26**, 3567–3583 (2006).

128. Timmermann, L. *et al.* Ten-Hertz stimulation of subthalamic nucleus deteriorates motor symptoms in Parkinson's disease. *Movement Disorders* **19**, 1328–1333 (2004).

129. Eusebio, A. *et al.* Effects of low-frequency stimulation of the subthalamic nucleus on movement in Parkinson's disease. *Experimental Neurology* **209**, 125–130 (2008).

130. Brown, P. Oscillatory nature of human basal ganglia activity: relationship to the pathophysiology of Parkinson's disease. *Mov. Disord.* **18**, 357–363 (2003).

131. Starr, P. A., Vitek, J. L. & Bakay, R. A. Ablative surgery and deep brain stimulation for Parkinson's disease. *Neurosurgery* **43**, 989–1013; discussion 1013-1015 (1998).

132. Chen, R., Garg, R. R., Lozano, A. M. & Lang, A. E. Effects of internal globus pallidus stimulation on motor cortex excitability. *Neurology* **56**, 716–723 (2001).

133. Gradinaru, V., Mogri, M., Thompson, K. R., Henderson, J. M. & Deisseroth, K. Optical Deconstruction of Parkinsonian Neural Circuitry. *Science* **324**, 354–359 (2009).

134. Cunic, D. *et al.* Effects of subthalamic nucleus stimulation on motor cortex excitability in Parkinson's disease. *Neurology* **58**, 1665–1672 (2002).

135. Boraud, T., Bezard, E., Bioulac, B. & Gross, C. E. From single extracellular unit recording in experimental and human Parkinsonism to the development of a functional concept of the role played by the basal ganglia in motor control. *Progress in Neurobiology* **66**, 265–283 (2002).

136. Malekmohammadi, M., Elias, W. J. & Pouratian, N. Human Thalamus Regulates Cortical Activity via Spatially Specific and Structurally Constrained Phase-Amplitude Coupling. *Cereb. Cortex* **25**, 1618–1628 (2015).

137. Steiner, L. A. *et al.* Subthalamic beta dynamics mirror Parkinsonian bradykinesia months after neurostimulator implantation. *Movement Disorders* **32**, 1183–1190 (2017).

138. Perera, T. *et al.* Deep brain stimulation wash-in and wash-out times for tremor and speech. *Brain Stimulation: Basic, Translational, and Clinical Research in Neuromodulation* **8**, 359 (2015).

139. Cooper, S. E., McIntyre, C. C., Fernandez, H. H. & Vitek, J. L. Association of deep brain stimulation washout effects with Parkinson disease duration. *JAMA Neurol* **70**, 95–99 (2013).

140. Aru, J. *et al.* Untangling cross-frequency coupling in neuroscience. *Current Opinion in Neurobiology* **31**, 51–61 (2015).

141. Canolty, R. T. & Knight, R. T. The functional role of cross-frequency coupling. *Trends in Cognitive Sciences* **14**, 506–515 (2010).

142. Allen, E. A. *et al.* Components of Cross-Frequency Modulation in Health and Disease. *Front Syst Neurosci* **5**, (2011).

143. Swann, N. C. *et al.* Motor System Interactions in the Beta Band Decrease during Loss of Consciousness. *J Cogn Neurosci* **28**, 84–95 (2016).

144. Sejnowski, T. J. & Paulsen, O. Network Oscillations: Emerging Computational Principles. *J. Neurosci.* **26**, 1673–1676 (2006).

145. Vaz, A. P., Yaffe, R. B., Wittig, J. H., Inati, S. K. & Zaghloul, K. A. Dual origins of measured phase-amplitude coupling reveal distinct neural mechanisms underlying human episodic memory in the human cortex. *Neuroimage* **148**, 148–159 (2017).

146. Lian, T.-H. *et al.* Tremor-Dominant in Parkinson Disease: The Relevance to Iron Metabolism and Inflammation. *Front Neurosci* **13**, 255 (2019).

147. Banker, L. & Tadi, P. Neuroanatomy, Precentral Gyrus. in *StatPearls* (StatPearls Publishing, 2021).

148. Randazzo, M. J. *et al.* Three-dimensional localization of cortical electrodes in deep brain stimulation surgery from intraoperative fluoroscopy. *Neuroimage* **125**, 515–521 (2016).

149. Malekmohammadi, M. *et al.* Propofol-induced Changes in α-β Sensorimotor Cortical Connectivity. *Anesthesiology* **128**, 305–316 (2018).

150. Dale, A. M., Fischl, B. & Sereno, M. I. Cortical surface-based analysis. I. Segmentation and surface reconstruction. *Neuroimage* **9**, 179–194 (1999).

151. Ratib, O. & Rosset, A. Open-source software in medical imaging: development of OsiriX. *Int J CARS* **1**, 187–196 (2006).

152. Welch, P. The use of fast Fourier transform for the estimation of power spectra: A method based on time averaging over short, modified periodograms. *IEEE Transactions on Audio and Electroacoustics* **15**, 70–73 (1967).

153. Bokil, H., Purpura, K., Schoffelen, J.-M., Thomson, D. & Mitra, P. Comparing spectra and coherences for groups of unequal size. *Journal of Neuroscience Methods* **159**, 337–345 (2007).

154. Cohen, M. X. Analyzing Neural Time Series Data. *The MIT Press* https://mitpress.mit.edu/books/analyzing-neural-time-series-data (2014).

155. Holm, S. A Simple Sequentially Rejective Multiple Test Procedure. *Scandinavian Journal of Statistics* **6**, 65–70 (1979).

156. Varela, F., Lachaux, J.-P., Rodriguez, E. & Martinerie, J. The brainweb: Phase synchronization and large-scale integration. *Nat Rev Neurosci* **2**, 229–239 (2001).

157. Nolte, G. *et al.* Identifying true brain interaction from EEG data using the imaginary part of coherency. *Clin Neurophysiol* **115**, 2292–2307 (2004).

158. Vinck, M., Oostenveld, R., van Wingerden, M., Battaglia, F. & Pennartz, C. M. A. An improved index of phase-synchronization for electrophysiological data in the presence of volume-conduction, noise and sample-size bias. *NeuroImage* **55**, 1548–1565 (2011).

159. Cole, S. R. *et al.* Nonsinusoidal Beta Oscillations Reflect Cortical Pathophysiology in Parkinson's Disease. *The Journal of Neuroscience* **37**, 4830–4840 (2017).

160. López-Azcárate, J. *et al.* Coupling between Beta and High-Frequency Activity in the Human Subthalamic Nucleus May Be a Pathophysiological Mechanism in Parkinson's Disease. *J. Neurosci.* **30**, 6667–6677 (2010).

161. Khan, S. *et al.* Local and long-range functional connectivity is reduced in concert in autism spectrum disorders. *PNAS* **110**, 3107–3112 (2013).

162. Moran, L. V. & Hong, L. E. High vs Low Frequency Neural Oscillations in Schizophrenia. *Schizophr Bull* **37**, 659–663 (2011).

163. Miskovic, V. *et al.* Changes in EEG Cross-Frequency Coupling During Cognitive Behavioral Therapy for Social Anxiety Disorder. *Psychol Sci* **22**, 507–516 (2011).

164. Wach, C. *et al.* Effects of 10Hz and 20Hz transcranial alternating current stimulation (tACS) on motor functions and motor cortical excitability. *Behavioural Brain Research* **241**, 1–6 (2013).

165. Tort, A. B. L., Komorowski, R., Eichenbaum, H. & Kopell, N. Measuring Phase-Amplitude Coupling Between Neuronal Oscillations of Different Frequencies. *Journal of Neurophysiology* **104**, 1195–1210 (2010).

166. Malekmohammadi, M., Elias, W. J. & Pouratian, N. Human Thalamus Regulates Cortical Activity via Spatially Specific and Structurally Constrained Phase-Amplitude Coupling. *Cereb. Cortex* **25**, 1618–1628 (2015).

167. Pollok, B. *et al.* Motor-cortical oscillations in early stages of Parkinson's disease. *The Journal of Physiology* **590**, 3203–3212.

168. Cagnan, H. *et al.* Temporal evolution of beta bursts in the parkinsonian cortical and basal ganglia network. *PNAS* **116**, 16095–16104 (2019).

169. Hosaka, R., Nakajima, T., Aihara, K., Yamaguchi, Y. & Mushiake, H. The Suppression of Beta Oscillations in the Primate Supplementary Motor Complex Reflects a Volatile State During the Updating of Action Sequences. *Cereb. Cortex* bhv163 (2015) doi:10.1093/cercor/bhv163.

170. Womelsdorf, T. *et al.* Modulation of Neuronal Interactions Through Neuronal Synchronization. *Science* **316**, 1609–1612 (2007).

171. Buzsaki, G. *Rhythms of the Brain*. (Oxford University Press, U.S.A., 2011).

172. Belitski, A., Panzeri, S., Magri, C., Logothetis, N. K. & Kayser, C. Sensory information in local field potentials and spikes from visual and auditory cortices: time scales and frequency bands. *J Comput Neurosci* **29**, 533–545 (2010).

173. Arroyo, S. *et al.* Functional significance of the mu rhythm of human cortex: an electrophysiologic study with subdural electrodes. *Electroencephalography and Clinical Neurophysiology* **87**, 76–87 (1993).

174. Buzsáki, G., Czopf, J., Kondákor, I. & Kellényi, L. Laminar distribution of hippocampal rhythmic slow activity (RSA) in the behaving rat: Current-source density analysis, effects of urethane and atropine. *Brain Research* **365**, 125–137 (1986).

175. Hentschke, H., Perkins, M. G., Pearce, R. A. & Banks, M. I. Muscarinic blockade weakens interaction of gamma with theta rhythms in mouse hippocampus. *European Journal of Neuroscience* **26**, 1642–1656 (2007).

176. Buzsáki, G., Rappelsberger, P. & Kellényi, L. Depth profiles of hippocampal rhythmic slow activity ('theta rhythm') depend on behaviour. *Electroencephalogr Clin Neurophysiol* **61**, 77–88 (1985).

177. Belluscio, M. A., Mizuseki, K., Schmidt, R., Kempter, R. & Buzsáki, G. Cross-Frequency Phase–Phase Coupling between Theta and Gamma Oscillations in the Hippocampus. *J. Neurosci.* **32**, 423–435 (2012).

178. Pietersen, A. N. J., Patel, N., Jefferys, J. G. R. & Vreugdenhil, M. Comparison between spontaneous and kainate-induced gamma oscillations in the mouse hippocampus in vitro. *European Journal of Neuroscience* **29**, 2145–2156 (2009).

179. Cole, S. R. & Voytek, B. Brain Oscillations and the Importance of Waveform Shape. *Trends in Cognitive Sciences* **21**, 137–149 (2017).

180. Sherman, M. A. *et al.* Neural mechanisms of transient neocortical beta rhythms: Converging evidence from humans, computational modeling, monkeys, and mice. *PNAS* **113**, E4885–E4894 (2016).

181. Kühn, A. A., Kupsch, A., Schneider, G.-H. & Brown, P. Reduction in subthalamic 8–35 Hz oscillatory activity correlates with clinical improvement in Parkinson's disease. *European Journal of Neuroscience* **23**, 1956–1960 (2006).

182. Buzsáki, G., Logothetis, N. & Singer, W. Scaling brain size, keeping timing: evolutionary preservation of brain rhythms. *Neuron* **80**, 751–764 (2013).

183. Jackson, N., Cole, S. R., Voytek, B. & Swann, N. C. Characteristics of Waveform Shape in Parkinson's Disease Detected with Scalp Electroencephalography. *eNeuro* **6**, (2019).

184. Yanagisawa, T. *et al.* Regulation of Motor Representation by Phase–Amplitude Coupling in the Sensorimotor Cortex. *J. Neurosci.* **32**, 15467–15475 (2012).

185. Little, S. & Brown, P. The functional role of beta oscillations in Parkinson's disease. *Parkinsonism & Related Disorders* **20, Supplement 1**, S44–S48 (2014).

186. Hatsopoulos, N. G. Encoding in the Motor Cortex: Was Evarts Right After All? Focus on "Motor Cortex Neural Correlates of Output Kinematics and Kinetics During Isometric-Force and Arm-Reaching Tasks". *Journal of Neurophysiology* **94**, 2261–2262 (2005).

187. Evarts, E. V. ReIation of pyramidal tract activity to force exerted during voluntary movementJ. Neurophysiol. 3 1 : 14-27. 1968. E.V. Activity of pyramidal tract neurons during postural fixation. *J* 32–375 (1969).

188. Rougeul, A., Bouyer, J. J., Dedet, L. & Debray, O. Fast somato-parietal rhythms during combined focal attention and immobility in baboon and squirrel monkey. *Electroencephalography and Clinical Neurophysiology* **46**, 310–319 (1979).

189. Heinrichs-Graham, E. *et al.* Hypersynchrony despite pathologically reduced beta oscillations in patients with Parkinson's disease: a pharmaco-magnetoencephalography study. *J Neurophysiol* **112**, 1739–1747 (2014).

190. Murthy, V. N. & Fetz, E. E. Coherent 25- to 35-Hz oscillations in the sensorimotor cortex of awake behaving monkeys. *Proc Natl Acad Sci U S A* **89**, 5670–5674 (1992).

191. Friston, K. J. Transients, Metastability, and Neuronal Dynamics. *NeuroImage* **5**, 164–171 (1997).

192. Neumann, W.-J. *et al.* Subthalamic synchronized oscillatory activity correlates with motor impairment in patients with Parkinson's disease. *Movement Disorders* **31**, 1748–1751 (2016).

193. Miller, K. J. *et al.* Human Motor Cortical Activity Is Selectively Phase-Entrained on Underlying Rhythms. *PLoS Comput Biol* **8**, (2012).

194. Toro, C. *et al.* Event-related desynchronization and movement-related cortical potentials on the ECoG and EEG. *Electroencephalography and Clinical Neurophysiology/Evoked Potentials Section* **93**, 380–389 (1994).

195. Miller, K. J. *et al.* Human Motor Cortical Activity Is Selectively Phase-Entrained on Underlying Rhythms. *PLoS Comput Biol* **8**, (2012).

196. Cassim, F. *et al.* Brief and sustained movements: differences in event-related (de)synchronization (ERD/ERS) patterns. *Clinical Neurophysiology* **111**, 2032–2039 (2000).

197. van Driel, J., Cox, R. & Cohen, M. X. Phase-clustering bias in phase-amplitude cross-frequency coupling and its removal. *J Neurosci Methods* **254**, 60–72 (2015).

198. Siderowf, A. & Stern, M. B. Preclinical diagnosis of Parkinson's disease: are we there yet? *Curr Neurol Neurosci Rep* **6**, 295–301 (2006).

199. Brown, P. *et al.* Dopamine Dependency of Oscillations between Subthalamic Nucleus and Pallidum in Parkinson's Disease. *J. Neurosci.* **21**, 1033–1038 (2001).

200. Airaksinen, K. *et al.* Somatomotor mu rhythm amplitude correlates with rigidity during deep brain stimulation in Parkinsonian patients. *Clin Neurophysiol* **123**, 2010–2017 (2012).

201. Xiao, R., Malekmohammadi, M., Pouratian, N. & Hu, X. Characterization of pallidocortical motor network in Parkinson's disease through complex network analysis. *J Neural Eng* **16**, 066034 (2019).

202. Choi, J. W. *et al.* Altered Pallidocortical Low-Beta Oscillations During Self-Initiated Movements in Parkinson Disease. *Front Syst Neurosci* **14**, 54 (2020).

203. Shimamoto, S. A. *et al.* Subthalamic Nucleus Neurons Are Synchronized to Primary Motor Cortex Local Field Potentials in Parkinson's Disease. *J. Neurosci.* **33**, 7220–7233 (2013).

204. Wang, H. C., Lees, A. J. & Brown, P. Impairment of EEG desynchronisation before and during movement and its relation to bradykinesia in Parkinson's disease. *J Neurol Neurosurg Psychiatry* **66**, 442–446 (1999).

205. Pfurtscheller, G., Graimann, B., Huggins, J. E., Levine, S. P. & Schuh, L. A. Spatiotemporal patterns of beta desynchronization and gamma synchronization in corticographic data during self-paced movement. *Clinical Neurophysiology* **114**, 1226–1236 (2003).

206. Yoshida, T., Masani, K., Zabjek, K., Chen, R. & Popovic, M. R. Dynamic cortical participation during bilateral, cyclical ankle movements: effects of aging. *Scientific Reports* **7**, 44658 (2017).

207. Roeder, L., Boonstra, T. W. & Kerr, G. K. Corticomuscular control of walking in older people and people with Parkinson's disease. *Scientific Reports* **10**, 2980 (2020).

208. Miller, K. J. *et al.* Spectral Changes in Cortical Surface Potentials during Motor Movement. *J. Neurosci.* **27**, 2424–2432 (2007).

209. Friston, K. J. Another neural code? *Neuroimage* **5**, 213–220 (1997).

210. Vinding, M. C. *et al.* Reduction of spontaneous cortical beta bursts in Parkinson's disease is linked to symptom severity. *Brain Communications* **2**, (2020).

211. Little, S., Bonaiuto, J., Barnes, G. & Bestmann, S. Human motor cortical beta bursts relate to movement planning and response errors. *PLoS Biol* **17**, e3000479 (2019).

212. Pollok, B. *et al.* Increased SMA–M1 coherence in Parkinson's disease — Pathophysiology or compensation? *Experimental Neurology* **247**, 178–181 (2013).

213. Arce-McShane, F. I., Ross, C. F., Takahashi, K., Sessle, B. J. & Hatsopoulos, N. G. Primary motor and sensory cortical areas communicate via spatiotemporally coordinated networks at multiple frequencies. *PNAS* **113**, 5083–5088 (2016).

214. Brovelli, A. *et al.* Beta oscillations in a large-scale sensorimotor cortical network: Directional influences revealed by Granger causality. *PNAS* **101**, 9849–9854 (2004).

215. Kato, K. *et al.* Bilateral coherence between motor cortices and subthalamic nuclei in patients with Parkinson's disease. *Clin Neurophysiol* **126**, 1941–1950 (2015).

216. Swann, N. C. *et al.* Elevated synchrony in Parkinson disease detected with electroencephalography: Elevated Synchrony in PD. *Annals of Neurology* **78**, 742–750 (2015).

217. Yeh, C.-H. *et al.* Waveform changes with the evolution of beta bursts in the human subthalamic nucleus. *Clinical Neurophysiology* **131**, 2086–2099 (2020).

218. McCarthy, M. M. *et al.* Striatal origin of the pathologic beta oscillations in Parkinson's disease. *PNAS* **108**, 11620–11625 (2011).

219. Kouli, A., Torsney, K. M. & Kuan, W.-L. Parkinson's Disease: Etiology, Neuropathology, and Pathogenesis. in *Parkinson's Disease: Pathogenesis and Clinical Aspects* (eds. Stoker, T. B. & Greenland, J. C.) (Codon Publications, 2018).

220. Schrag, A., Horsfall, L., Walters, K., Noyce, A. & Petersen, I. Prediagnostic presentations of Parkinson's disease in primary care: a case-control study. *The Lancet Neurology* **14**, 57–64 (2015).

221. Braak, H. *et al.* Staging of brain pathology related to sporadic Parkinson's disease. *Neurobiology of Aging* **24**, 197–211 (2003).

222. Feingold, J., Gibson, D. J., DePasquale, B. & Graybiel, A. M. Bursts of beta oscillation differentiate postperformance activity in the striatum and motor cortex of monkeys performing movement tasks. *PNAS* **112**, 13687–13692 (2015).

223. Picazio, S. *et al.* Prefrontal Control over Motor Cortex Cycles at Beta Frequency during Movement Inhibition. *Curr Biol* **24**, 2940–2945 (2014).

224. Darch, H. T., Cerminara, N. L., Gilchrist, I. D. & Apps, R. Pre-movement changes in sensorimotor beta oscillations predict motor adaptation drive. *Scientific Reports* **10**, 17946 (2020).

225. Jones, S. R. When brain rhythms aren't "rhythmic": implication for their mechanisms and meaning. *Curr Opin Neurobiol* **40**, 72–80 (2016).

226. Little, S. *et al.* Adaptive deep brain stimulation in advanced Parkinson disease. *Annals of Neurology* **74**, 449–457 (2013).

227. Parvizi, J. & Kastner, S. Human Intracranial EEG: Promises and Limitations. *Nat Neurosci* **21**, 474–483 (2018).

228. Schnitzler, A. & Gross, J. Normal and pathological oscillatory communication in the brain. *Nat Rev Neurosci* **6**, 285–296 (2005).

229. Chiang, S. & Haneef, Z. Graph theory findings in the pathophysiology of temporal lobe epilepsy. *Clin Neurophysiol* **125**, 1295–1305 (2014).

230. Donoghue, J. P., Sanes, J. N., Hatsopoulos, N. G. & Gaál, G. Neural Discharge and Local Field Potential Oscillations in Primate Motor Cortex During Voluntary Movements. *Journal of Neurophysiology* **79**, 159–173 (1998).

231. Hayward, T. How to kill a lobster is as much about our moral code as science. *Financial Times* (2021).

232. Hartung, T. Thoughts on limitations of animal models. *Parkinsonism & Related Disorders* **14**, S81–S83 (2008).

233. Wendel, K. *et al.* EEG/MEG Source Imaging: Methods, Challenges, and Open Issues. *Computational Intelligence and Neuroscience* **2009**, e656092 (2009).

234. Savage, N. How AI and neuroscience drive each other forwards. *Nature* **571**, S15–S17 (2019).

235. Ch, Y. *et al.* Waveform changes with the evolution of beta bursts in the human subthalamic nucleus. *Clin Neurophysiol* **131**, 2086–2099 (2020).

236. Kwon, G. *et al.* Individual differences in oscillatory brain activity in response to varying attentional demands during a word recall and oculomotor dual task. *Front Hum Neurosci* **9**, 381 (2015).